# Effect Of Heavy Metal(loid)s On The Level Of Gonadal Hormone During The Sexual Maturity And Breeding Period Of Catfish, *Clarias batrachus* (L.).

Dr. Nilanjana Bhattacharyya Nath

Assistant Professor & HOD,

Department of Biotechnology,

Swami Vivekananda Institute of Modern Science, Sonarpur, Kolkata-103, West Bengal, India.

***Abstract :*** Natural sexual steroid hormones play a major role in controlling sex differentiation and reproduction in fish. Additionally, physiological concentrations of these hormones are essential for the maintenance of cell proliferation, growth and several other biological activities. Imbalance in hormonal status caused by higher level of endogenous hormones as well as by exposure to exogenous steroid-like compounds is known to produce adverse effects on reproductive processes. In the present investigation, *Clarias batrachus* treated with three different heavy metals at different doses. Lead, mercury and arsenic exposed fish had significantly decreased gonadosomatic index. In case of control fish, in the month of June, the level of 17β estradiol was 0.75 $ngml^{-1}$ where as in the treated fish the amounts were 0.70 $ngml^{-1}$ for Lead, 0.60 $ngml^{-1}$ for Mercury and 0.63 $ngml^{-1}$ for Arsenic and the level of testosterone in both control and treated group were 1.61 $ngml^{-1}$ and 1.47 $ngml^{-1}$, 1.27 $ngml^{-1}$and 1.43 $ngml^{-1}$ respectively. Among the three heavy metals, the level of gonadal hormone of *Clarias batrachus* treated with any chemical was disturbed and in case of mercury exposed fish the reduction was maximum.

***Index Terms*** **- Lead, Mercury, Arsenic, Gonadosomatic Index, Estradiol, Testosterone, *Clarias batrachus*.**

## I. INTRODUCTION

In all fishes investigated development of secondary sexual characteristics has been shown to depend on gonadal steroids. Several androgens (male sexual hormones like testosterone) and estrogens (the female equivalent) have been identified from the tissues and blood of fishes. Among the steroids found are testosterone, androstenedione, 17β estradiol, androsterone, 11keto testosterone, conjugated testosterone and progesterone. Various studies have demonstrated that many environmental contaminants adversely affect embryonic development. Thus, a disruption of the normal hormonal signals can permanently modify the organization and future functioning of the reproductive system. Over 65 different types of chemicals have been identified as being endocrine disruptors (Keith, 1997), including PAHs, PCBs, dioxins and furans, several trace elements, organochlorine, organophosphate and carbamate pesticides, triazine herbicides and synthetic steroids (Gross and others, 2003). Determinations of steroid hormones and gonad condition during the annual reproductive cycles of various teleosts have been reported (Singh and Singh, 1987; Matsuyama *et al.*, 1991). Moreover, alterations of steroid hormones have implications in studying the effects of the environment (temperature, photoperiod, pollution or habitat degradation) on the reproductive biology of fish (Bromage *et al.*, 1982; Okuzawa *et al.*, 1989; Shimizu *et al.*, 1994).

Several studies document the greatest variance in sex steroid concentrations during spawning, yet hormone levels from individuals at the same site have been shown to vary up to 30-fold during gonadal recrudescence (Chang and Chen, 1990; Down *et al.*, 1990; Folmar *et al.*, 1996). There is also evidence that the stress of collecting, holding, and obtaining blood from fish may affect hormone concentrations (Jardine *et al.*, 1996; McMaster *et al.*, 1994; Van den Heuvel *et al.*, 1995; Barton and Iwama, 1991; Magri *et al.*, 1982). The sex steroids, a class of hormones derived from cholesterol and synthesized by the gonads in response to circulating levels of GTH-I and GTH-II, collectively control the development of the gonads and gametes, secondary sexual characteristics and reproductive behavior (Liley and Stacey, 1983; Fostier *et al.*, 1983). Kumar and Pant (1984) found that lead, copper and zinc caused reabsorption of oocytes from the ovaries of an Indian teleost fish. Reabsorption of oocytes indicates potential hormonal disruption within the endocrine system.

Therefore, the objective of the present research was to test whether the continuous exposure of Clarias *batrachus* to lead, mercury and arsenic may affect the level of gonadal hormone during the sexual maturity and breeding period of *Clarias batrachus.*

## II. MATERIAL AND METHODS

About eighty (80) *Clarias batrachus* weighing 100+10g were purchased from the local fish market and acclimated to the laboratory conditions for 15 days, prior initiating the experiment. They were divided into eight groups of 10 each. Group I served as control and other seven groups were treated with Lead Nitrate (3.0 ppm, 5.0 ppm and 7.0 ppm), Mercuric Chloride (0.05$mgl^{-1}$) and Sodium Arsenate (5.0 ppm, 10.0 ppm and 15.0 ppm). Both controls and experimental were fed with minced goat liver every

alternate day before the aquaria water was changed. The experiment was initiated in the month of February with Lead, Mercury and Arsenic when the gonads were immature and terminated in June when the gonads in the control fish were fully matured. Blood serum of all those groups was collected and assayed for serum Eestradiol and Tesrosterone by ELISA reader (Method followed by Lone *et al.*, 2001).

## III. RESULTS

The major estrogen in female fish, 17β estradiol (E2), is produced primarily in the ovary by the follicular cells. In addition to their importance in eliciting reproductive behavior and the development and maintenance of secondary sex characteristics, the estrogens and androgens are involved in the production of gametes (Bone *et al.*, 1995). 17β estradiol was at low levels in the previtellogenic phase, increased rapidly in the vitellogenic phase and attained their peaks in the late vitellogenic phase. Gonadosomatic index (GSI) was low in the previtellogenic phases and increased in the vitellogenic and postvitellogenic phases. In control *Clarias batrachus*, Plasma testosterone levels increased in a stepwise fashion, the first significant increase occurring in the previtellogenic phase (March) and the second in the early vitellogenic phase (May). The levels remained elevated till the early postvitellogenic phase and reached basal levels in the regressed phase. In treated groups, level of 17 β estradiol and testosterone were reduced significantly. From the month February to June, the level of gonadal hormone was decreased.

Table 1 : Gonadosomatic Index (GSI) of *Clarias batrachus* Both Control And Treated.

| Group | Gonadosamatic Index (GSI) | |
|---|---|---|
| | Female | Male |
| Control | 6.73 + 0.72 | 0.29 + 0.01 |
| Lead treated | 2.17 + 0.01 | 0.12 + 0.02 |
| Mercury treated | 2.14 + 0.03 | 0.10+ 0.03 |
| Arsenic treated | 2.15 + 0.12 | 0.11 + 0.02 |

[Figures Represent Mean ± S.D. Each Data Is A Mean Of Five Separate Determinations.]

Table 2 : The Amount Of 17 β-Estradiol Of Control And Lead Treated *Clarias batrachus* At Highest Dose**.**

| Month | Control (ng $ml^{-1}$) | Treated (ng $ml^{-1}$) |
|---|---|---|
| February | $0.05^a$ | $0.05^a$ |
| March | $0.12^a$ | $0.11^b$ |
| April | $0.22^a$ | $0.20^b$ |
| May | $0.40^a$ | $0.37^b$ |
| June | $0.75^a$ | $0.70^b$ |

[The different superscripts in a row are significantly different at $p \leq 0.05$]

Each data is a mean of five separate determinations.

Table 3 : The Amount Of 17 β-Estradiol Of Control And Mercury Treated *Clarias batrachus* At Highest Dose.

| Month | Control (ng $ml^{-1}$) | Treated (ng $ml^{-1}$) |
|---|---|---|
| February | $0.05^a$ | $0.05^a$ |
| March | $0.12^a$ | $0.10^b$ |
| April | $0.22^a$ | $0.18^b$ |
| May | $0.40^a$ | $0.32^b$ |
| June | $0.75^a$ | $0.60^b$ |

[The different superscripts in a row are significantly different at $p \leq 0.05$]
Each data is a mean of five separate determinations.

Table 4 : The Amount Of 17 β-Estradiol Of Control And Arsenic Treated *Clarias batrachus* At Highest Dose.

| Month | Control (ng $ml^{-1}$) | Treated (ng $ml^{-1}$) |
|---|---|---|
| February | 0.05 [a] | 0.05 [a] |
| March | 0.12 [a] | 0.11 [b] |
| April | 0.22 [a] | 0.19 [b] |
| May | 0.40 [a] | 0.34 [b] |
| June | 0.75 [a] | 0.63 [b] |

[The different superscripts in a row are significantly different at $p \leq 0.05$]
Each data is a mean of five separate determinations.

Table 5 : The Amount Of Testosterone Of Control And Lead Treated *Clarias batrachus* At Highest Dose.

| Month | Control (ng $ml^{-1}$) | Treated (ng $ml^{-1}$) |
|---|---|---|
| February | 0.32 [a] | 0.32 [a] |
| March | 0.52 [a] | 0.48 [b] |
| April | 0.82 [a] | 0.75 [b] |
| May | 1.17 [a] | 1.07 [b] |
| June | 1.61 [a] | 1.47 [b] |

[The different superscripts in a row are significantly different at $p \leq 0.05$]
Each data is a mean of five separate determinations.

Table 6 : The Amount Of Testosterone Of Control And Mercury Treated *Clarias batrachus* At Highest Dose.

| Month | Control (ng $ml^{-1}$) | Treated (ng $ml^{-1}$) |
|---|---|---|
| February | 0.32 [a] | 0.32 [a] |
| March | 0.52 [a] | 0.42 [b] |
| April | 0.82 [a] | 0.65 [b] |
| May | 1.17 [a] | 0.94 [b] |
| June | 1.61 [a] | 1.27 [b] |

[The different superscripts in a row are significantly different at $p \leq 0.05$]
Each data is a mean of five separate determinations.

Table 7 : The Amount Of Testosterone Of Control And Arsenic Treated *Clarias batrachus* At Highest Dose.

| Month | Control (ng $ml^{-1}$) | Treated (ng $ml^{-1}$) |
|---|---|---|
| February | 0.32 [a] | 0.32 [a] |
| March | 0.52 [a] | 0.46 [b] |
| April | 0.82 [a] | 0.71 [b] |
| May | 1.17 [a] | 0.99 [b] |
| June | 1.61 [a] | 1.43 [b] |

[The different superscripts in a row are significantly different at $p \leq 0.05$]
Each data is a mean of five separate determinations.


Figure 1 : Effect Of Lead Nitrate On The Level Of17 β-Estradiol
In *Clarias batrachus*

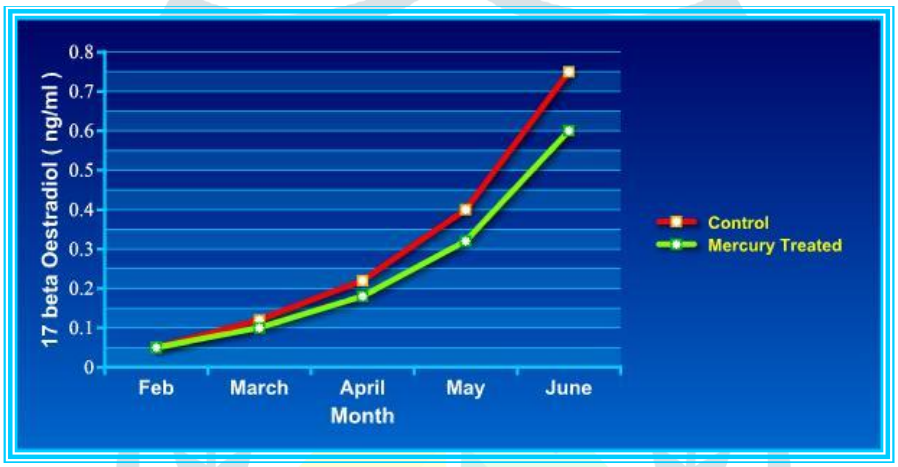


Figure 2 : Effect Of Mercuric Chloride On The Level Of 17 β-Estradiol
In *Clarias batrachus*

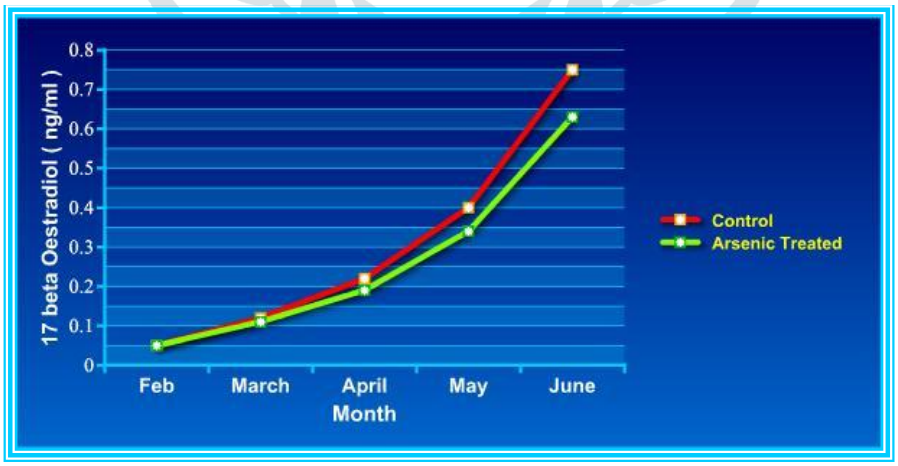


Figure 3 : Effect Of Sodium Arsenate On The Level Of 17 β-Estradiol
In *Clarias batrachus*

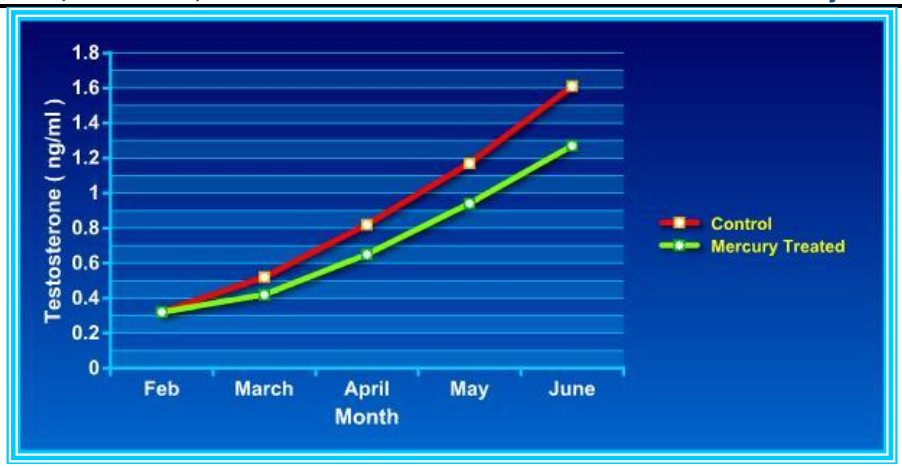


Figure 4 : Effect Of Mercuric Chloride On The Level Of Testosterone In *Clarias batrachus*


Figure 5 : Effect Of Lead Nitrate On The Level Of Testosterone In *Clarias batrachus*


Figure 6 : Effect Of Sodium Arsenate On The Level Of Testosterone In *Clarias batrachus*

## IV. DISCUSSION

The major androgens in fish include testosterone, 11-keto testosterone, and androstenedione. The predominant estrogens are 17β-estradiol and estrone. Sex steroids in immature fish probably influence gonadal differentiation, whereas these same hormones play an important role in gametogenesis, ovulation and spermiation in mature fish (Redding and Patino, 1993; Barry *et al*., 1990; Patino and Thomas, 1990a; Patino and Thomas, 1990b). Over the last few decades, sex steroid hormones have evolved as convenient biomarkers for detecting contaminant-induced biochemical alterations and fish have emerged as favorable models for examining the effects of environmental pollutants in aquatic ecosystems.

Endocrine disrupters includes pesticides such as the insecticides endosulfan (Chakravorty *et al.*, 1992), carbofuran (Sukumar and Karpagaganapathy, 1992), lindane (α-HCH) (Celius *et al.*, 1999), DDT (Khan and Thomas, 1998; Celius *et al.*, 1999) and the herbicide atrazine (Wetzel *et al.*, 1994), PCBs (Monosson *et al.*, 1994; Thomas, 1988; Thomas, 1989) and a number of metals including lead (Thomas, 1988), cadmium (Thomas, 1989; Ruby *et al.*, 2000; Kime *et al.*, 1996), and mercury (Rurangwa *et al.*, 1998). Some contaminants may affect the function of the endocrine system (Peterle, 1991). The endocrine system regulates hormone-dependent physiological functions that are necessary for survival and perpetuation of an organism. Chemicals that impact endocrine processes are called endocrine-disruptors (Ward, 1998). These particular chemicals are capable of eliciting or inhibiting responses typically induced by hormonal or steroidal activities (Gillesby and Zacharewski, 1998). Endocrine-disrupting agents may also interfere with production, release, transport, metabolism, binding or elimination of the natural hormones and steroids (Peterle, 1991; Arcand-Hoy and Benson, 1998; Rolland *et al.*, 1997). Some hormones and steriods are responsible for timing and rate of development in embryos, fry, juveniles and adults. If production of hormones and steroids is disrupted, these processes can be effectively altered (Roberts *et al.*, 1978). Reabsorption of oocytes indicates potential hormonal disruption within the endocrine system. Several fish species have been used for in vivo, multiple generational testing of endocrine disrupting compounds, including Japanese medaka (*Oryzias latipes*) (Patyna and others, 1999), zebrafish (*Pterois volitans*) (Nash and others, 2004), fathead minnow (*Pimephales promelas*) (Lange and others, 2001) and mummichog (*Fundulus heteroclitus*) (Bordeau and others, 2004).

The purpose of the present investigation was to report the changes in plasma levels of gonadal hormones after heavy metal exposure. In present investigation, common catfish, *Clarias batrachus* exposed to three chemicals such as Lead, Mercury and Arsenic showed reduction on the 17β estradiol and Testosterone in comparison with the control one. In case of control fishes, in the month of June, the level of 17β estradiol was 0.75 $ngml^{-1}$ where as in the treated fish the amounts were 0.70 $ngml^{-1}$ for Lead, 0.60 $ngml^{-1}$ for Mercury and 0.63 $ngml^{-1}$ for Arsenic and the level of Testosterone in both control and treated group were 1.61, 1.47, 1.27 and 1.43 $ngml^{-1}$ respectively. Among the three heavy metals, the level of gonadal hormone of *Clarias batrachus* treated with any chemical was disturbed and in case of mercury exposed fish the reduction was maximum.

## V. CONCLUSION

In case of control group the annual cycle of steroids indicated that high plasma levels of 17β oestradiol in females and testosterone in males correspond well with high gonadal activity (high GSI index and active vitellogenesis or spermatogenesis). Whereas, high levels of circulating 17β- oestradiol stimulate the liver to synthesize and release vitellogenin, a glycolipophospho-protein egg yolk precursor. So, in case of treated group gonadal maturation was retarded which directly correlated with the changes of both 17β oestradiol and testosterone. From the above data I may conclude that this decrease of 17β estradiol and Testosterone directly affect the whole process of gametogenesis and also the reproductive success of *Clarias batrachus* (L.).

## VI.REFERENCES

**[I].**Ali Annabi et al. (2013) : Cadmium: Toxic Effects and Physiological Impairments in Fishes. International Journal of Advanced Research, Volume 1, Issue3, 372-382.

**[II].**Alam, M. K. and O. E. Maughan (1995) **:** Acute toxicity of heavy metals to common carp (*Cyprinus carpio*). J. Environ. Sci. Health 30A (8) **:** 1807 - 1816.

**[III].**Blazquez, M., P. T. Bosma, E. J. Fraser, K. J. W. Van Look and V. L. Trudeau (1998a) **:** Fish as model for the neuroendocrine regulation of reproduction and growth. Comparative Biochemistry and Physiology. Part C. 119 **:** 345 - 364.

**[IV].**Barcellos, L. J. G., S. Nicolaiewsky, S. M. J. de Souza and F. Lulhier (1999) **:** Plasmatic levels of cortisol in the response to acute stress in Nile tilapia, *Oreochromis niloticus* (L.), previously exposed to chronic stress. Aquaculture Research 30**,** 437 - 444.

**[V].**Claper Rebecca, Christopher B. Rees, Paul Drevnick, Daniel Weber, Mark Sandheinrich and Michael J. Carvan (2006) **:** Gene Expression Changes Related to Endocrine Function and Decline in Reproduction in Fathead Minnow (*Pimephales promelas*) after Dietary Methylmercury Exposure. Environmental Health Perspective. 114(9).

**[VI].**Ebrahimi, M.;Taherianfard, M.(2011): The effects of heavy metals exposure on reproductive systems of cyprinid fish from Kor River. Iranian Journal of Fisheries Sciences 10(1)13-24.

**[VII].**Folmar, L. C., N. D. Denslow, V. Rao, M. Chow, D. A. Crain, J. Enblom, J. Marcino, and L. J. Guillette, Jr (1996) : Vitellogenin induction and reduced serum testosterone concentrations in feral male carp (*Cyprinus carpio*) captured near a major metropolitan sewage treatment plant. Environ Health Perspect. 104(10) : 1096 – 1101.

**[VIII].**Geeta J. Gautam,Radha(2018): ChaubeDifferential Effects of Heavy Metals (Cadmium, Cobalt, Lead and Mercury) on Oocyte Maturation and Ovulation of the Catfish *Heteropneustes fossilis*: an In Vitro Study. Turkish Journal of Fisheries and Aquatic Sciences 18: 1205-1214.

**[IX].**Katti, S. R. and A. G. Sathyanesan (1985) : Chronic effects of lead and cadmium on the testis of the catfish, *Clarias batrachus*. Environ. Ecol. 3(1) : 596 -598

**[X].**Kasuppasumy, R. (2001) : Evaluation of acute toxicity levels and behavioural responses of *Channa punctatus* (Block) to phenyl mercuric acetate. Ecol. Env. & cons 7(1) : 75 – 78.

**[XI].**Levesque, M. Haude, Jocelyn Dorval, Alice Hontela, Glen J. Van Der Kraak and Peter G. C. Campbell (2003) : Hormonal, morphological and physiological responses of yellow perch (*Perca flavescens*) to chronic environmental metal exposures. Journal of Toxicology and Environmental Health. 66(7) : 657 - 676.

**[XII].**XII.Masud Sahar, J. J. Singh and R. N. Ram (2001) : Testicular recrudescence and related changes in *Cyprinus Carpio* after long term exposure to a mercurial compound. J. Ecophysion. Oocup. Hlth. 1 : 109 – 120.

**[XIII].**Marte, Clarissa L. and T. J. Lam (2004) : Hormonal changes accompanying sexual maturation in captive milkfish (*Chanos chanos* Forsskal). Fish Physiology and Biochemistry 10 (4) : 267 - 275.

**[XIV].**Mohammad MN Authman et al.(2015) : Use of fish as bio-indicator of the effects of heavy metals pollution. J Aquac Res Development, 6:4.

**[XV].**Sindhe, V. R., M. U. Veeresh and R. S. Kulkjarvi (2002) : Ovarian changes in the response to Heavy metal exposure to the fish, *N. notopterus* (Pallas). J. Environ. Biol.23 (2) : 137 – 141.

**[XVI].**Seul Min Choi, Sun Dong Yoo and Byung Mu Lee (2003) : Toxicological Characteristics of Endocrine-Disrupting Chemicals: Developmental Toxicity, Carcinogenicity, and Mutagenicity. Journal of Toxicology and Environmental Health. 7 (1) : 1 - 23.

**[XVII].**Sumera Sajjad et al. (2018) : Changes in Growth Hormone and Cortisol Profile due to Lead Induced Toxicity in *Labeo rohita.* Turkish Journal of Fisheries and Aquatic Sciences 18: 921-926.

Int J Env Tech Sci 7: 244–248 © 2019 http://www.kalyanishineindia.org/index.php/journal Kalyani Shine India ORIGINAL ARTICLE

# Lead nitrate induced biochemical change on gonad and gonadal development of Catfish (*Clarias batrachus* (L.)


**Nilanjana B. Nath[1], Bidhan C. Patra[2]**

[1]*Swami Vivekananda Institute Of Modern Science Department of Biotechnology;Sonarpure Kolkata-103,West Bengal,India*
[2]*Department Of Zoology, Vidyasagar University, Midnapore,West Bengal, India*

**ARTICLE INFO**

**Article history:**
Received– 03 January, 2019
Revised– 02 April, 2019
Accepted– 30 April, 2019
Available– 06 May, 2019
(online)

**Keywords:**
Lead nitrate
Fish gonad
Histological changes
*Clarias batrachus*

**Corresponding Author:**
Nilanjana B. Nath
Email: nbhattacharyyanath@hotmail.com

**ABSTRACT**

The present paper deals with the effect of Lead nitrate on the gonads and the gonadal development of common Indian catfish, *Clarias batrachus* (L.). It has been observed that the Gonadosomatic Index of both male and female were reduced significantly in case of lead treated fish. A great increase of primary (non-yolky) oocytes was observed in treated ovary. Mature oocytes were totally disappeared and atretic follicles were found. Whereas, control ovary had fully mature vitellogenic stage IV oocytes. The lead treated testis was completely devoid of spermatids and mature sperms. Cells of vas deferens were crumpled often with inter-cellular spaces having irregular nuclei. All the cross sections of control testis were occupied by the sperms that filled several tubules. Summarily, it can be concluded that the Lead nitrate has severe adverse impacts on gonadal development showing biochemical alterations.

## 1. Introduction

Lead is potent toxic metal, the quantity of which is progressively increasing in our environment (Choudhury and Mudipalli 2008; Directive 2000; Bhakta et al. 2012; Bhakta and Munekage 2012). Most of the lead salts find their way into aquatic systems through rain, sewages and effluents. Absorption of lead by aquatic animals is affected by the age, gender and diet of the organism, as well as the particle size, chemical species of lead and presence of other compounds in the water. Lead is known to affect the structure and function of various organs and tissues. It is highly toxic to aquatic organisms, especially fish. Fish from polluted areas do build up substantial concentrations of lead in muscle tissue and whole-body analysis of fish for lead is still recommended for general environmental monitoring. The biological effects in sublethal concentrations of lead include delayed embryonic development, suppressed reproduction, inhibition of growth, increased mucous formation, neurological problems, enzyme inhibition and kidney dysfunction. Sublethal effects of lead on pituitary function of rainbow trout during exogenous vitellogenesis were studied by Ruby et al. (2000). Alados and Daniel (1999) reported the effect of lead on the predictability of reproductive behavior in fathead minnows, *Pimephales promelas.* The fish, *Clarias batrachus* is a hardy fish and highly valued in India specially West Bengal. It would therefore be of interest to study the quantity of lead that can be accumulated within its tissues. So, this work is therefore aimed to assess the toxic effect of lead on the ovary and testis of *Clarias batrachus* (L.).

## 2. Materials and methods

About 80 catfishes, *Clarias batrachus* measuring 20 – 22 cm and weighing 90 – 100 g were brought from local market and were acclimatized to laboratory conditions for about 2 weeks prior starting the experiment. They were kept in tap water. The fishes were divided into four groups of 20 each. Three groups were exposed continuously to 3.0, 5.0 and 7.0 ppm lead nitrate for 150 days and the fourth group was given no treatment and served as control. The water temperature varied from 20 – 35°C from February to June. They were fed

with minced goat liver and the water was changed every alternate day after feeding the fish. At the end of the experiment, the fish were weighed and sacrificed, gonads were dissected out within 1 – 2 min, rapidly frozen and processed for various biochemical analysis. The significance of analysis was ratified through student's t-test. For histological preparation, ovary and testis from both the experimental and control groups were fixed in Bouin's fixative for 24 hours. After that, paraffin blocks containing the tissue were sectioned at 6 µm thickness and then stained by double staining (Haematoxylene and Eosin) method.

## 3. Results

The fish, *Clarias batrachus* is an annual breeder and it spawns during the monsoon months starting from late June to early September. The treatment of lead nitrate was given in February when the gonads were in resting phase and terminates in June when they were fully matured in the controls. Histology of treated fish was largely made up of stage-I oocytes. However, few stage II oocytes and some larger oocytes were also encountered (Plate 1a). In some cases larger oocytes showed signs of atresia. The control ovary had fully mature vitellogenic stage IV oocytes (Plate 1b). The testis of treated fish had only spermatogonial cells and spermatocytes whereas, in the control, the tubular lumen was filled with sperm. Comparatively from 3.0 ppm, in the 5.0 ppm lead exposed fish, the colour becomes darker which is more pronounced in the tail. Marginal erosion and extravasation of blood in the tail region of some was noticed after 90 days of treatment. When exposed to7.0 ppm such changes were obvious after 40 days. Table 1 shows the significant decreases of primary oocytes, GSI and ova diameter in the lead treated fish when compared to that of controls.

Histological examination of the testis following chronic exposure of the fish to lead nitrate showed a very significant decrease of the testicular diameter. The lead treated testis was completely devoid of sparmatids and spermatozoa. The area occupied by the spermatids and sperms were largely filled with amorphous masses containing dark stained nuclei and few irregular cells (Plate 2a). In the lead treated fish, living cells of vas deferens were crumpled often with intercellular spaces having irregular nuclei. The blood supply appeared more conspicuous than controls and the process of spermiogenesis was affected. Whereas, in the control fish the testis is divided into lobes and lobules separated by intralobular stromal fibres and several nest of pre spermiogenic germ cells and vast masses of spermatids and sperms were noticed. In fact, a significant area of the cross sections of the testis was occupied by the sperms that filled several tubules (Plate 2b).

**Table 1.** Effect of lead nitrate on the ovary of *Clrias batrachus.* Figures represent mean ± S.D

| Parameters | Control | Treated |
|---|---|---|
| Gonadosomatic index | 6.73 ±0.72 [a] | 2.17 ±0.01 [b] |
| Ovary diameter(um) | 8212.00 ±188.20 [a] | 1871.01±137.70 [b] |
| Oogonia | 15.00 ± 1.08 [a] | 21.00 ± 0.80 [b] |
| Primary (non-yolky) oocytes | 19.00 ±0.64 [a] | 46.00 ± 2.16 [b] |
| Primary(yolky) oocytes | 32.00 ±078 [a] | 2.00 ± 0.04 [b] |
| Mature oocytes | 41.00 ± 1.40 [a] | Absent |
| Atretic follicles | 2.00 ± 0.25 [a] | 34.00 ± 4.21 [b] |

[The different superscripts in a row are significantly different at p≤0.05] Each data is a mean of five separate determinations.

**Plate 1** a) treated ovary and b) control ovary

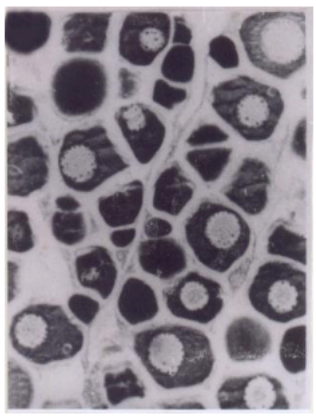

(a)

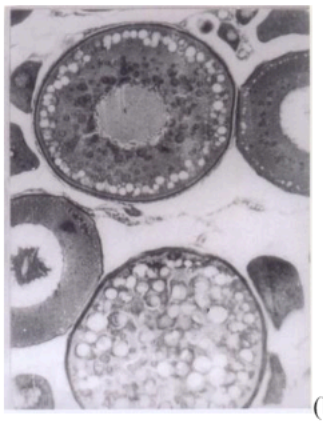

(b)

**Plate 2** a) treated testis and b) control testis

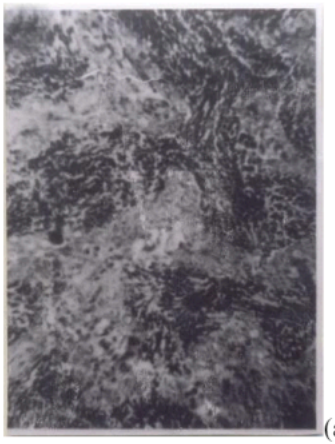
(a)

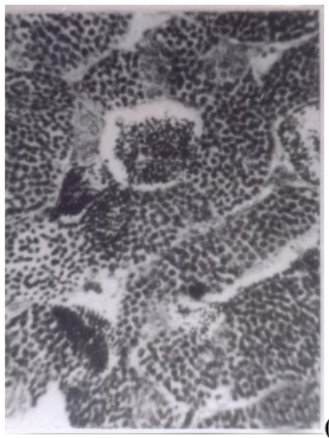
**(b)**

**Table 2.** Effect of lead nitrate on the testis of *Clarias batrachus*. Figures represent mean ± S.D.

| Parameters | Control | Treated |
|---|---|---|
| Gonadosomatic index | 0.29 ± 0.01 [a] | 0.12 ± 0.02 [b] |
| Testicular diameter (μm) | 5789.25 ± 298.60 [a] | 1369.40 ± 140.25[b] |
| Primary spermatogonia | 19.00 ± 0.56 [a] | 28.00 ± 1.65 [b] |
| Secondary spermatogonia | 22.00 ± 1.10 [a] | 35.00 ± 0.85 [b] |
| Primary spermatocytes | 32.00 ± 1.45 [a] | 71.00 ± 1.39 [b] |
| Secondary spematocytes | 77.00 ± 1.00 [a] | 13.00 ± 0.23 [b] |
| Spermatids | 90.00 ± 1.00 [a] | Absent |
| Spermatozoa | 448.00 ± 2.00 [a] | Absent |

[The different superscripts in a row are significantly different at $p \leq 0.05$]. Each data is a mean of five separate determinations.

The data recorded in Table 1 and 2 showed the mean value of variation in GSI, gonadal diameter, differential count and cytomorphology of germinal cells in the ovary and testis of both lead treated and control fish which are statistically quite significant. Gonadal development and maturation are intimately correlated with GSI. In present investigation, GSI of control groups were higher than treated groups and in case of treated groups gonadal development was also affected. So, it showed that the reduction of GSI was directly correlated with gonad maturity.

Upto 90 days of experiment, the mortality rate was nil. After 150 days, in case of both the control and treated fishes with first dose of Lead Nitrate (3.0 ppm) there was no mortality observed (Fig 1). But fishes with next two doses that were 5.0ppm and 7.0 ppm, there observed 2% and 6% mortality respectively due to prolong treatment of Lead Nitrate (Table 3).

**Table 3.** The mortality percentage after 150 days of both control and treated fish

| Group | Doses | Mortality % |
|---|---|---|
| Control | | NIL |
| Treated | 3 ppm | NIL |
| | 5 ppm | 2% |
| | 7 ppm | 6% |

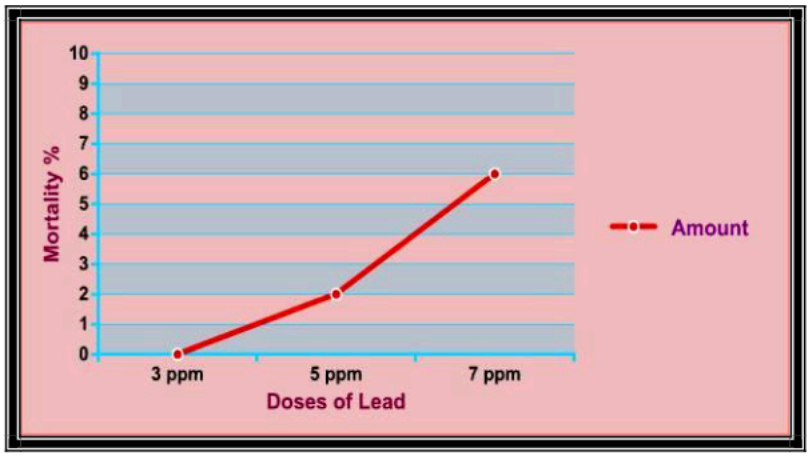


**Fig 1** Mortality percentage of *Clarias batrachus* (L.) in different doses of Lead nitrate treatment

## 4. Discussion

All measured effects of lead on living organisms are adverse, including those related to survival, growth, learning, reproduction, development, behavior and metabolism. Lead interferes with biochemical, physiological, morphological and behavioral parameters of fish. Lead functions as a cumulative poison. Lead is a heavy metal which is very toxic to aquatic organisms, especially fish. Various experiments were conducted about the toxicity of heavy metals with fresh water fish but little work has been done about the effects of Lead (Pb) in the sub lethal concentration on the gonadal development of fresh water fish. As reported in mammals including man (Vallee and Ulmar 1972) and in a few fish, changes in the activities of some enzymes were reported in response to exposure to sub lethal level of Lead. According to Tulasi et al. (1989) accumulation studies indicated that lead accumulated in the brain of *Anabas testudineus*, probably changing specific gonadal functions, resulting in an altered reproductive potential. They also found that the exposure of lead hastened the spawning of *A. testudineus*, possibly due to elevated corticosteriod levels. James et al. (1996) reported the effects of lead on respiratory enzyme activity, glycogen and blood sugar levels of the teleost, *Oreochromis mossambicus* (Peters) during accumulation and depuration. Olaifa et al. (2003) studied the toxic effect of lead on *Clarias gariepinus* (African catfish) fingerlings.

The toxic stress of lead on fish was tested employing a 96-hour bioassay test. The experimental fish used were *Clarias gariepinus* fingerlings. Lead in the form of lead chloride was used to prepare the stock solution. The concentrations of lead used for the experiment were 0, 1.8, 3.2, and 5.6, and 10.0mgl$^{-1}$. Kasthuri and Chandran (1997) studied the sublethal effect of Lead on feeding energetics, growth performance, biochemical composition and accumulation of the estuarine catfish, *Mystus gulio* (Hamilton). Lead has to decreasing trend in feeding energetics, growth rate and biochemical composition when compared to their respective controls. Of the three size groups, fingerlings seemed to be more sensitive to lead poisoning followed by the immature and then by the mature fish.

In the recent investigation with *Clarias batrachus*, Lead caused degenerative changes in the both gonads. In the control ovary, matured vitellogenic Stage IV oocytes were found whereas, in case of treated fish mainly Stage I and few Stage II oocytes were encountered. The testis of treated fish had only spermatogonial cells and spermatocytes but in the control fish, mature sperms were seen. Thus the present study reveals that long term exposure to lead caused retardation of gonadal growth, reducing gonadosomatic index which was directly related with reduced gonad weight and reduction of mature oocytes and sperms.

## 4. Conclusion

The present study revealed the severe adverse impacts of Lead nitrate on gonadal development of *Clarias batrachus* along with biochemical alterations.

### References

Alados CL, Daniel NW (1999) Lead effects on the predictability of reproductive behavior in fathead minnows (*Pimephales promelas*). Environmental Toxicology and Chemistry. 18 (10) **:** 2392–2399.

Bhakta JN, Munekage Y, Ohnishi K, Jana BB (2012) Isolation and identification of cadmium and lead resistant lactic acid bacteria for applying as metal removing probiotic. International Journal of Environmental Science and Technology 9:433–440.

Bhakta JN, Ohnishi K, Munekage Y, Iwasaki K, Wei M (2012) Characterization of lactic acid bacteria-based probiotics as heavy metals sorbents. Journal of Applied Microbiology 112:1193–1206.

Choudhury H, Mudipalli A (2008) Potential considerations andconcerns in the risk characterization for the interaction profiles of metals. Indian J Med Res 128:462–483.

Directive 2000/60/EC (2000) Water Framework Directive of theEuropean Parliament and of the Council of 23 Oct 2000

James R, Sampath K and Alagrathinam S (1996) Effects of lead on respiratory enzyme activity, glycogen and blood sugar levels of the teleost, *Oreochromis mossambicus* (Peters) during accumulation and depuration. Asian Fish. Sc. 9(2): 87–100.

Kasthuri J and Chandran MR (1997) : Sublethal effect of lead on feeding energetics, growth performance, biochemical composition and accumulation of the estuarine catfish, *Mystus gulio* (Hamilton). J Environ Bio, 18(1): 95–101.

Olaifa FE, Olaifa AK, Lewis OO (2003) Toxic stress of Lead on *Clarias gariepinus* (African catfish) fingerlings. African Journal of Biomedical Research 6(2).

Roberts JR (1999) Metal toxicity in children. In: training manual on pediatric environmental health: putting it into practice. Emeryville, CA, Children's Environmental Health Network. http://www.cehn.org/cehn/training manual/(pdf/manual-full.pdf).

Ruby SM, Jaroslawski P, Hull R (1993) Lead and cyanide toxicity in sexually maturing rainbow trout, *Oncorhynchus mykiss* during spermatogenesis. Aquat. Toxicol. 26(3-4): 225–238.

Tulasi SJ, Reddy PUM, Ramano Rao J.V (1989) Effects of lead on the spawning potential of the fresh water Fish, *Anabas testudineus*. Bull. Environ.Contam. Toxicol. 43: 8–863.

Vallee BL, Ulmer DD (1972) Biochemical effects of mercury, cadmium and lead. Ann. Rev. Biochem 4: 91–128.

International Journal of Advances in Engineering and Management (IJAEM)
Volume 4, Issue 6 June 2022, pp: 1235-1241 www.ijaem.net ISSN: 2395-5252

# Skin Bioprinting: An Innovative Technology Forskin Reconstruction

Nilanjana Bhattacharyya Nath,Meghali Sen Majumder and Ena Kundu

*Swami Vivekananda Institute of Modern Science. Department of Biotechnology, Sonarpur, Kolkata-103, West Bengal, India.*

Submitted: 05-06-2022 Revised: 17-06-2022 Accepted: 20-06-2022

**ABSTRACT**
3D bioprinting is an advanced technology that can easily create skin grafts for the patient by using different biomaterials and cells in less time and cost. 3D bioprinting can fabricate skin tissue which can help to reconstruct skin in severe skin disease and burn patients. This technology improves the production process of the covering skin that covers the entire burn bound. With the help of this technology, scientists can create skin transplants of specific shape and size as per patient's requirement and which is also suitable for the patient's injury.
**Keyward:** 3D bioprinting, skin grafting, reconstruction of skin

## I. INTRODUCTION

The largest and complicated organ of human body is skin. Skin is the outermostcovering of human body which protects the muscles, ligaments and variousinternal organs. Skin acts as the first line of defense hence, any injury firstattacks the outermost layer of the body. So, various regeneration methods ofskin tissue is necessary. Day by day need for organ donors are increasing.
Using3Dbioprintingregenerationoforgansandtissues arepossibleinthelaboratory (Ai L & L. Weng,2013). Skin wounds are common which may result from trauma, skin diseases, burn or removal of skin during surgery (Coyer et al., 2015). Nowadays, skin injuries due to burns is a verycommoncase.Even minor defects bring psychological distress on the affected individuals. There are several options of skin tissue engineering such as autografts, allografts, xenografts etc. Though each technique has some demerits like creation of secondary wounds, risk of immune reactions etc. Everyyear,around11millionpeopleneedmedicalhelp. Theburninjuries are life-long ache whose survival rates are high among the patients (M. Bacakova&Musilkova J, Riedel T et al., 2016). In this regard, tissue engineering holds great promises for improving the treatment of skin defectsand it is a viable method in the tissue and organ reconstruction (J. B. Jank et al., 2017). Tissue-engineered skin (TES) is mainly composed of biomaterials, cells, and bioactive factors. It can completely cover skin wounds, accelerating wound healing and promoting the vascularization of dermal substitutes. However, there are also many limitations such as non-pigmented skin, insufficient elasticity of dermis, long-term postoperative scars, and loss of skin appendages etc. (T. Weng et al., 2021). Therefore, these limitations of TES have been resolved by the development of three-dimensional (3D) printing technology with its accuracy and high resolution.

Bioprinting is a process where biomaterials are used to create tissue likestructures which looks similar to the original tissue. 3D bioprinting is a type of Additive Manufacturing (AM) technology that becomes widely used in the medical sector for reconstruction of the burn injuries with the help of computer-aided design (CAD) model inputs.This technology helps to create better skin grafts which is also cost effective (P. He et al. & P. Rider et al., 2018). Inkjet 3D printing and laser assist 3D printing is used commonly. In future, this technology can create 3D tissue-engineered structures that can rectify the defect in a patient-specific organ (Md. Javaid & A. Haleem, 2021). Though it involves somerisks such as developing cancer, teratoma etc. Bioink is used to create thesestructureslayerbylayer (L. Bai, D. D. Ginty& A. Zimmerman, 2014).Inbioprinting,mostlyuseoflivingcellsareencouragedwhereasin3Dbioprintingmostlyplasticisusedtomakethemodels. Three dimensional bioprinting works on the principle of deposition ofbiomaterials

International Journal of Advances in Engineering and Management (IJAEM)
Volume 4, Issue 6 June 2022, pp: 1235-1241 www.ijaem.net ISSN: 2395-5252

layer by layer in the infected area (H. Bien, C.Y. Chung & X. Zong,2005). 3D bioprinting is used to develop complicatedorgansandtissueswhichlooksverysimilartotheoriginalorgansandtissues (A. Chaudhari et al.,2017).
The3basicstepsof3Dbioprintinginvolves(C.M. Chuong et al.,2012):

- Pre-printinginvolvesimagingofthetargettissue,
- developmentwithCAD/CAMsoftwaresandselectinga biomaterial
- Post-printinginvolvesmaturationand implantationoftissues

Within 5-7 years,the bioprinting market will increase by 15.7% and by 2025 it will cross $4.70billion. With the advent of skin bioprinting it will mark the end of the testing ofdrugs on animals (3). It is a promising technique with the aim to produce 3Dtissues or organs. Skin bioprinting involves the replacement of skin injury with skinsubstitutesbytheprocessofreconstruction.

## II. SKIN BIOPRINTING – AN UNORTHODOX APPROACH

Overtheformerdecennium,therehasbeenan outstandingadvancement towards the evolution of substitutes which are in vitro-engineered. These invitro-engineered substitutes help to imitate human skin. It either acts as an aidto grafts for the substituting lost skin, or for the initiating in vitro model.Anewanduniqueplanofactionhasevolvedknownastissueengineering.Thishasprogressedbyutilizingthecontemporaryadvancesin diverse areas. These fields of action include stem cell research, bioengineering,polymer engineering and nano medicine. Lately, a growth in the area of 3Dprinting technology and its advancements are being used for a larger benefit.This is popularly known as bio printing. This helps to formulate cell loadedscaffoldswhichinturnfabricatesmaterialsmore complimentarytotheoriginal,indigenous tissue. Bio printing works on smoothening out the process of theconcurrent and highly unequivocal skin cells deposition of multiple types andbiomaterials.Thisisaprocedurewhichrequiresadvancementtowardstraditional tissue-engineering of skin. Bio printed skin replaces or acts as acounterpart to equivalents consisting of dermal as well as epidermal elements.Suchconstituentsputforwardahopefulperspectiveinthefieldofskinbioengineering. Numerous mediums which include either naturalor syntheticbiopolymers and cells, in addition to or without adding a warning towardsmoleculessuchasgrowthelementswhichareb eingavailedtoassembleeffective skin constructs. This applied science makes an impressive appearanceas a fresh and unique policy plan to prevail over the topical constrictions in theengineeringofskintissuesuchasestablishmentofs weatglands,weakvascularization, andnon-appearanceofhairfollicles.

**Advantages**

- Growth components, extracellular matrix as well as units which are epidermal can be easily located in the necessary places which makes them extremely reproductive.
- Affability, extensibility, inflated yield and improved plasticity.
- We can mark and reprint the matrix of blood vessels to make it much more remarkable for an extended endurance of the operation.

**Disadvantages**

- The cost is very much high. It needs expensive biological printers and manpower.
- Bio printing technology has not yet developed enough. Bio printed skin constructs may originate some security complications, more so, if it is applied straight away to clinical implementation.

## III. WOUND HEALING AND BIOPRINTING

Skin is a complicated and most sensitive part of our body hence, if there is any wound or burn injury we need to treat it immediately. Skin bioprinting treatment by darning of wounds diminishes gap. But it is difficult to treat a patient with extensive burns. With age skin tends to become thin and sensitive. Hence, wound healing becomes a tough job. Skin biotechnology is one of the promising technique which involves the use of it in various medicinal lines such as growth of tissues and cells in laboratory etc. Skin bioprinting helps in the treatment of wounds by darning wounds and alleviating, lessen the chance of contamination, reduce blemishes, upgrade cosmetic consequences etc.

There are different kinds of bioprinting technologies. Among them four of which are widely used at present: Inkjet-based printing, Extrusion-based printing, Laser-assisted printing and DLP-based printing—dynamic optical projection stereolithography (DOPsL).

There are two basic styles for skin bioprinting - In vitro and in situ bioprinting.L.

International Journal of Advances in Engineering and Management (IJAEM)
Volume 4, Issue 6 June 2022, pp: 1235-1241 www.ijaem.net ISSN: 2395-5252

Koch et al., (2012) reported that 20 layers of fibroblasts (murine NIH-3 T3) and 20 layers of keratinocytes (human immortalizedHaCaT) embedded in collagen were printed by a Laser-assisted BioPrinter to generate simple 3D skin which is similar with dermis and epidermis (Fig. 2). In 2013, V. Lee et al. demonstrated that the 3D Printed skin samples on collagen layers retained their form and shape, whereas manually deposited structures shrank and became concave shapes. Separately Michael et al. (2013) demonstrated that bi-layered constructs formed dermis and epidermis. After 11 days of transplantation, some blood vessels from the wound bed could be observed.

In case of in situ bioprinting, amniotic fluid-derived stem cells (AFSCs) and bone marrow-derived mesenchymal stem cells (MSCs) were suspended in fibrin-collagen gel, mixed with the thrombin solution and then printed onto the wound site. The bioprinter was used to deposit two layers of a fibrin-collagen gel by depositing a layer of thrombin, a layer of fibrinogen/collagen, a second layer of thrombin, a second layer of fibrinogen/collagen, and a final layer of thrombin.

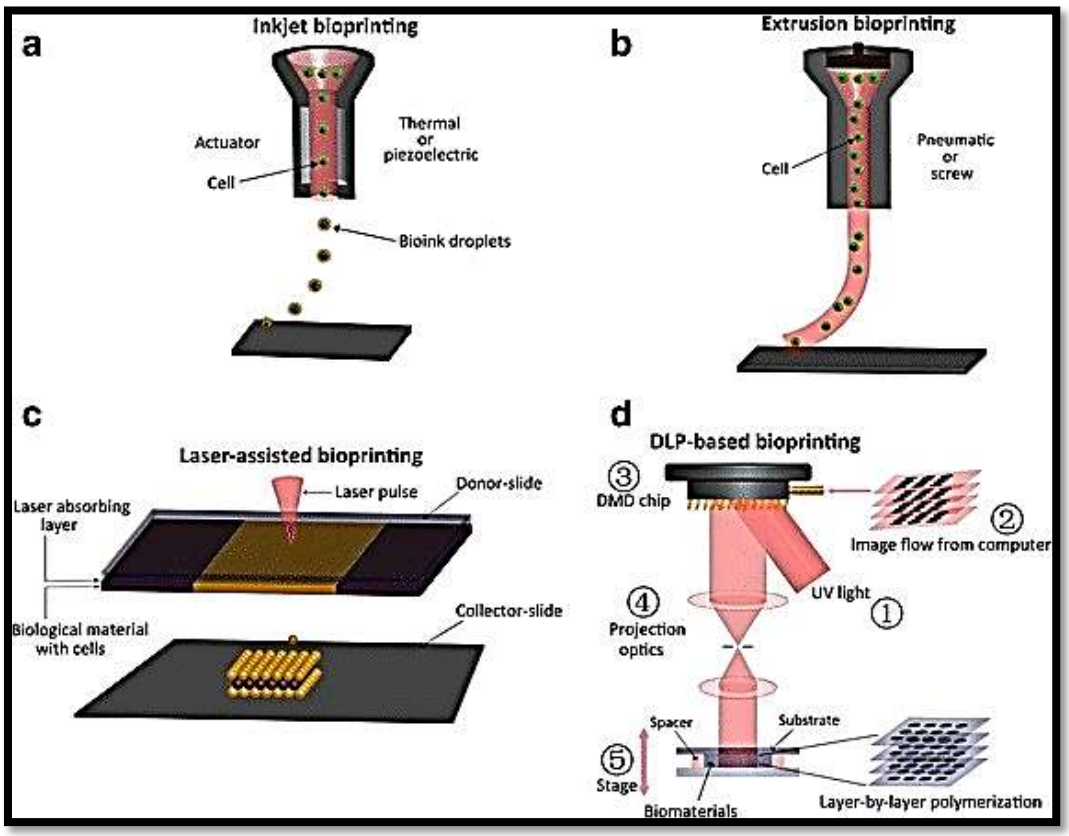


**Fig1:**Bioprinting techniques. **a.** Inkjet bioprinter eject small droplets of cells and hydrogel sequentially to build up tissues. **b.** Extrusion bioprinter use pneumatics or manual force to continuously extrude a liquid cell–hydrogel solution. **c.** Sketch of the laser printer setup. **d.** Schematic of the DLP based bioprinter—dynamic optical projection stereolithography (DOPsL).

(**Picture curtsy:** P. He, J. Zhao, J. Zhang, B. Li, Z. Gou, M. Gou, X. Li Bioprinting of skin constructs for wound healing.Burns Trauma, 6 (2018), p. 5)

International Journal of Advances in Engineering and Management (IJAEM)
Volume 4, Issue 6 June 2022, pp: 1235-1241 www.ijaem.net ISSN: 2395-5252

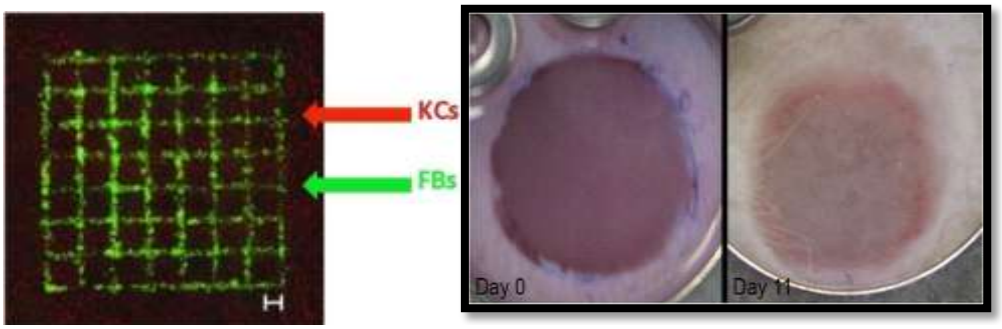


**(a) (b)**

**Fig2:**In vitro bioprinting.

**a.**Fibroblasts (green) and keratinocytes (red) was printed by the laser printing technique.
(**Picture curtsy:** Koch L, Deiwick A, Schlie S, Michael S, Gruene M, Coger V, et al. Skin tissue generation by laser cell printing. BiotechnolBioeng. 2012; 109(7):1855–1863. doi: 10.1002/bit.24455.).
**b.**Skin construct inserted into the wound directly after the implantation (day 0) and on day 11.
(**Picture curtsy:** Michael S, Sorg H, Peck CT, Koch L, Deiwick A, Chichkov B, et al. Tissue engineered skin substitutes created by laser-assisted bioprinting form skin-like structures in the dorsal skin fold chamber in mice. PLoS One. 2013; 8(3):e57741.)

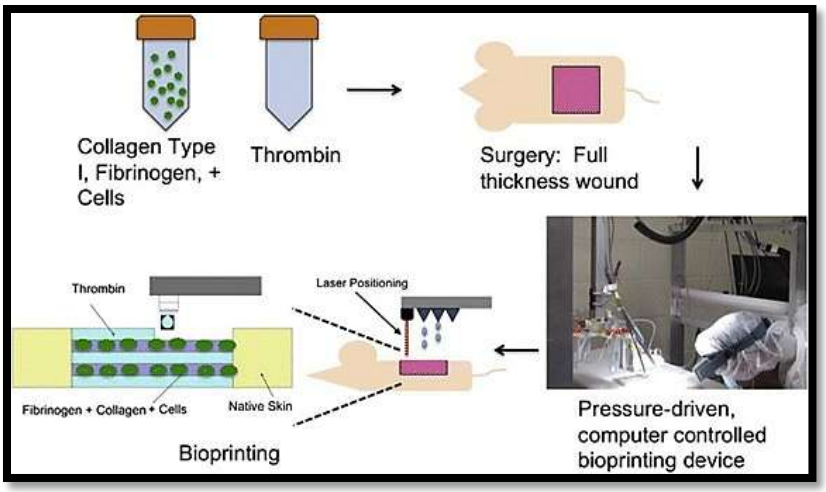


**Fig3:**In situ bioprinting.

(**Picture curtsy:** Skardal A, Mack D, Kapetanovic E, Atala A, Jackson JD, Yoo J, et al. Bioprinted amniotic fluid-derived stem cells accelerate healing of large skin wounds. Stem Cells Transl Med. 2012; 1(11):792.)

## IV. BIOINK & CREATING BIOINK

The bioinks are the most important ingredient for 3D bioprinting. It is used forthe development and regeneration of various organs and tissues. An ideal bioink should have few physicochemical properties, such as proper mechanical, rheological, chemical, and biological characteristics. Itisamixtureofcells, biomaterials,growthfactorsandnutrients.In3Dbiopri ntingmainlytwotypesofbioinkbiomaterialsareused:

**Natural biomaterials used as bioink**

Hydrogels-based bioinks are biocompatible and typically biodegradable. Hydrogel biomaterials include alginate, gelatin, collagen, fibrin/fibrinogen, gellan gum, hyaluronic acid (HA), agarose, chitosan, silk, decellularized extracellular matrix (dECM), poly(ethylene glycol) (PEG), and Pluronic. As collagen is the main structural protein in the extracellular matrix (ECM) of mammalian cells, several scientists used collagen as bioink.Gelatin is one of the most widely used natural polymers for its thermo sensitivity and ability to form a hydrogel at lower

International Journal of Advances in Engineering and Management (IJAEM)
Volume 4, Issue 6 June 2022, pp: 1235-1241 www.ijaem.net ISSN: 2395-5252

temperatures. For bioprinting applications, gelatin has been used as a bioink and/or as a composite with other polymers.Gelatin-alginate composite bioinks also used for bioprinting (T. Zhang et al., 2013). Alginate was also widely used as a bioink in the LaBP method. In tissue engineering, fibrinogen and fibrin are mainly used to construct functional tissue for the replacement of damaged tissues for wound healing. They are biocompatible, biodegradable, non-immunogenicand they also induce cell attachment, proliferation, and ECM formation (T. Rajangam, 2013, X. Cue & T. Boland, 2009). Silk is a naturaI Polymer and it has long been utilized as a scaffoIding material for both soft and hard tissue engineering applications.Gellan gum is an anionic polysaccharide produced by bacteria. Like alginate, it forms a hydrogel at low temperatures when blended with monovalent or divalent cations (AH Bacelar et al., 2016). Dextran and agarose are natural polysaccharide that has been widely used in tissue engineering applications

**Synthetic biomaterials used as bioink**

PEG is a synthetic polymer synthesized by polymerization of ethylene oxide which faciIitate the bioprinting processes. PEG with reactive groups (PEGX) is a valuable tool to modify the bioink's properties and to increase the bioink options. Pluronic is a type of poloxamer which has good printability and temperature-responsive gelation. Due to these properties, it is well-suited for use in bioinks (C. C. Chang et al., 2011).

There are a few commerciaI biomaterials that have been recentIy introduced such as Dermamatrix, NovoGeI, CELLINK etc. Recently nanomaterials [e.g. silver nanoparticles (AgNPs), gold nanorods (AuNRs)]have been used for producing conductive bioinks (P. S. G. Ozkerim et al., 2018).

## V. CHALLENGES

An updated applied science becoming more and more evident for assemblingartificialskin is the 3D bio printing mechanization. Nevertheless, there still existsomeremarkabletechnologicaldisputesintheoccurrenceofbio-mimeticpracticalskin forclinicalimplementation.

A single question which is majorly looked out on skin bio printing is the one ofbio ink. The fundamental units of original, local skin are the quantity-seedingunits. In spite of the recent up gradation in cell culture methodology for givingrise to cells for bio printing, concerns are still present as to whether there areadequate units which can very well be created willingly for bio printing of skinestablishmentforclinicalutilization.Thepotentialityofcellsresentduringtoday's recent times, could be sustained in biological substances, but suchmediums have the need of bio-elasticity of the raw and original skin. Thesemediums which are acceptable, not only for 3D scaffold impression but also forseeding units. These also include the electrophysiology of the nude skin whichacts in a much better way for skin bio printing. Hence, developments of all thefacts and figures used to engrave scaffolds have become a crucial provocationforfutureanalysis.

## VI. APPLICATION

Bio printing necessitates the application of 3D printing mechanism to formepithelial tissues as well as organs. This operation has been tested and tried ondiverse research spheres incorporating transplantation, grafting and clinics, useofprogenitorcellstoproducetissuessynonymously appliedtothetermregenerative medicine, research on carcinoma, drug testing along with drugscreening and (HTS) high-throughput screening enabling the testing of largenumbersof chemicalsubstancesforactivityindiverseareas ofbiology.

## VII. FUTURE

Inthenearfuture,theappliedsciencebasedon 3Dbioprintingcouldextendanaspiration amongst people. At present, these people count on donor organs.Falseorgansprintedbyavailingbioinkcreatedfromcellsbelongingtoapatienthimselfcouldabolishtherequirementofatransplantaltogether.Thiscouldalsodoawaywiththerequirementfororgandonorsandbringingdowntheprobablethreatoftransplantrejection.Crucialevolutionintheoperationoftissueswhich are 3D bio printed could be expected for the following 10–15 years. To beginwith, this works by concentrating on simple, uninvolved prototype tissues fordrug screening and cosmetic testing. This operation is backed by an expandingnumber of experiments on animals and clinical investigation of 3D bio printedmuscle or epithelial tissue in the coming 10 years.We can expect a great dealofexcitingpossibilitiesintheupcomingtransplantationprocedures.Someofthemore updated possibilities comprises of the transfer of a vascularized humanbody part containing multiple tissue types (such as skin, muscle, bone, nervesand blood vessels), conventions authorized the fortunate deprecation or evencessation of amantadine or immunosuppressant drugs, and the application ofbody's raw materials for organ restoration. Availing the facilities of bio printingwill qualify the integration of different

International Journal of Advances in Engineering and Management (IJAEM)
Volume 4, Issue 6 June 2022, pp: 1235-1241 www.ijaem.net ISSN: 2395-5252

varieties of cells in the membrane whichincludes foramen (sweat) and oleaginous or sebaceous glands as well as hairfollicles. This in turn will sanction the renewal of Keratinocytes or in a simplerlanguage,ourskintissue,withtheformationan dcellularconstructionbearingaresemblancetothenati veorindigenous tissue.

## VIII. CONCLUSION

Thetechnologywhichhasmadeanimmensei mpactbecauseofitshugecapability to make a smoother fabrication of anatomical and body relevanttissue as well as qualifying improved, more compatible practical solutions incases of burn patients is none other than the skin bio printing technology. Theapplication of bio printing in cases of skin restoration after burns is definitelypromising. Bio printing authorizes an error-free placement of the innumerableoriginalskincellclassificationswithallmi nutedetails.Italsoenablesmanufacturing clonable constructs to restore bruised or damaged skin. Theapplicationof3Dbioprintingforrelievingmutilati onmakessuchhealingsmuchfaster, which is analytical in cases of large-scale, serious damage caused due toburning.Anadvancedandinitialmediationwilllesse nthepossibilitiesforsepticemia and provide lesser scarring, secured and speedy healing, as well asmuch superior cosmetic after-effects. This will also come up with a decrease inthequantityofsurgeriesessentiallyneededandthelon gdurationforwhichthepatients require to stay behind in the hospital. To make clinical translationsuccessfully possible by taking advantage of the benefit of bio printing forwound restoration, the damaged product evolved needs to be uncomplicated.The injury should also be able to integrate in an uninterrupted manner into thesurgicalprocedureandtheoperativeactivity.Morea dditionalprogressinterm of occurrence of clinical grade 3D bio printers in a systematized approach andbiocompatible or microporous bio inks will allow broader utilization of thistechnology in surgery. Universally, these all-inclusive facts help us to comprehend that 3D bio printingis an extremely life-changing technology, and its application for reformation ofwoundwillactasarevolutionaryaswellasfundament alchangeinconsequencesofallpatients.

## REFERENCES

[1]. A. H. Bacelar, Silva-Correia J, Oliveira JM and Reis RL, J. Mater. Chem. B(2016): 4, 6164–6174. [Google Scholar]
[2]. A. Chaudhari et al. (2017): Advances in skin regeneration using tissue engineering. Int J MolSci; 18: 789.
[3]. A. M. Hocking, Honari S, Thompson C.M et al. (2013): Genetic risk factors for hypertrophic scar development. J Burn Care Res; 34: 477–482.
[4]. A. Zimmerman, Bai, L, Ginty, D. D. (2014): The gentle touch receptors of mammalian skin. Science; 346: 950–954.
[5]. A. Skardal, Mack D, Kapetanovic E, Atala A, Jackson JD, Yoo J, et al. (2012):Bioprinted amniotic fluid-derived stem cells accelerate healing of large skin wounds. Stem Cells Transl Med;1(11):792. doi: 10.5966/sctm.2012-0088. [PMC free article] [PubMed] [CrossRef] [Google Scholar]
[6]. B. J. Jank, Goverman J, Guyette JP, et al. (2017): Creation of a bioengineered skin flap scaffold with a perfusable vascular pedicle. Tissue Eng Part A;23: 696–707.
[7]. C.M. Chuong, Randall VA, Widelitz RB, et al. (2012): Physiological regeneration of skin appendages and implications for regenerative medicine. Physiology; 27: 61–72.
[8]. C. Kleinhans, Kluger P. J., Novosel E. C. (2011): Vascularization is the key challenge in tissue engineering. Adv Drug Deliv Rev; 63: 300–311.
[9]. C. M. Thompson, Hocking, AM, Honari, S, et al. (2013): Genetic risk factors for hypertrophic scar development. J Burn Care Res; 34: 477–482.
[10]. C. C. Chang, Boland ED, Williams S. K and Hoying J. B, J. Biomed. Mater. Res., Part B,(2011):98, 160–170. [PMC free article] [PubMed] [Google Scholar]
[11]. E. C. Novosel, Kleinhans, C, Kluger, P. J. (2011): Vascularization is the key challenge in tissue engineering. Adv Drug Deliv Rev; 63: 300–311.
[12]. E. V. Badiavas, Maranda E.L, Rodriguez-Menocal L, Badiavas, E. V. (2017): Role of mesenchymal stem cells in dermal repair in burns and diabetic wounds. Curr Stem Cell Res Ther; 12: 61–70.
[13]. F. Groeber, Hampel M,Holeiter M et al. (2011): Skin tissue engineering—in vivo and in vitro applications. Adv Drug Deliv Rev; 63: 352–366.
[14]. F. Coyer, Gardner A, Doubrovsky A, et al. (2015): Reducing pressure injuries in critically ill patients by using a patient skin integrity care bundle (inspire) Am J Crit Care; 24:199–209.

[15]. G. S. Liu, Yan, X, Yan, F. F et al. (2018): In situ electrospinning iodine-based fibrous meshes for antibacterial wound dressing. Nanoscale Res Lett; 13: 309.
[16]. H. Bien, Chung C.Y, Zong X, et al. (2005): Electrospun fine-textured scaffolds for heart tissue constructs. Biomaterials; 26: 5330–5338.
[17]. J.S. Miller, Paulsen S. J. (2015): Tissue vascularization through 3D printing: will technology bring us flow? Dev Dyn;244:629–40.
[18]. K. Vig, Chaudhari, A, Tripathi, S, et al., (2017): Advances in skin regeneration using tissue engineering. Int J MolSci; 18: 789.
[19]. L. Ai, Weng L. (2013): Heat shock sweat gland cells induce phenotypic transformation of human bone marrow mesenchymal stem cells. Chin J Tissue Eng Res;17: 985–991.
[20]. L. Bai, Ginty D. D, Zimmerman A. (2014): The gentle touch receptors of mammalian skin. Science; 346: 950–954.
[21]. L. Moroni, de Wijn, JR, van Blitterswijk, CA., (2006): 3D fiber-deposited scaffolds for tissue engineering: influence of pores geometry and architecture on dynamic mechanical properties. Biomaterials; 27: 974–985.
[22]. L. Koch, Deiwick A, Schlie S, Michael S, Gruene M, Coger V, et al., (2012): Skin tissue generation by laser cell printing. Biotechnol Bioeng;109(7):1855–1863. doi: 10.1002/bit.24455.
[23]. M. Bacakova, Musilkova J, Riedel T, et al. (2016): The potential applications of fibrin-coated electrospunpolylactidenanofibers in skin tissue engineering. Int J Nanomed; 11: 771–789.
[24]. M. Paulsson (1992): Basement membrane proteins: structure, assembly, and cellular interactions. Crit Rev BiochemMol Biol;27: 93–127.
[25]. M. Bacakova, Musilkova, J, Riedel, T, et al., (2016): The potential applications of fibrin-coated electrospunpolylactidenanofibers in skin tissue engineering. Int J Nanomed; 11: 771–789.
[26]. Mohd. Javaid et al., (2021): 3D bioprinting applications for the printing of skin: A brief study. Sensors International. Vol 2.
[27]. P. He, J. Zhao, J. Zhang, B. Li, Z. Gou, M. Gou, X. Li (2018): Bioprinting of skin constructs for wound healing.Burns Trauma, 6, p. 5
[28]. P. Rider, Alkildani S. KačarevićŽP, S. Retnasingh, M. Barbeck (2018): Bioprinting of tissue engineering scaffolds. J. Tissue Eng., 9.
[29]. R. H. Dong, Jia Y.X, Qin C. C. et al., (2016): In situ deposition of a personalized nanofibrous dressing via a handy electrospinning device for skin wound care. Nanoscale; 8: 3482–3488.
[30]. S. Michael, Sorg H, Peck CT, Koch L, Deiwick A, Chichkov B, et al., (2013): Tissue engineered skin substitutes created by laser-assisted bioprinting form skin-like structures in the dorsal skin fold chamber in mice. PLoS One;8(3):e57741. doi: 10.1371/journal.pone.0057741. [PMC free article] [PubMed] [CrossRef] [Google Scholar]
[31]. S. Huang, Wu C, Xu Y et al., (2010): In vitro constitution and in vivo implantation of engineered skin constructs with sweat glands. Biomaterials; 31: 5520–5525.
[32]. S. Huang, Xu, Y, Wu, C, et al., (2010): In vitro constitution and in vivo implantation of engineered skin constructs with sweat glands. Biomaterials; 31: 5520–5525.
[33]. T. Zhang, Yan K. C., Ouyang L. and Sun W., (2013): Biofabrication, 5, 045010. [PubMed] [Google Scholar]
[34]. T. Rajangamet al., (2013): Int. J. Nanomed, 8, 3641–3662. [PMC free article] [PubMed] [Google Scholar]
[35]. V. Lee, Singh G., Trasatti J. P., Bjornsson C., Xu X., Tran T. N. et al., (2013): Design and fabrication of human skin by three-dimensional bioprinting. Tissue Eng Part C Methods. 20(6):473–484. doi: 10.1089/ten.tec.2013.0335. [PMC free article] [PubMed] [CrossRef] [Google Scholar]
[36]. X. Zong, Bien, H, Chung, CY, et al., (2005):Electrospun fine-textured scaffolds for heart tissue constructs. Biomaterials; 26: 5330–5338.
[37]. X. Cui and Boland T., (2009):Biomaterials, 30, 6221–6227. [PubMed] [Google Scholar]

# Extra pulmonary manifestations in covid-19: A review on histopathological alterations.

**Nilanjana Bhattacharyya Nath[1]*, Anjali Smita[2], Abhijit Dutta[3]**

[1]Department of Biotechnology, Swami Vivekananda Institute of Modern Science, Kolkata, West Bengal, India.
[2]Department of Zoology, Nirmala College, Ranchi, Jharkhand, India.
[3]Department of Zoology, Ranchi University, Ranchi, Jharkhand, India.

## Abstract

**COVID-19 is a major health issue, responsible for more than three million deaths worldwide as of June 2021. COVID-19 is most well-known for causing acute respiratory pathology, but it can also result in several extra pulmonary manifestations. In serious condition, SARS-CoV-2 causes a systemic disease, with possible cardiovascular, gastrointestinal, hepatobiliary, thrombotic, neurological, renal, dermatologic, reproductive, and psychologic manifestations. Histopathological alterations are mostly found within lungs and blood vessels. Recent investigations through full autopsy or minimally invasive autopsy of COVID-19 patients revealed that SARS-CoV-2 hijacked angiotensin converting enzyme-2 (ACE2) for entry into target cells to cause severe pathologic changes in the lungs and multiple extra pulmonary organs/tissues. To understand its morbidity, mortality and the pathogenesis, histopathological findings are essential. The histopathological features of COVID-19 significantly help therapists to improve disease treatment and outcome. So, more studies and evidence on tissue samples are required to establish the degree of involvement of other organs and tissues which are indeed affected by COVID-19. In this article, we have tried to provide comprehensive information regarding the multisystemic involvement of COVID-19 based on the evidence and experiences from the researchers worldwide.**

**Keywords**: COVID-19, ACE2, Histopathological alterations, Extra pulmonary manifestations.

## Introduction

Coronavirus disease 2019 (COVID-19) is a severe acute respiratory syndrome, caused by coronavirus-2 (SARS-CoV-2) which is zoonotic in origin and most spread through respiratory droplets and has caused a big threat to humankind [1]. First detected in December 2019 in Wuhan (China) and declared by World Health Organization (WHO) a pandemic in March 2020. Till now it presents a great challenge for the healthcare communities across the globe.

Coronaviruses envelop a single-stranded large RNA. It is a virus that infects humans as well as a wide range of animals. Their spherical morphology with a core shell and glycoprotein projections form their envelope and gives them a "crown-like" appearance; therefore, they are termed coronaviruses [2]. The genome size ranges from 27 to 32 kB, which is mostly the largest genome among all RNA viruses. Their four main structural genes encode the nucleocapsid protein (N), the spike protein (S), the small membrane protein (SM), and the membrane glycoprotein (M) [3].

The spike protein of the virus, through its Receptor Binding Domain (RBD) attaches to a human cell surface receptor Protein - Angiotensin Converting Enzyme-2 (ACE-2), encoded by the ACE2 gene, followed by its priming through auxiliary protein TMPRSS2 (trans membrane protease, serine 2). The TMPRSS2 is a cell-surface protein, expressed by epithelial cells of specific tissues including those in the aero digestive tract. ACE-2, which acts as a viral host cell entry receptor, distributed all over the organs. SARS- CoV-2 in severe cases affects entire body - the kidneys, the heart and blood vessels, the liver, the pancreas and regulates alterations in circulating lymphocytes and the immune system [4-6]. From the human protein atlas dataset [7], the maximum expression of the ACE-2 receptors is present in small intestine, duodenum, and colon, followed by kidney, testis, gall bladder, heart, thyroid gland, adipose tissue, rectum, and Lungs.

Fundamental in the pathophysiology of multi-organ injury caused by SARS-CoV-2 infection include: (i) direct virus-mediated cell damage; (ii) dysregulation of the renin–angiotensin–aldosterone system (RAAS) as a consequence of the down regulation of ACE2 related to viral entry; (iii) endothelial cell damage with subsequent inflammation and generation of a thrombotic milieu; and (iv) dysregulation of the immune response and cytokine release syndrome [8].

***Correspondence to:** Nilanjana Bhattacharyya Nath, Department of Biotechnology, Swami Vivekananda Institute of Modern Science, Kolkata, West Bengal, India, US, E-mail: nbn0305@gmail.com

***Received:** 17-Jun-2022, Manuscript No. AAPDB-22-66863; **Editor assigned:** 20-Jun-2022, PreQC No. AAPDB-22-66863(PQ); **Reviewed:** 27-Jun-2022, QC No. AAPDB-22-66863; **Published:** 05-Jul-2022, DOI: 10.35841/aapdb-6.4.116*

***Citation:** Nath NB, Smita A, Dutta A. Extra pulmonary manifestations in covid-19: A review on histopathological alterations. J Pathol Dis Biol. 2022;6(4):116*

Primarily identified as a typical pneumonia known as COVID pneumonia, it has developed into severe acute respiratory distress syndrome (ARDS), a multi-organ dysfunction with associated fatality. Other extra pulmonary conditions include thrombotic complications, myocardial dysfunction and arrhythmia, acute coronary syndromes, acute kidney injury, gastrointestinal symptoms, hepatocellular injury, hyperglycemia and ketosis, neurologic illnesses, ocular symptoms, and dermatologic complications [8].

The aim of this review is to describe the main histopathological alterations and the immunopathological mechanisms underlying COVID-19, with particular attention to extra pulmonary manifestations.

## Pathophysiology

SARS-CoV-1 and SARS-CoV-2 have the same mechanism of action; both can cause rapid production of multiple cytokines in body fluids following infection, leading to acute respiratory distress and multiple organ failure. This is the main reason most COVID-19 patients have mild symptoms at the onset of the disease, while conditions of a few affected patients are suddenly worsened after being diagnosed in hospital. This severity may be related to the excessive production of cytokines after the disease, leading to 'cytokine storm' in the body. The association of viral infection with any comorbidity such as hypertension, diabetes and renal failure has shown more serious form of clinical presentations such as respiratory failure to multiple organ failure [9]. Post-mortem studies have shown pulmonary, renal, and small vessel injury with particles resembling virus observed in the kidney by electron microscopy [10-12]. Benjamin T Bradley done post- mortem examinations on fourteen people who died with COVID-19 at the King County Medical Examiner's Office (Seattle, WA, USA) and Snohomish County Medical Examiner's Office (Everett, WA, USA) in negative-pressure isolation suites during February and March 2020. Tissue examination done by light microscopy, immunohistochemistry, electron microscopy, and quantitative RT-PCR. Coronavirus-like particles were detected in the respiratory system, kidney, and gastrointestinal tract. Lymphocytic myocarditis was observed in one patient with viral RNA detected in the tissue. All patients were median aged (range 42–84) with different comorbidities (hypertension, chronic kidney disease, obstructive sleep apnea and metabolic disease including diabetes and obesity). The pathological findings identified in the COVID-19 suggested that SARS-CoV-2 can widely spread in the epithelial lining of the respiratory tract, digestive tract, distal convoluted tubules of the kidney, the sweat glands of the skin and testicular epithelium including spermatogonia and Sertoli cells [13]. SARS-CoV-2 can bind angiotensin converting enzymes 2 (ACE2) receptors, expressed in multiple extra pulmonary tissues and this can lead to a direct viral tissue damage [8,14,15].

### *Histopathological findings in liver*

COVID-19 primarily causes pulmonary injury, but has been implicated to cause hepatic injury, both by serum markers and histologic evaluation. ACE2 expressed highly in the endothelial layer of small blood vessels, but not in the sinusoidal endothelium. ACE2 cell surface receptor was expressed highly in cholangiocytes (59.7%) than hepatocytes (2.6%) [16]. The level of ACE2 in cholangiocytes was like that in type 2 alveolar cells of the lungs suggesting that the liver could be another potential target for viral RNA.

Xu first reported the post-mortem findings of a COVID-19 patient and stated micro vesicular steatosis and mild inflammatory infiltrates in the hepatic lobule and portal tract. Stephen studied histology of liver of forty patients who died of complications of COVID-19 [17]. Infected patients showed elevated level of hepatic enzymes, such as alanine aminotransferase (ALT) and aspartate aminotransferase (AST). Macro vesicular steatosis was detected in thirty patients (75%). Mild lobular necro inflammation and portal inflammation were present in twenty cases each (50%). Tian reported the post-mortem liver biopsies in four patients with COVID-19 showing mild sinusoidal dilatation and focal macro vesicular steatosis [11]. There was mild lobular lymphocytic infiltration, which was not the normal feature of portal areas (Figure 1). Viral RNA was isolated from liver tissue in one of the patients through RT- PCR. Histopathological examinations showed hepatocyte degeneration with lobular focal necrosis, congestion of hepatic sinuses with microthrombus, fibrosis of portal tract, proliferation of portal vein branches, and mononuclear leukocyte and neutrophil infiltration within the portal area [18,19]. Sonzogni also found alteration of vascular structure, both acute (thrombosis, luminal ectasia) and chronic (fibrous thickening of vascular wall or phlebosclerosis, and abnormal asset of portal intrahepatic system) [20]. They observed typical arrangement of intrahepatic blood vessels with CD34 staining, decorating a Periportal network of sinusoidal vessels, which may show increased arterial pressure.

Though autopsies had limitations, death may occur long interval after the acute liver injury and the histological changes. At the time of the acute injury, it would be important to perform a liver biopsy for better histopathological study. However, liver biopsies are not performed in COVID-19 patients. Fiel presented the report of two liver biopsies of COVID 19 patients without pulmonary injury [21]. The first one was a 63-year- old post–liver transplant patient with different comorbidities (chronic renal failure, hypertension, and diabetes) reported following manifestations:- abnormal liver enzymes (alanine aminotransferase level - 1761 U/L, bilirubin, and an alkaline phosphatase level-1568 U/L). Significant bile duct injury was also identified. The second patient was a 36-year-old woman without other known comorbidities developed high aminotransferase levels and jaundice. Biopsy performed after one week of hospital admission showed histopathological findings like the first patient, with acute hepatitis and prominent bile duct injury. Though researchers suggested that COVID is responsible for the association of viral infection and biochemical liver injury and the histologic findings of acute hepatitis and bile duct injury.

### *Histopathological findings in gastrointestinal tract*

Common gastrointestinal symptoms of COVID-19 positive patients reported were diarrhea, anorexia, nausea, vomiting,

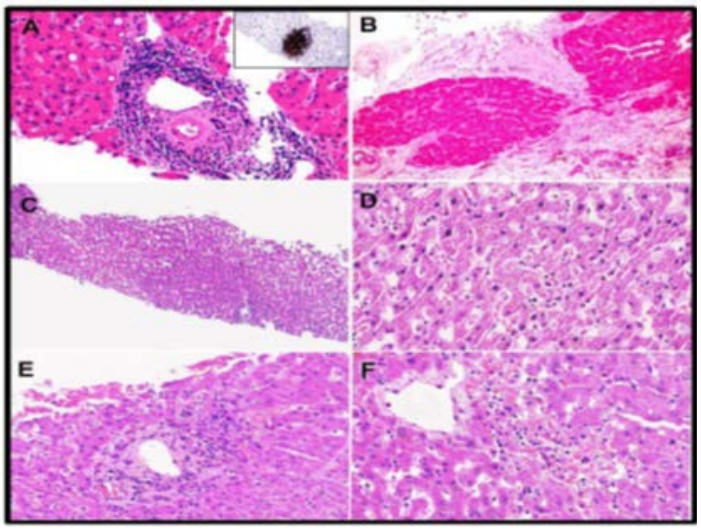


***Figure 1.*** *Histopathological changes in Liver of COVID-19 patients.*

*(A) Hepatocytes showing glycogenated nuclei and atypical small lymphocytes densely infiltrating the area of portal triad and showing CD20 positivity (inset). Dense portal infiltration.* by atypical small lymphocytes (inset: CD20 Immunostaining) and focal glycogenated nuclei in hepatocytes have also been observed.

*(B) Hepatic nodules showing fibrosis, indicative of cirrhosis. Cirrhotic nodules with thick fibrosis.*

*(C) Hepatic sinusoids are dilated and filled with lymphocytes. Mild sinusoidal dilatation with increased lymphocytic infiltration.*

*(D) High power view showing sinusoidal lymphocytes.*

*(E, F) Periportal and centrilobular areas show necrosis, indicative of injury.*

abdominal pain, and gastrointestinal bleeding during the onset and after hospitalization [18]. Microscopically, the gastrointestinal tract may show epithelial damage, endothelitis and ischemic enterocolitis [21,22]. There is few evidence of stenosis of the small intestine. Gastric tissue may show epithelial degeneration, necrosis and shedding of the mucosa with the presence of dilated and congested small blood vessels in lamina propria and sub mucosa. Endocrine pancreas may show evidence of tissue degradation [23].

The lower GI (LGI) tract is more involved than upper GI (UGI). Viral RNA detected in GI tissue by RT-PCR correlates with disease severity and is more dependable than RNA detected in the stool [24]. Although most cases had neither significant gross nor histological pathological changes in esophagus, stomach nor duodenum [23]. Barton has described gaseous stomach, punctate gastric and duodenal hemorrhages, and multifocal gastric hemorrhage in COVID patients [10].

## *Histopathological findings in kidney*

Though respiratory and immune systems are the major targets of Coronavirus (COVID-19), acute kidney injury and proteinuria was also observed. Su Hua [25] reported twenty-five kidney abnormalities in twenty-six autopsies of patients with COVID-19. Out of twenty-six, nine patients showed clinical signs of kidney injury which included systemic hypoxia, abnormal coagulation, and drug or hyperventilation-relevant rhabdomyolysis.

They also observed increased serum creatinine and/or new-onset proteinuria. Electron microscopic study showed clusters of coronavirus-like particles with distinctive spikes in the tubular epithelium and podocytes. The diameter of virus-like particle varied from about 65 nm to 136 nm, with distinctive spikes, around 20 to 25 nm, presenting in a solar "corona" appearance. Immunostaining with SARS-CoV nucleoprotein antibody was also positive in tubules.

ACE2 attached to the cell membranes of cells in the lungs, arteries, heart, kidney, and intestines. Cell entry of corona virus depends on binding of the viral spike (S) proteins to cellular receptors and on S protein priming by host cell proteases. SARS-CoV2 uses the SARS-CoV receptor ACE2 for entry and the serine protease, TMPRSS2, for S-protein priming. Xu found that ACE2 and TMPRSS2 are significantly co-expressed in podocytes and proximal convoluted tubules which provide direct viral involvement of the kidneys.

Akalin reported that transplanted kidney patients have an increased risk from Covid-19. In New York, the Montefiore Medical Center reported twenty-six transplant patients with Covid-19 those who had secondary risk factors. An extremely high early mortality (28% at 3 weeks) was found among kidney transplant recipients with Covid-19. Two thirds of the patients died [26].

Clinically, the incidence of acute kidney injury in COVID-19 varies from 0.9% to 29% with new onset proteinuria. The significant microscopic changes were proximal tubule injury with loss of brush border, swollen glomerular endothelial cells, presence of thrombus in the capillaries, tubular epithelial cell oedema and vacuolar degeneration (Figure 2A & B). Yao mentioned the occasional findings include segmental fibrin thrombus, podocyte vacuolation, focal segmental glomerulosclerosis and shrinkage of capillary loops and accumulation of plasma in Bowman's space (Figure 2G & H) [9].

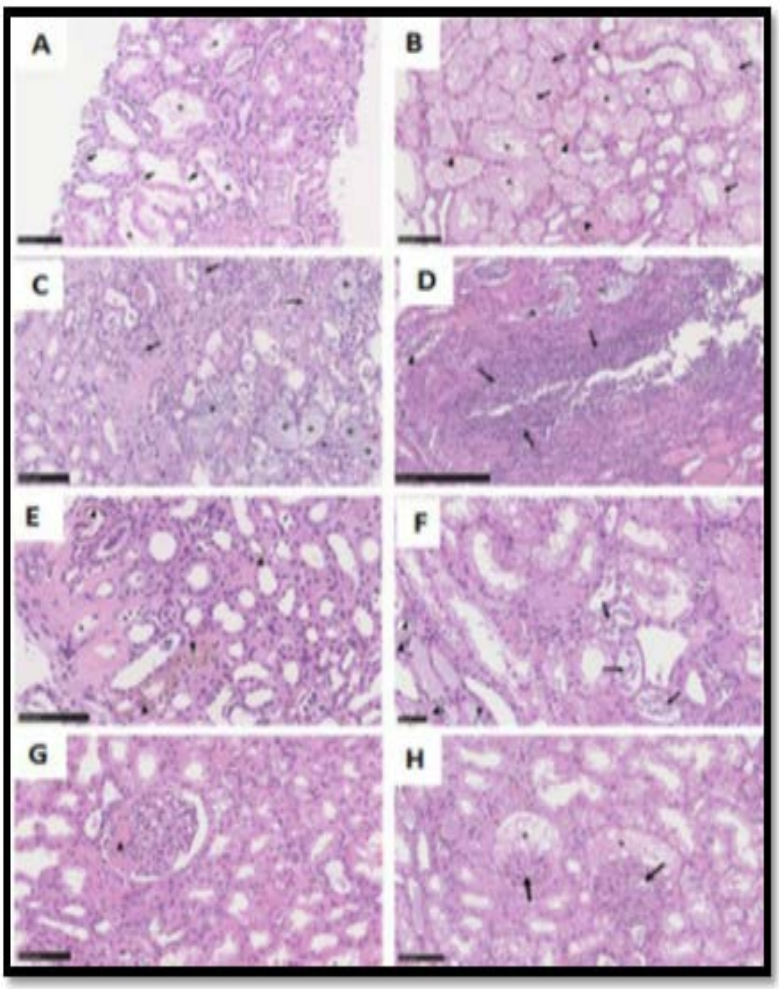


***Figure 2.*** *Histopathological changes in kidneys of COVID-19 patients.*

*(A) Epithelium of proximal convoluted tubules shows decreased/ loss of the brush border.*

*(B)Tubular epithelial cells show vacuolar degeneration (arrows), leading to collection of necrotic debris in the lumen (asterisks). Blocked peritubular capillaries due to erythrocytic aggregates (arrowheads).*

*(C,D) Inflammatory cells (arrowhead) infiltrate the tubules and arcuate artery (arrows), Bacterial foci (asterisks) is also observed.*

*(E,F) Tubular deposition of hemosiderin granules, calcium deposits (arrowhead) and pigmented cast (arrow).*

*(G,H) Glomeruli show ischemic contraction (arrows) and fibrin thrombi (arrowhead). Bowman's space show presence of leaked accumulated plasma; hematoxylin and eosin. Bars = (F) 50 µm, (A–C, E, G, H) 100 µm, and (D) 250 µm.*

### *Histopathological findings in Heart*

Several researchers reported cardiovascular damages in COVID-19 patients including myocardial infarction, acute coronary syndrome, cardiomyopathy, arrhythmias, and cardiogenic shock. Especially in pre-existing cardiovascular diseases, myocardial injury occurred in more than 20% of hospitalized patients infected with corona virus. Bengaluru presented a case study of eighteen patients with ST segment elevation on ECG that showed six patients had coronary obstruction leading to myocardial infarction, two were diagnosed with myocardial infarction as wall abnormalities on echocardiogram and ten had non-coronary myocardial injury [27]. Cardiac arrhythmias and ventricular arrhythmias have been frequently reported during COVID-19 disease, 17% among hospitalized patients and 44% among those admitted in intensive care units. Few case reports described the occurrence of myocarditis as the first manifestation of COVID-19 even in absence of respiratory symptoms or radiological features of interstitial pneumonia.

### *Histopathological findings in nervous system*

Histopathological examination of the brain showed no infiltration of inflammatory cells or neural cell degeneration though neurological symptoms in COVID-19 have been frequently reported. Autopsy findings of a Covid-19 patient showed haemorrhagic white matter lesions with axonal injuries and Perivascular acute disseminated encephalomyelitis (ADEM)-like appearance as well as neocortical microscopic infarcts were also observed [27].

Dizziness and headache were most common CNS manifestations, while taste and smell impairment were the most common peripheral nervous system symptoms [28]. Occasional neurological symptoms were stroke, acute encephalopathy, convulsions, ataxia, or nerve demyelination

found in some patients. Autopsied brain tissue displayed signs of acute hypoxic ischemic injury like hyperaemia, oedema, and neuronal degeneration [29]. A post-mortem examination study in COVID-19 patients showed widespread brain lesions [30].

### *Histopathological findings in skin*

The virus reaches the cutaneous tissue through the blood vessels where the ACE-2 can easily bind to the viral spike protein and facilitate viral invasion into the skin tissue. Like other viral infection, a COVID-19 patient may also show signs of erythematous rash, dermatitis, urticaria, chicken pox-like vesicles purpuric papulovesicular rash which may even be painful, pseudo-chilblains on fingertips and toes, macular/ maculopapular exanthems, livedo reticularis lesions, and petechiae (Figure 3). Histopathological findings of biopsy samples of infected persons showed superficial and deep perivascular dermatitis, blood vessels surrounded by lymphocytes, focal acantholytic suprabasal clefts, dyskeratotic and ballooning herpes-like keratinocytes, necrosis of keratinocytes, mucin deposition in the dermis and hypodermis, and nests of Langerhans cells within the epidermis [31,32].

### *Histopathological findings in Spleen and lymph nodes*

Researchers stated that viral nucleocapsid protein (NP) could be seen in splenic tissue. Histopathologic examinations of some autopsy samples showed reduction of cell composition, atrophy of white pulp, neutrophil and plasma cell infiltration, reduction, or absence of lymph follicles, increase in red pulp to white pulp proportion, reduction of T and B cells due to necrosis and apoptosis, and atrophy of corpuscles in the spleen of infected cases [33]. Other than these symptoms, congestion and haemorrhagic appearance were also visualized in the spleen.

### *Histopathological findings in placenta & testis*

SARS-Cov-2 alter placenta in pregnant women. Pathologic findings of biopsy samples revealed low grade fetal vascular malperfusion, intramural fibrin deposition, intramural nonocclusive thrombi, and meconium macrophages. Fetal thrombotic vasculopathy has also been reported [34].

ACE2 is also present in seminiferous tubules, Leydig cells, Sertoli cells and spermatogonia. When viral protein bound with the testicular cells expressing ACE2 receptor, it not only damages the testicular tissue but also forms a potential shelter for the virus. Different studies showed that Sertoli cells are more susceptible than germ cells as more than 90% Sertoli cells expressed ACE-2 receptors. All COVID-19 infected testes demonstrated extensive germ cell destruction and decreased spermatogenesis in the seminiferous tubules [13].

The basement membrane becomes thickened with peritubular fibrosis. Sertoli cells showed swelling, vacuolation and cytoplasmic rarefaction. One of the evident phenomena in the COVID-19 testis is leucocyte infiltration (Figure 4D). These cells could affect the function of Leydig cells and thus directly decrease the production of testosterone (Figure 4C). These infiltrated cells the lymphocytes and histiocytes also damage the blood–testis barrier and destroy the seminiferous tubules directly (Figure 4E & F). Like other viruses like HIV, mumps and hepatitis B virus, SARS-CoV- 2 also may lead to activation of inflammatory cytokines, which may initiate the autoimmune response as well as may result in the testicular damage leading to infertility and sterility. These symptoms may further increase the chances of testicular tumours [35].

RT-PCR result was not found any positive report for the semen or testicular biopsy specimen. So, it can be suggested that it will not be transmitted through the sexual route [36].

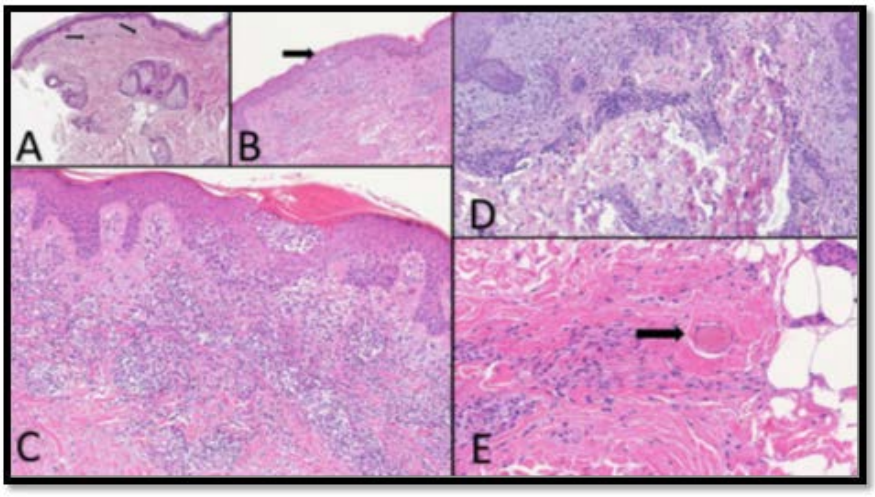


***Figure 3.*** *Histopathological changes in skin of COVID-19 patients.*

*(A) Arrow showing telangiectatic blood vessels in early exanthematous rash.*

*(B) Epidermis (arrow) showing groups of Langerhans cells in the later phase of exanthematous rash. Superficial dermis also shows perivascular infiltration of lymphocytes.*

*(C) An intraepidermal group of Langerhans cell seen in papulovesicular rash.*

*(D) Micrographic feature in a Maculo-papular eruption.*

*(E) Capillary thrombosis (arrow) along with diffuse haemorrhage in an exanthemous*

***Citation:*** *Nath NB, Smita A, Dutta A. Extra pulmonary manifestations in covid-19: A review on histopathological alterations. J Pathol Dis Biol. 2022;6(4):116*

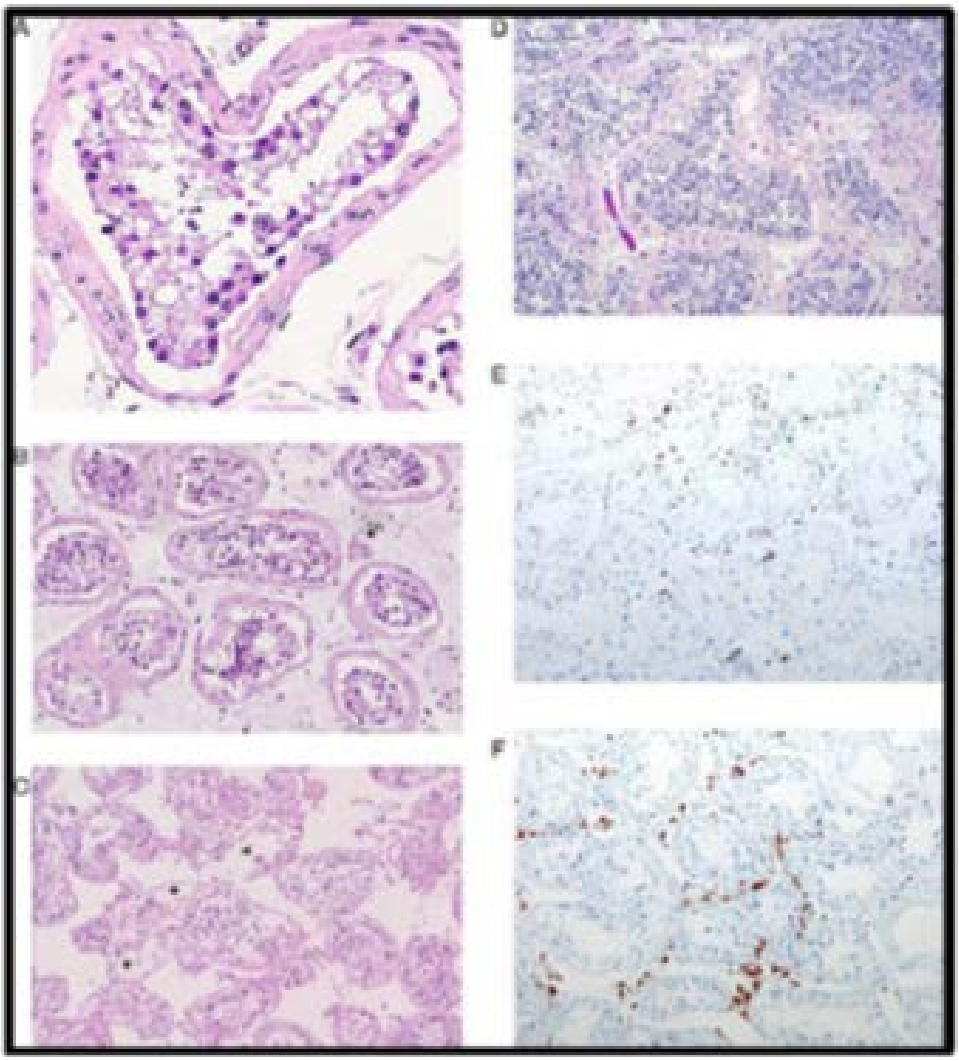

***Figure 4.*** *Pathological changes observed in testes from patients with COVID-19.*

*(A, B) Defoliated and oedematous Sertoli cells with vacuoles along with reduced spermatogenesis and scattered Leydig cells.*

*(C) Tubular cells show sloughing into the lumen (asterisks) indicative of injury. There is marked interstitial oedema.*

*(D) Non-Covid testis with protracted disease showing interstitial edema with infiltration of inflammatory cells.*

*(E) Immunohistochemical findings showing CD3-positive+ T lymphocytes and*

*(F) CD68-positive+ histiocytes.*

## Conclusion

Varga published endothelial infection by the virus & stated that SARS-CoV-2 infection facilitates the induction of endothelitis in several organs as a direct consequence of viral involvement. SARS-CoV-2 infects the host using the angiotensin converting enzyme 2 (ACE2) receptor which is expressed in several organs including the lung, heart, kidney, intestine & testis more often if comorbidities are present [22]. Thus, no vascular tissue is safe.

In this article, we try to describe the histopathological changes caused by COVID-19 and special emphasis with extra pulmonary manifestations. This description is up to date as of now, but every day new experiences are pouring from different parts of the world, newer knowledge and information will appear by the time this article is published.

## References


1. Wang W, Yoneda M. Determination of the optimal penetration factor for evaluating the invasion process of aerosols from a confined source space to an uncontaminated area. Sci Total Environ. 2020;740:140113.
2. Velavan TP, Meyer CG. The COVID-19 epidemic. Trop Med Int Health. 2020;25(3):278.
3. Li F. Structure, function, and evolution of coronavirus spike proteins. Annu Rev Virol. 2016;3(1):237..
4. Huang C, Wang Y, Li X, et al. Clinical features of patients infected with 2019 novel coronavirus in Wuhan, China. lancet. 2020;395(10223):497-506.
5. Xu Z, Shi L, Wang Y, et al. Pathological findings of COVID-19 associated with acute respiratory distress syndrome. Lancet Respir Med 2020; 8: 420–22.



***Citation:*** *Nath NB, Smita A, Dutta A. Extra pulmonary manifestations in covid-19: A review on histopathological alterations. J Pathol Dis Biol. 2022;6(4):116*

6. Mehta P, McAuley DF, Brown M, et al. COVID-19: consider cytokine storm syndromes and immunosuppression. The Lancet. 2020;395(10229):1033-4.
7. The Human Protein Atlas. Tissue expression of ACE2 - Summary.
8. Gupta A, Madhavan MV, Sehgal K, et al. Extrapulmonary manifestations of COVID-19. Nat Med. 2020;26(7):1017-32.
9. Yao XH, Li TY, He ZC, et al. A pathological report of three COVID-19 cases by minimal invasive autopsies. Chin J Pathol. 2020;49(5):411-7.
10. Barton LM, Duval EJ, Stroberg E, et al. Covid-19 autopsies, Oklahoma, USA. Am J Clin Pathol. 2020;153(6):725-33.
11. Tian S, Xiong Y, Liu H, et al. Pathological study of the 2019 novel coronavirus disease (COVID-19) through postmortem core biopsies. Mod Pathol. 2020;33(6):1007-14.
12. Magro C, Mulvey JJ, Berlin D, et al. Complement associated microvascular injury and thrombosis in the pathogenesis of severe COVID-19 infection: a report of five cases. Transl Res. 2020;220:1-3.
13. Deshmukh V, Motwani R, Kumar A, et al. Histopathological observations in COVID-19: a systematic review. J Clin Pathol. 2021;74(2):76-83.
14. Lan J, Ge J, Yu J, et al. Structure of the SARS-CoV-2 spike receptor-binding domain bound to the ACE2 receptor. Nature. 2020;581(7807):215-20.
15. Indexed at, Google Scholar, Cross Ref
16. Shang J, Ye G, Shi K, et al. Structural basis of receptor recognition by SARS-CoV-2. Nature. 2020;581(7807):221-4.
17. ai X, Hu L, Zhang Y, et al. Specific ACE2 expression in cholangiocytes may cause liver damage after 2019-nCoV infection. Biorxiv. 2020.
18. Lagana SM, Kudose S, Iuga AC, et al. Hepatic pathology in patients dying of COVID-19: a series of 40 cases including clinical, histologic, and virologic data. Mod Pathol. 2020;33(11):2147-55.
19. Sonzogni A, Previtali G, Seghezzi M, et al. Liver and COVID 19 infection: a very preliminary lesson learnt from histological post-mortem findings in 48 patients.
20. Li J, Fan JG. Characteristics and mechanism of liver injury in 2019 coronavirus disease. J Clin Transl Hepatol. 2020;8(1):13.
21. Fiel MI, El Jamal SM, Paniz-Mondolfi A, et al. Findings of hepatic severe acute respiratory syndrome Coronavirus-2 infection. Cell Mol Gastroenterol Hepatol. 2021;11(3):763-70.
22. Wichmann D, Sperhake JP, Lütgehetmann M, et al. Autopsy findings and venous thromboembolism in patients with COVID-19: a prospective cohort study. Ann Internal Med. 2020;173(4):268-77.
23. Varga Z, Flammer AJ, Steiger P, et al. Endothelial cell infection and endothelitis in COVID-19. The Lancet. 2020;395(10234):1417-8.
24. Yao XH, He ZC, Li TY, et al. Pathological evidence for residual SARS-CoV-2 in pulmonary tissues of a ready-for-discharge patient. Cell Res. 2020;30(6):541-3.
25. Lin L, Lu L, Cao W, et al. Hypothesis for potential pathogenesis of SARS-CoV-2 infection–a review of immune changes in patients with viral pneumonia. Emerg Microb Infec. 2020;9(1):727-32.
26. Su H, Yang M, Wan C, et al. Renal histopathological analysis of 26 postmortem findings of patients with COVID-19 in China. Kidney Intern. 2020;98(1):219-27.
27. Akalin E, Azzi Y, Bartash R, et al. Covid-19 and kidney transplantation. N Engl J Med. 2020;382(25):2475-7.
28. Bangalore S, Sharma A, Slotwiner A, et al. ST-segment elevation in patients with Covid-19—a case series. New Engl J Med. 2020;382(25):2478-80.
29. Mao L, Jin H, Wang M, et al. Neurologic manifestations of hospitalized patients with coronavirus disease 2019 in Wuhan, China. JAMA Neurol. 2020;77(6):683-90.
30. Zubair AS, McAlpine LS, Gardin T, et al. Neuropathogenesis and neurologic manifestations of the coronaviruses in the age of coronavirus disease 2019: a review. JAMA Neurol. 2020;77(8):1018-27.
31. Remmelink M, De Mendonça R, D'Haene N, et al. Unspecific post-mortem findings despite multiorgan viral spread in COVID-19 patients. Critic Care. 2020;24(1):1-0.
32. Gianotti R., Veraldi S, Recalcati S, et al. Cutaneous clinico-pathological findings in three COVID-19-positive patients observed in the metropolitan area of Milan, Italy. Acta Derm. Venereol. 23;100(8):adv00124.
33. El Hachem M, Diociaiuti A, Concato C, et al. A clinical, histopathological and laboratory study of 19 consecutive Italian paediatric patients with chilblain-like lesions: lights and shadows on the relationship with COVID-19 infection. J Eur Acad Dermatol Enereol. 2020;34(11):2620-9.
34. Tabary M, Khanmohammadi S, Araghi F, et al. Pathologic features of COVID-19: A concise review. Pathol Res Prac. 2020;216(9):153097.
35. Baergen RN, Heller DS. Placental pathology in Covid-19 positive mothers: preliminary findings. Pediatric Dev Pathol. 2020;23(3):177-80.
36. Xu J, Qi L, Chi X, et al. Orchitis: a complication of severe acute respiratory syndrome (SARS). Biol Reprod. 2006;74(2):410-6.
37. Song C, Wang Y, Li W, et al. Absence of 2019 novel coronavirus in semen and testes of COVID-19 patients. Biol Reprod. 2020;103(1):4-6.


***Citation:*** *Nath NB, Smita A, Dutta A. Extra pulmonary manifestations in covid-19: A review on histopathological alterations. J Pathol Dis Biol. 2022;6(4):116*

WORLD JOURNAL OF PHARMACY AND PHARMACEUTICAL SCIENCES
SJIF Impact Factor 8.025
Volume 13, Issue 5, 813-823 Research Article ISSN 2278 – 4357

# A COMPARATIVE STUDY OF ANTIMICROBIAL ACTIVITY OF CLOVE, CINNAMON AND BAY LEAF EXTRACTS AGAINST *E. COLI* & *S. AUREUS.*

**Nilanjana Bhattacharyya Nath[1]*, Gargi Gupta[1], Arya Baidya[2] and Shovik Roy[3]**

[1]Department of Biotechnology. Swami Vivekananda Institute of Modern Science. Sonarpur, Kolkata-103, West Bengal, India.

[2]Department of Biochemistry & Medical Biotechnology. Calcutta School of Tropical Medicine (WBUHS). Kolkata-73, West Bengal, India.

[3]Department of Biotechnology. Amity University, Kolkata, West Bengal, India.

Article Received on
13 March 2024,

Revised on 03 April 2024,
Accepted on 23 April 2024

DOI: 10.20959/wjpps20245-27225

***Corresponding Author**
**Nilanjana Bhattacharyya Nath**
Department of Biotechnology. Swami Vivekananda Institute of Modern Science. Sonarpur, Kolkata-103, West Bengal, India.

## ABSTRACT

Spices traditionally have been used as flavouring agents, colouring agents, preservatives, food additives, medicine and antimicrobial agents. All over India clove, cinnamon and bay leaves are popular culinary herbs as well as important ingredients of Indian "garam masala" which not only enhance the flavour of any dish but also have health benefits. The present work aimed to find out the antimicrobial activity of clove, cinnamon and bay leaf as an alternative to antibiotics in order to arrest the infection of *E. coli* and *S. aureus*. Aqueous, alcohol and acetone extract of three spices were prepared and used against *E. coli* and *S. aureus*. The acetone extract of bay leaves had the highest zone of inhibition against the tested bacterial strains *(E. coli & S. aureus*) and aqueous extract of both clove and cinnamon shown the lowest zone of inhibition against both *E. coli & S. aureus*.

**KEYWORDS:** Anti-Microbial Activity, Spices, Clove, Cinnamon, Bay Leaf.

## INTRODUCTION

Spices play a vital role in Indian cuisine since long time. These are the some of the most valuable items of domestic as well as industrial kitchens. Spices for example, fenugreek,

coriander, turmeric, cinnamon, cumin, clove are being used medicinally. Spices are one of the most commonly used natural antimicrobial agents in foods and have been used traditionally for thousands of years by many cultures for preserving foods and as food additives to enhance aroma and flavor (O. P. Snyder, 1997). Researchers are collecting evidences that many of the herbs and spices such as garlic, black cumin, cloves, cinnamon, thyme, allspices, bay leaves, mustard, and rosemary have medicinal properties that alleviate symptoms or prevent diseases (P. K. Lai & J. Roy, 2004). The clove has several beneficial properties such as pain -relieving, anti-viral, anti-microbial, anti-helminthics, anti-diabetic, calming, antithrombotic, analgesic etc. (S. Kundu *et al*., 2014). Cinnamon is utilized as an adjuvant in stomachic and carminative prescriptions and is additionally managed in instances of anorexia, inflammation, spewing, and tubercular ulcers (D. M. Cheng *et al*., 2012). Hasanzade *et al*. in their study found that taking cinnamon at a dose of 1 g daily for 30 and 60 days has no effect in decreasing the blood glucose of type II diabetes patients (F. Askari *et al*., 2014). The Bay leaf belongs to Lauraceae family and it is endemic in the Mediterranean region. Lauraceae, is an aromatic plant frequently used as a spice and a traditional medicine for the treatment of several infectious disease (B. Siriken *et al*., 2018).

Antimicrobial activity refers to the process of killing or preventing the growth of the disease-causing microbes. The antimicrobial agents may be antibacterial, antifungal or antiviral and they all are having different modes of action by which they act to suppress the infection caused by their respective microbials. The growing concern about food safety has recently led to the development of natural antimicrobials to control food borne pathogens and spoilage bacteria. D. S. Arora and J. Kaur (1999) compared the sensitivity of some human pathogenic bacteria and yeasts to various spice extracts and commonly employed chemotherapeutic substances. A. L. Shelef (1983) documented the antimicrobial properties of some spices and their components. Previous studies confirmed that garlic, onion, cinnamon, cloves, thyme, sage, and other spices inhibit the growth of both gram positive and gram-negative food borne pathogens or spoilage bacteria, yeast, and molds. Clove (*Syzygium aromaticum*) oil extracts possessed antimicrobial activity against all bacteria and yeast tested. Their water extracts exhibited lower antimicrobial activity (B. C. Nzeako *et al*., 2006). Its antimicrobial potential was established when its essential oil extracts killed many gram-positive and gram-negative organisms including some fungi (G. F. Gislene *et al*., 2000). The antimicrobial activity of clove is attributable to eugenol, oleic acids and lipids found in its essential oils (A. K. Hammer *et al*., 1999). Eugenol is a class of phenylpropanoid compound. It is a clear to pale

yellow oil especially extracted from clove oil, nutmeg, cinnamon, and bay leaf (K Pandima Devi *et al*., 2013). Thyme and clove oils shows antimicrobial activity against *S. aureus*, *E. coli*, *P. aeruginosa* as well as *S. pyogenes*, *Corynebacterium*, *Salmonella*, *Bacteroides* and *C. albicans* at various dilutions of the extracts (B. C. Nzeako *et al*., 2006). Major antimicrobial component in cinnamon have been reported to be cinnamaldehyde, which has been reported to inhibit the growth of *S. aureus*, *E. coli*. It was determined by C. Jiang *et al*., (2022) that the main active compounds in the essential oils of cassia bark, bay fruits and cloves were cinnamaldehyde (78.11%), cinnamaldehyde (61.78%) and eugenol (75.23%), respectively. Generally cinnamon essential oil has the strongest antibacterial activity, while laurel fruit has the lowest antibacterial activity. M. De *et al*., (1999) reported that the clove, cinnamon, bishop's weed, chilli, horse raddish, cumin, tamarind, black cumin, pomegranate seeds, nutmeg, garlic, onion, tejpat, celery, cambodge have potent antimicrobial activities against *Bacillus subtilis*, *Escherichia coli* and *Saccharomyces cerevisiae*. R. Dhiman *et al*. (2015) studied in vitro antimicrobial activity of different spice extracts against microbes associated with juices and stated that Gram-positive bacteria are more sensitive to the spice extracts than the Gram-negative bacteria and yeast. The methanol leaf extracts of *Acacia nilotica, Sida cordifolia, Tinospora cordifolia, Withania somnifer* and *Ziziphus mauritiana* showed significant antibacterial activity against *Bacillus subtilis, Escherichia coli, Pseudomonas fluorescens, Staphylococcus aureus* and *Xanthomonas axonopodis* pv. *mahacearum* and antifungal activity against *Aspergillus flavus, Dreschlera turcica* and *Fusarium verticillioides* when compare to root/bark extracts (B. Mahesh & S. Satish, 2008).

Therefore, the main objective of this study was to examine the *in vitro* antimicrobial activity of clove, cinnamon and bay leaves extracts and to compare the effect of different solvents for antimicrobial activity against *E. coli & S. aureus*.

## MATERIALS AND METHODS

The spices namely Clove (*Syzygium aromaticum*), Cinnamon (*Cinnamomum verum*) & Bay leaf (*Laurus nobilis*) samples were collected from the local market and used for the present study.

### Preparation of spice extracts

Spices were taken and dried in hot air oven at 55°C for 15-20 min. Then grinded them properly to get powder of sample. 5 gm. of each sample were mixed separately with ethanol,

water & acetone by using electrical shaker and kept three mixtures in room temperature for 3 hours. After that they were filtrated & kept at 4°C until further uses.

**The microorganism**

Two bacterial strains (*Escherichia coli* and *Staphylococcus aureus*) were selected for the experiment depending on their pathogenic activity in humans.

**Preparation of bacterial culture**

Nutrient broth and agar media were prepared. All the materials kept in autoclave for 30 min in 15 Psi & 125°C for optimum sterilization. Each bacterial strains were taken & inoculated in the broth media and kept it in incubation at 37°C for 24 hours & then store it in 4°C. After solidifying the agar media, streak plates were prepared.

**Anti-microbial assay**

The concentration of spice at which no growth of the organism was observed, considered as Minimum inhibitory concentration of the spice for the microorganism. The result was expressed as the growth (+ve) or inhibition of growth (-ve) in the presence of spices. 5 µl, 10 µl and 20 µl of each sample solutions were taken for Kirby-Bauer disc diffusion test. All the plates were kept in incubator for 24 hrs in 37°C. Finally, area of zone of inhibition were calculated to measure the antimicrobial activity of each sample.

**RESULTS**

**Table 1: Effect of Bayleaf, clove and cinnamon on growth of test organisms (+ = growth, - = no growth).**

| SPICE | SOLVENT | DOSE | TEST ORGANISM | |
|---|---|---|---|---|
| | | | *E. coli* | *S. aureus* |
| **Bayleaf** | **Acetone** | 5 µl | + | + |
| | | 10 µl | + | + |
| | | 20 µl | - | - |
| | **Alcohol** | 5 µl | + | + |
| | | 10 µl | + | + |
| | | 20 µl | - | - |
| | **Aquous** | 5 µl | + | + |
| | | 10 µl | + | + |
| | | 20 µl | - | - |
| | | | | |
| **Clove** | **Acetone** | 5 µl | + | + |
| | | 10 µl | + | + |
| | | 20 µl | - | - |

| | | | | |
|---|---|---|---|---|
| | **Alcohol** | 5 µl | + | + |
| | | 10 µl | + | + |
| | | 20 µl | - | - |
| | **Aquous** | 5 µl | + | + |
| | | 10 µl | + | + |
| | | 20 µl | - | - |
| | | | | |
| **Cinnamon** | **Acetone** | 5 µl | + | + |
| | | 10 µl | + | + |
| | | 20 µl | - | - |
| | **Alcohol** | 5 µl | + | + |
| | | 10 µl | + | + |
| | | 20 µl | - | - |
| | **Aquous** | 5 µl | + | + |
| | | 10 µl | + | + |
| | | 20 µl | - | - |

**Table 2: Comparative study of the antimicrobial activity of clove, cinnamon and bay leaves (Dose = 20 µl).**

| ANTIMICROBIAL ACTIVITY OF CLOVE, CINNAMON & BAYLEAF | | | | | |
|---|---|---|---|---|---|
| | | ***E. coli*** | | ***S. aureus*** | |
| **Spices** | **Solvent** | **Radius (cm)** | **$\pi r^2$ ($cm^2$)** | **Radius (cm)** | **$\pi r^2$ ($cm^2$)** |
| **Bayleaf** | **Acetone** | 0.65 | 1.33 | 1.00 | 3.14 |
| | **Alcohol** | 0.55 | 0.95 | 0.80 | 2.01 |
| | **Aqueous** | 0.50 | 0.78 | 0.55 | 0.95 |
| | | | | | |
| **Clove** | **Acetone** | 0.70 | 1.54 | 0.55 | 0.95 |
| | **Alcohol** | 0.65 | 1.33 | 0.65 | 1.33 |
| | **Aqueous** | 0.60 | 1.13 | 0.50 | 0.78 |
| | | | | | |
| **Cinnamon** | **Acetone** | 0.90 | 2.54 | 0.60 | 1.13 |
| | **Alcohol** | 0.75 | 1.76 | 0.75 | 1.76 |
| | **Aqueous** | 0.65 | 1.33 | 0.50 | 0.78 |

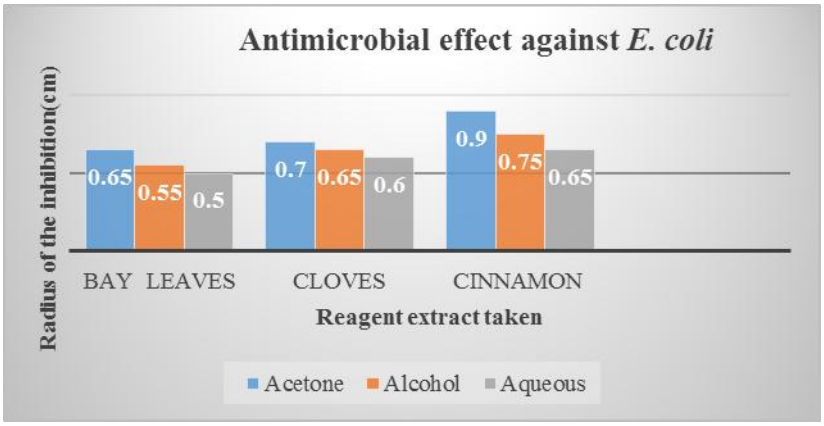


**Fig. 1: Radius of zone of inhibition formed by the antimicrobial effect of Bay leaf, clove and cinnamon against *E. coli*.**

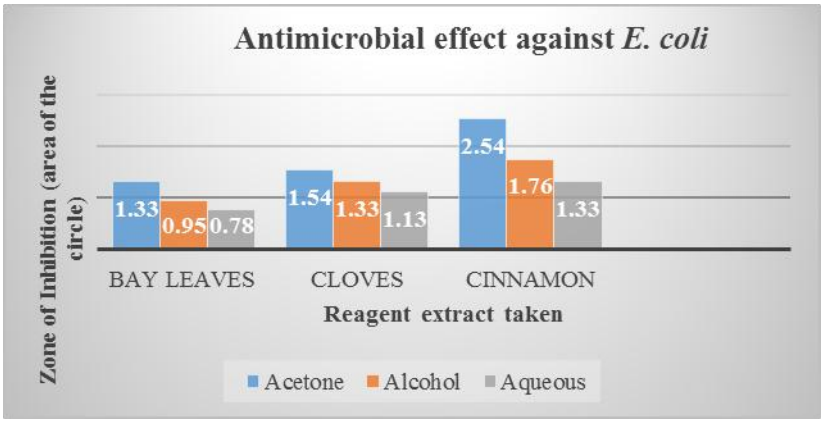


**Fig. 2: Total area of zone of inhibition formed by the antimicrobial effect of Bay leaf, clove and cinnamon against *E. coli*.**

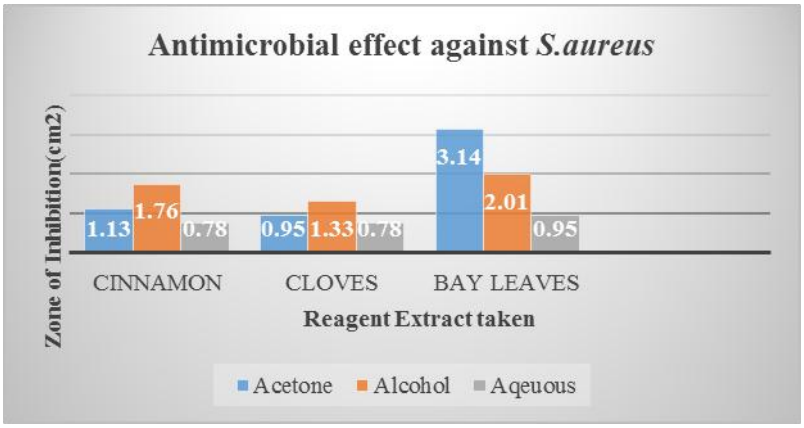


**Fig. 3: Radius of zone of inhibition formed by the antimicrobial effect of Bay leaf, clove and cinnamon against *S. aureus*.**

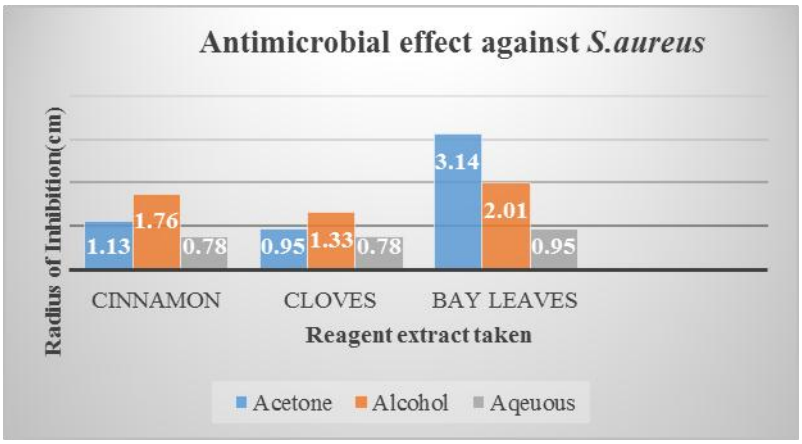


**Fig. 4: Total area of zone of inhibition formed by the antimicrobial effect of Bay leaf, clove and cinnamon against *S. aureus.***

In the present study, antimicrobial activity of three spices - clove, cinnamon and bay leaf were done. Fig -1, 2, 3 & 4 and Table -1 shown the antimicrobial activity of spices extracted

in acetone, alcohol and aqueous against *E. coli* and *S. aureus*. The acetone extract of bay leaves had the highest zone of inhibition against the tested bacterial strains *(E. coli & S. aureus*) and aqueous extract of both clove and cinnamon shown the lowest zone of inhibition against both *E. coli & S. aureus*.

**FIG. 5. A**

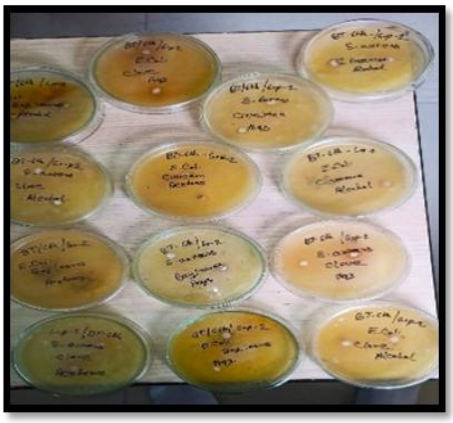

**FIG. 5. B**

**FIG. 5. A & B: Agar plate with *E. coli & S. aureus* and the effect of different solvents of clove, cinnamon and bay leaves extracts.**

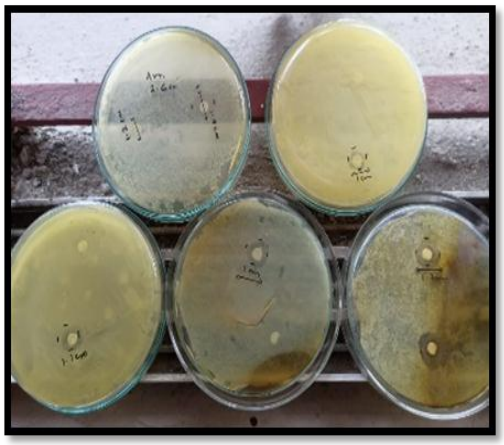

**FIG 6. A**

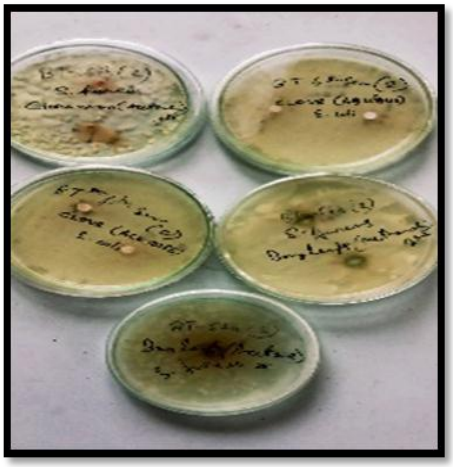

**FIG 6. B**

**FIG. 6. A & B: The anti microbial activity of clove, cinnamon and bay leaves extracts shown by Disc diffusion method in terms of zone of inhibition.**



**FIG 7. A** **FIG 7. B** **FIG 7. C**

**FIG. 7. A, B & C: Measurement of zone of inhibition formed due to anti microbial activity of clove, cinnamon and bay leaves extract respectively.**

## DISCUSSION

We got the highest value from Acetone and alcohol respectively & least from aqueous. The zone of inhibition indicates the antimicrobial activity of clove, cinnamon & bay leaves against *E. coli* & *S. aureus*. All three extracts of clove, cinnamon & bay leaves contain pharmacological active substances with antimicrobial properties.

The average zone of inhibition for the different extracts indicating antibacterial potential. The acetone extract of bay leaves was the most effective against the tested bacterial strains *(E. coli & S. aureus*) with highest zone of inhibition. Whereas the alcohol extracts of clove and cinnamon had the highest zone of inhibition against *E. coli and S. aureus*. The lowest antimicrobial activity as well as zone of inhibition than rest of two readings has been shown by aqueous solution. In comparison with the control, the inhibition of the microbe was absent in the control than in spices extract namely acetone, alcohol and aqueous as depicted in the picture.

The use of spices as colorants and preservatives is becoming fashion in the food industry, and among these spices, *Syzygium aromaticum* is of great important (Jessica Elizabeth, Gassara, Kouassi, Brar, & Belkacemi, 2017). Clove could destroy cell walls and cell membranes of microorganisms and enter the cells, then inhibit the normal synthesis of DNA and proteins (G. J. Xu *et al*., 2016). The major component of clove is eugenol which could inhibit the production of amylase and proteases in *Bacillus cereus* and has the ability of cell wall deterioration and cell lysis (S. Burt, 2004). Cinnamon extract showed the highest activities

against *B. cereus* among bacteria, and *Penicillium* sp. among fungi (Q. Liu *et al*., 2017). The major component of cinnamon is cinnamaldehyde which possesses antimicrobial effects on microorganisms by inhibiting cell wall biosynthesis, membrane function, and specific enzyme activities. More specific cellular targets of cinnamaldehyde are still required to be studied in detail (S. Sreaz *et al*., 2016).

The major significance of clove, cinnamon and bay leaf is to reduce stomach ulcers, prevent cough & cold, kill bacteria, cure digestive problems, relief from respiratory problem, increase immune system, fights against infection, cure sore throats, prevent diarrhoea, prevent skin infection etc. They can also use as natural preservatives to solve various problems regarding microbial resistance as well as they can be a good alternative to chemical and synthetic compounds (I. D. Dewijanti *et al*., 2017).

## CONCLUSION

The present work demonstrates the antimicrobial potential of clove, cinnamon, bay leaf extract by using various solvents. The results indicate that ethanol and acetone are better than aqueous for the extraction of the antibacterial properties of spices. The results also indicate that only the bayleaf extracts have least antibacterial effect on the *E. coli*, whereas acetone extracts of both clove and cinnamon shown the highest antimicrobial activity as well as zone of inhibition against the organism. The observed inhibition of Gram-positive bacteria, *Staphylococcus aureus*, suggests that sample of clove, cinnamon, bay leaf compounds containing antibacterial properties that can effectively suppress the growth when extracted using acetone or ethanol as the solvent. On the basis of the present findings, clove, cinnamon and bay leaf – these three spices can act as natural antimicrobial agents against infections and/or diseases caused by *E. coli* and *S. aureus* as they all contain eugenol in different percentage (Saima Batol *et al*., 2020; L. Nunez *et al*., 2012). Comparisons with related data from the literature indicate that according to the different methodologies of studies on antibacterial activity, the most diverse outcomes can be obtained. This study provides scientific insight to further determine the antimicrobial principles and investigate other pharmacological properties of extracts of clove, cinnamon and bay leaf.

## ACKNOWLEDGMENT

This research work was supported by our institute Swami Vivekananda Institute of Modern Science. We are thankful to our Director Dr. Nandan Gupta for his continuous support and encouragement.

## REFERENCES


1. Arora D. S. and J. Kaur. Antimicrobial activity of spices. International Journal of Antimicrobial Agents, 1999; 12(3): 257–262.
2. Askari F, Rashidkhani B., Hekmatdoost A. Cinnamon may have therapeutic benefits on lipid profile, liver enzymes, insulin resistance, and high-sensitivity C-reactive protein in nonalcoholic fatty liver disease patients. Nutr Res. 2014; 34(2): 143–8.
3. Burt S. Essential oils: Their antibacterial properties and potential applications in foods - A review. Int. J. Food Microbiol, 2004; 94: 223–253. doi: 10.1016/j.ijfoodmicro.2004. 03.022.
4. Cheng D. M., Kuhn P., Poulev A., Rojo L. E., Lila M. A., Raskin I. In vivo and in vitro antidiabetic effects ofaqueous cinnamon extract and cinnamon polyphenol-enhanced food matrix. Food Chem, 2012; 135(4): 2994–3002.
5. De M., De A.K., Banerjee A.B. Antimicrobial screening of some Indian spices. Phytother. Res., 1999; 13: 616–618. doi: 10.1002/(SICI)1099-1573(199911)13:7<616:: AID-PTR475>3.0.CO;2-V. [PubMed] [CrossRef] [Google Scholar]
6. Devi K. P., Sakthivel R., Arif N. S., Suganthy N., Karutha S. Eugenol alters the integrity of cell membrane and acts against the nosocomial pathogen *Proteus mirabilis*. Arch Pharm Res., 2013; 36(3): 282-92.
7. Dhiman R., N. K. Aggarwal, and M. Kaur. Comparative evaluation of antimicrobial activities of commonly used indian spices against microbes associated with juices. *Research Journal of Microbiology*, 2015; 10(4): 170–180.
8. Dewijanti I. D. *et al*. Anti-microbial activity of Bay Leaf (*S. polyanthum* (Weight) Walp) extracted using various solvent. AIP Conference Proceedings, 2017; 2175(1): 020021. DOI:10.1063/1.5134585.
9. Elizabeth Jessica, F. Gassara, A. P. Kouassi, S. K. Brar, and K. Belkacemi. Spice use in food: Properties and benefits. Crit Rev Food Sci Nutr, 2017; 57(6): 1078-1088.
10. Gislene G. F., Paulo C., Giuliana L. Antibacterial Activity of Plant Extracts and Phytochemicals onAntibiotic Resistant Bacteria. Braz J Microbiol, 2000; 31: 314–325.
11. Hammer K. A., Carson C. F., Riley T. V. Antimicrobial Activity of Essential Oils and Other Plant Extracts. JAppl Microbiol, 1999; 86: 985–990.
12. Jiang C. Antibacterial activity of essential oils extracted from the unique Chinese spices cassia bark, bay fruits andcloves. Arch Miocrobiol, 2022; 18; 204(11): 674.

13. Lai P.K., Roy J. Antimicrobial and chemopreventive properties of herbs and spices. Curr. Med. Chem, 2004; 11: 1451–1460. doi: 10.2174/0929867043365107. [PubMed] [CrossRef] [Google Scholar]
14. Kundu S., Ghosh R., Choudhary P., Prakash A. Health benefits of various Indian culinary herbs and comparative statistical analysis for organoleptic properties of Indian teas by using analysis of variance (ANOVA). Int J Pharm Pharm Sci., 2014; 6: 621–5.
15. Mahesh B. and S. Satish. Antimicrobial activity of some important medicinal plant against plant and human pathogens. World Journal of Agricultural Sciences, 2008; 4: 839–843.
16. Nzeako B. C. *et al*. Antimicrobial Activities of Clove and Thyme Extracts. Sultan Qaboos Univ Med J., 2006; 6(1): 33–39.
17. Pandey B., Shabina Khan and Sheetal Singh. A Study of antimicrobial activity of some spices. Int. J. Curr. Microbiol. App. Sci, 2014; 3(3): 643-650.
18. Qing Liu *et al*. Antibacterial and Antifungal Activities of Spices. Int J Mol Sci., 2017; 18(6): 1283.
19. Shreaz S., Wani W.A., Behbehani J.M., Raja V., Irshad M., Karched M., Ali I., Siddiqi W.A., Hun L.T. Cinnamaldehyde and its derivatives, a novel class of antifungal agents. Fitoterapia, 2016; 112: 116–131. doi: 10.1016/j.fitote.2016.05.016.
20. Siriken B. *et al*. Antibacterial Activity of *Laurus nobilis*: A review of literature. Medical Science and Discovery, 2018; 5; 11.
21. Snyder, O. P. Antimicrobial effects of spices andherbs. Hospitality Institute of Technology and Management. St. Paul, Minnaesota, 1997; https://www.hitm.com /Documents/Spices.html.
22. Xu J.G., Liu T., Hu Q.P., Cao X.M. Chemical composition, antibacterial properties and mechanism of action of essential oil from clove buds against *Staphylococcus aureus*. Molecules, 2016; 21: 1194. doi: 10.3390/molecules21091194.

Healthcare Analytics 5 (2024) 100294

Contents lists available at ScienceDirect

Healthcare Analytics

journal homepage: www.elsevier.com/locate/health

# An intuitionistic fuzzy differential equation approach for the lake water and sediment phosphorus model

Ashish Acharya [a], Sanjoy Mahato [b], Nikhilesh Sil [c], Animesh Mahata [d,*], Supriya Mukherjee [e], Sanat Kumar Mahato [b], Banamali Roy [f]

[a] Department of Mathematics, Swami Vivekananda Institute of Modern Science, Karbala More, Kolkata -700103, West Bengal, India
[b] Department of Mathematics, Sidho-Kanho-Birsha University, Purulia West Bengal, 723104, India
[c] Department of Mathematics, Narula Institute of Technology, 81, Nilgunj Road, Agarpara, Kolkata -700109, West Bengal, India
[d] Department of Mathematics, Sri Ramkrishna Sarada Vidya Mahapitha, Kamarpukur, Hooghly, West Bengal -712612, India
[e] Department of Mathematics, Gurudas College, 1/1, Suren Sarkar Road, Narkeldanga, Kolkata, 700054, West Bengal, India
[f] Department of Mathematics, Bangabasi Evening College, Kolkata -700 009, West Bengal, India

ARTICLE INFO

*Keywords:*
Intuitionistic fuzzy differential equation
Phosphorus model in lake water and sediment
Generalized Hukuhara derivative
Fuzzy valued function
Trapezoidal intuitionistic fuzzy number

ABSTRACT

Intuitionistic fuzzy sets cannot consider the degree of indeterminacy (i.e., the degree of hesitation). This study presents an intuitionistic fuzzy differential equation approach for the lake water and sediment phosphorus model. We examine the proposed model by assuming generalized trapezoidal intuitionistic fuzzy numbers for the initial condition. Feasible equilibrium points, along with their stability criteria, are evaluated. We describe the characteristics of intuitionistic fuzzy solutions and clarify the difference between strong and weak intuitionistic fuzzy solutions. Numerical simulations are performed in MATLAB to validate the model results.

## 1. Introduction

Nowadays application of continuous stirred tank reactor (CSTR) has been extended to cover a large number of problems. As an example the compartmental model which have been widely used to analyze a variety of problems in biological and environmental engineering. Let us consider the case of phosphorus release in lake water through compartmental model. Release of phosphatic and nitrogenous substances into a water body through anthropogenic activities causes 'eutrophication', due to the eutrophication phytoplankton, periphyton and macrophytes grows excessively, which creates problem in lake water such as loss of dissolved oxygen, odor, color and aquatic life problems (Schnoor, 2006). Let us consider the case when the lake receives wastewater containing phosphates. The phosphates partly settle down with the sediments. In the stratified condition, only little oxygen reaches the water at the bottom, and bottom sediment experiences essentially anaerobic condition under which release of phosphorus into the water ('sediment feedback') occurs simultaneously. Some of the researcher devoted their time to model the release of phosphate in the lake water. Chapra and Canale (1991) [1] proposed a two-compartment model for the phosphate concentration in the sediment layer at the bottom of lake.

So many problem arises due to the release of phosphorus in to the lake water. In the last few decades the researchers devoted their time to develop the compartmental models to describe the problems of lake water due to the release of phosphorus [2–8]. Gentleman 2002 [9] describe the marine plankton models. But till now no action has been taken to describe the phosphorus release model in to the lake water mathematically.

Uncertainty plays a crucial role in the field of phosphorus release in the sediment layer of lake. Due to the lack of data, insufficient supply of data, technical fault and environmental fluctuation, uncertainty comes into the biological and environmental system. To handle these type of noise into the environment, nowadays the researchers are eager to frame there mathematical model of phosphorus release in the sediment of lake water through FDEs approach to get realistic scenario.

Fuzzy differential equation is widely explored in various fields such as engineering, biology, physics etc. [10–19]. Optimization of renewable resource by population in imprecise nature is given in [20]. Dynamical behavior of Malaria disease modsel is described in crisp and fuzzy environment [21]. Dynamical behavior of prey–predator model with MSY policy under different harvesting strategy is described in imprecise environment [22]. Fuzzy set theory plays an important role to model different type of real life situations. The concept of fuzzy number and fuzzy set is a major concern today. Zadeh [23] and Dubois and Parade [24] are the pioneer of fuzzy set theory. Intuitionistic fuzzy set theory (IFST) is the generalization of fuzzy set theory [23].

* Corresponding author.
*E-mail address:* animeshmahata8@gmail.com (A. Mahata).

https://doi.org/10.1016/j.health.2023.100294
Received 17 October 2023; Received in revised form 11 December 2023; Accepted 18 December 2023
Available online 19 December 2023

The pioneering work of intuitionistic fuzzy set theory was done by Atanassov [25–27] which is the generalization of fuzzy set theory developed by Zadeh [23] and Dubois and Parade [24]. The degree of belongingness and non belongingness is considered in fuzzy set theory but there is a hesitation in the degree of membership function, whereas IFST is the most applicable method to model the hesitation and uncertainty with the help of additional degree of the membership function and non-membership function [28].

In the last few years intutionistic fuzzy set theory (IFST), becomes more demandable. It is used in several industries, robotics, to control the complex process, in transmission of energy, in audiovisual systems etc. So many researchers devoted their time to develop intuitionistic fuzzy set theory. Atanassov mention the notion of intuitionistic fuzzy set theory [25–27]. Melliani et al. [29] give the conception of intuitionistic fuzzy metric space. Melliani et al. [30] established the existence and uniqueness theorem of the solution of intuitionistic fuzzy differential equation with nonlocal condition. So many researchers devoted their time to study intuitionistic fuzzy differential equation numerically [31–34]. The theories of interval valued IFST and its application are described in [35–37]. The theory of triangular Atanassov intuitionistic fuzzy set theory are described in [38]. The application of IFST is a major concern today [39–41]. So nowadays intuitionistic fuzzy set theory is a well defined theory, which is nothing but the generalization of fuzzy set theory proposed by Zadeh. Unfortunately till now it is not widely used to describe the dynamical behavior of mathematical model of environmental system.

Furthermore we can develop our model with the help of neutrosophic fuzzy set theory. Because neutrosophic fuzzy set theory is more generalization of intutionistic fuzzy set theory [42–45].

In this paper, apply the theory of IFST in a compartmental model of phosphorus release in the sediment of lake water and analyze the dynamics of it with uncertainty. The Preliminaries are given in Section 2, In the next section i.e. in Section 3, we introduce the formulation of mathematical model. Section 4 is devoted for model analysis in intuitionistic fuzzy environment when the both compartment i.e. first compartment $c_1(t)$ and second compartment $c_2(t)$ are i-gH differentiable, $c_1(t)$ is i-gH and $c_2(t)$ is ii-gH differentiable, $c_1(t)$ is ii-gH differentiable and $c_2(t)$ is i-gH differentiable and finally we present the model when both the population are in ii-gH differentiable and give the corresponding results respectively. In next section we give the numerical results of the fuzzy differential equation. Finally we end the paper with discussion and conclusion.

*Motivation and novelty*

In contemporary research, there is a notable shift towards addressing real-world issues within a dynamic context. The study by [10] highlights the environmental impact of carbon emissions from both warehouse electricity and generator fuel usage. Notably, all fuzzy-integrated Multi-Attributive Border Approximation Area Comparison (MABAC) methods consistently identify the same set of optimal and suboptimal healthcare suppliers, showcasing their effectiveness in handling decision makers' judgments and uncertainty related to qualitative criteria. A novel contribution to the optimization of time and cost in life-saving rescue operations is presented in [12]. The paper introduces a unique perspective through a pentagonal type-2 fuzzy variable (PT2FV) defuzzification method, providing a detailed explanation of its application in fuzzy logic. In the realm of health, [13] explores the dynamic behavior of HIV infection. Meanwhile, a gap in the research on two-compartmental phosphorus model in fuzzy environments is identified. While numerous articles have been published in crisp environments, the impact of environmental fluctuations and uncertainties remains unexplored. Fuzzy differential equations emerge as a powerful method to address this, leveraging fuzzy set theory as a crucial tool for modeling uncertain real-life scenarios. The significance of fuzzy set theory is underscored, particularly as fuzzy number theories gain popularity. It is crucial to note that traditional fuzzy set theory only considers the degree of belongingness and non-belongingness. This approach overlooks the level of uncertainty or non-determinacy, which is effectively addressed by intuitionistic fuzzy sets (IFS). Atanassov's work on IFS, characterized by membership and non-membership functions, offers a valuable extension of fuzzy set theory, allowing for a nuanced understanding of uncertainties where the sum of both values may be less than one. This perspective broadens the applicability of fuzzy set theories and aligns with the growing interest in fuzzy number theories and their practical applications. On the contrary, traditional fuzzy sets exclusively consider the degree of acceptance [25–27]. However, recent attention has shifted towards intuitionistic fuzzy sets (IFS), sparking extensive research and applications across various scientific and technological domains. Notably, this paper employs different generalized Hukuhara derivatives tailored for intuitionistic fuzzy-valued functions. The study serves as a model, elucidating the concentration of drugs in two distinct areas. Through the application of generalized Hukuhara intuitionistic fuzzy derivatives, both of type 1 and type 2, the paper establishes a comprehensive model for describing phosphorus model in lake water and sediment. The analysis encompasses stability criteria, exploring both strong and weak solutions for the proposed model. The paper argues for the adoption of intuitionistic fuzzy set theory over traditional fuzzy set theory to capture a more realistic depiction of the given system of differential equations. By delving into the nuances of intuitionistic fuzzy set theory, the research enhances our understanding of the system's behavior. This shift in perspective enables a more nuanced exploration of two compartment phosphorus dynamics, contributing to a broader comprehension of the complex interplay within the given system of differential equations.

### 1.1. Structure of the paper

Useful prerequisites concept put in Section 2. In Section 3 consists of model formulation of two-compartment phosphorus model intuitionistic fuzzy environment. Stability analysis of the model are discussed in Section 4. Section 5 deals with the numerical simulation for different values of $(\alpha, \beta)$-cut of the generalized trapezoidal intuitionistic fuzzy number. Section 6 consists of the conclusion.

## 2. Pre-requisite concept

**Definition 2.1** (*Intuitionistic Fuzzy Set (IFS) [46]*)**.** Let U be a set which is fixed. An IFS $\tilde{B}^i$ in U is an object having the form $\tilde{B}^i = \{\langle x, \chi_{\tilde{B}^i}(x), \rho_{\tilde{B}^i}(x)\rangle : x \in U\}$ where the $\chi_{\tilde{B}^i}(x) : U \to [0,1]$ and $\rho_{\tilde{B}^i}(x) : U \to [0,1]$ represents the degree of membership and degree of non-membership function respectively, for every element $x \in U$ of the set $\tilde{B}^i$ such that $0 \le \chi_{\tilde{B}^i}(x) + \rho_{\tilde{B}^i}(x) \le 1$

**Definition 2.2** (*Intuitionistic Fuzzy Number (IFN) [46]*)**.** An IFN $\tilde{B}^i$ is defined as follows

$(i)$ an intuitionistic fuzzy subject of real line.

$(ii)$ normal,i.e there exist $x_0 \in R$ such that

$\chi_{\tilde{B}^i}(x) = 1$ (so $\rho_{\tilde{B}^i}(x) = 1$

$(iii)$ a convex set for the membership function $\chi_{\tilde{B}^i}(x)$, i.e. $\chi_{\tilde{B}^i}(\lambda x_1 + (1-\lambda)x_2) \ge min(\chi_{\tilde{B}^i}(x_1), \chi_{\tilde{B}^i}(x_2))$ for all $x_1, x_2 \in R, \lambda \in [0,1]$

$(iv)$ a concave set for the non-membership function $\rho_{\tilde{B}^i}(x)$, i.e. $\rho_{\tilde{B}^i}(\lambda x_1 + (1-\lambda)x_2) \ge min(\rho_{\tilde{B}^i}(x_1), \rho_{\tilde{B}^i}(x_2))$ for all $x_1, x_2 \in R, \lambda \in [0,1]$

**Definition 2.3** (*$(\alpha, \beta)$-cut of IFN [47]*)**.** A set of $(\alpha, \beta)$-cut generalized by IFS $\tilde{B}^i$, where $(\alpha, \beta) \in [0,1]$,fixed number such that $\alpha+\beta \le 1$ is defined as $\tilde{B}^i_{(\alpha,\beta)} = \{\langle x, u_{\tilde{B}^i}(x), v_{\tilde{B}^i}(x)\rangle : x \in X, u_{\tilde{B}^i}(x) \ge \alpha, v_{\tilde{B}^i}(x) \le \beta; \alpha, \beta \in [0,1]\}$

$(\alpha, \beta)$-cut denoted by $\tilde{B}^i_{(\alpha,\beta)}$ as the crisp elements of $x$ belongs to $\tilde{B}^i$ at least to the degree $\alpha$ and which belongs to $\tilde{B}^i$ at most to the degree $\beta$

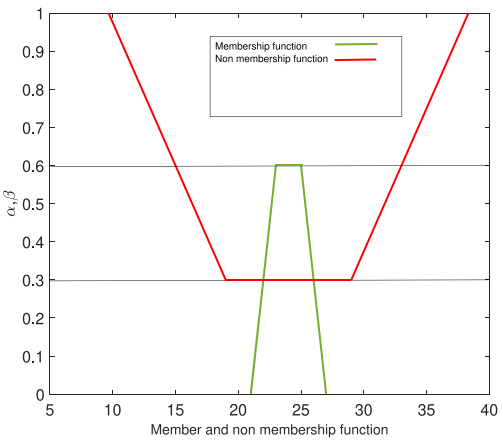


**Fig. 1.** Generalized trapezoidal intuitionistic fuzzy number.

**Definition 2.4** (*Generalized Trapezoidal Intuitionistic Fuzzy Number (Gtrifn): [48]*)**.** A generalized trapezoidal intuitionistic fuzzy number $\tilde{S}^i = \langle (b_1, b_2, b_3, b_4; \rho), (b_1', b_2, b_3, b_4'; \kappa)\rangle$ of IFN on subset of real number R,with following the membership and non-membership function of $\tilde{d}^i$ as,

$$\begin{aligned} &= \tfrac{y-b_1}{b_2-b_1}\rho, && if\, b_1 \le y < b_2 \\ u_{\tilde{d}^i}(y) &= \rho, && if\, b_2 \le y \le b_3 \\ &= \tfrac{b_4-y}{b_4-b_3}\rho, && if\, b_3 < y \le b_4 \\ &= 0, && otherwise \end{aligned}$$

$$\begin{aligned} &= \tfrac{b_2-y}{b_2-b_1'}\kappa, && if\, b_1' \le y < b_2 \\ u_{\tilde{d}^i}(y) &= \kappa, && if\, b_2 \le y \le b_3 \\ &= \tfrac{y-b_3}{b_4'-b_3}\kappa, && if\, b_3 < y \le b_4' \\ &= 0, && otherwise \end{aligned}$$

where $b_1' \le b_2 \le b_3 \le b_4', b_1 \le b_2 \le b_3 \le b_4$

A $(\alpha, \beta)$-cut of TIFN $\tilde{S}^i = \langle (b_1, b_2, b_3, b_4; \rho), (b_1', b_2, b_3, b_4'; \kappa)\rangle$, is a crisp subset of R, which is defined as, $\tilde{d}^i_\alpha = \{x : u_{\tilde{d}^i}(x) \ge \alpha\}$, $\tilde{d}^i_\beta = \{x : v_{\tilde{d}^i}(x) \le \beta\}$ where $0 \le \rho \le 1, 0 \le \kappa \le 1, 0 \le \rho + \kappa \le 1$ and its $(\alpha, \beta)$-cut can be as follows,

$$[L_{\tilde{d}^i}(\alpha), R_{\tilde{d}^i}(\alpha)] = [b_1 + \frac{\alpha}{\rho}(b_2 - b_1), b_4 - \frac{\alpha}{\rho}(b_4 - b_3)]$$

$$[L_{\tilde{d}^i}(\beta), R_{\tilde{d}^i}(\beta)] = [b_2 - \frac{\beta}{\kappa}(b_2 - b_1'), b_3 + \frac{\beta}{\kappa}(b_4' - b_3)]$$

**Example 1.** Pictorial diagram of GTrIFN is given in Fig. 1.

Consider the GTrIFN, $\tilde{A}_{IFN} = \langle (21, 23, 25, 27; 0.6), (19, 23, 25, 29; 0.3)\rangle$

The parametric form of GTrIFN represented as follows,

$A_{u_1}(\alpha) = 21 + \frac{2}{0.6}\alpha$, $A_{u_2}(\alpha) = 27 - \frac{2}{0.6}\alpha$, $A_{v_1}(\beta) = 23 - \frac{4}{0.3}\beta$, $A_{v_2} = 25 + \frac{4}{0.3}\beta$

**Definition 2.5** (*Generalized Hukuhara Derivative for Intuitionistic Fuzzy Valued (ifv) Function: [46]*)**.** Let $f_{gI} : (a, b) \to R_I$ be a IFV function and $x_0 \in (a, b)$. We say that the function $f_{gI}$ is Hukuhara differentiable at $x_0$ if there exist an element $f'_{gI}(x_0) \in R_I$, such that $\forall h > 0$ sufficiently small

$$f'_{gI}(x_0) = \lim_{h\to 0} \frac{f_{gI}(x_0 + h) \Theta_g f_{gI}(x_0)}{h} = \lim_{h\to 0} \frac{f_{gI}(x_0) \Theta_g f_{gI}(x_0 - h)}{h}$$

Note: Let, $f_{gI} : (a.b) \to R_I$ be a IFV function and $f_{gI}(x)$ is generalized Hukuhara intuitionistic fuzzy (GHIF) derivative at $x_0$ is defined by $f'_{gI}(x_0)$ and defined by,

$$\tilde{f}_{gI}(x) = \langle f_1(x, \alpha; w), f_2(x, \alpha; w), h_1(x, \beta; \sigma), h_2(x, \beta; \sigma)\rangle$$

for each $\alpha \in [0, w], \beta \in [\sigma, 1], 0 < w, \sigma \le 1$.

(i) If $\tilde{f}_{gI}(x)$ is GHIF derivative of type-1 and $f_1(x, \alpha; w), f_2(x, \alpha; w), h_1(x, \beta; \sigma), h_2(x, \beta; \sigma)$ are all differentiable, then

$$[\tilde{f}'_{gI}(x_0)]_{\alpha,\beta} = \langle f_1'(x, \alpha; w), f_2'(x, \alpha; w), h_1'(x, \beta; \sigma), h_2'(x, \beta; \sigma)\rangle$$

(ii) If $\tilde{f}_{gI}(x)$ is GHIF derivative of type-2 and $f_1(x, \alpha; w), f_2(x, \alpha; w), h_2(x, \beta; \sigma), h_1(x, \beta; \sigma)$ are all differentiable, then

$$[\tilde{f}'_{gI}(x_0)]_{\alpha,\beta} = \langle f_1'(x, \alpha; w), f_2'(x, \alpha; w), h_1'(x, \beta; \sigma), h_2'(x, \beta; \sigma)\rangle$$

(iii) If $\tilde{f}_{gI}(x)$ is GHIF derivative of type-3 and $f_1(x, \alpha; w), f_2(x, \alpha; w), h_1(x, \beta; \sigma), h_2(x, \beta; \sigma)$ are all differentiable, then

$$[\tilde{f}'_{gI}(x_0)]_{\alpha,\beta} = \langle f_2'(x, \alpha; w), f_1'(x, \alpha; w), h_1'(x, \beta; \sigma), h_2'(x, \beta; \sigma)\rangle$$

(iv) If $\tilde{f}_{gI}(x)$ is GHIF derivative of type-4 and $f_1(x, \alpha; w), f_2(x, \alpha; w), h_2(x, \beta; \sigma), h_1(x, \beta; \sigma)$ are all differentiable, then

$$[\tilde{f}'_{gI}(x_0)]_{\alpha,\beta} = \langle f_1'(x, \alpha; w), f_2'(x, \alpha; w), h_2'(x, \beta; \sigma), h_1'(x, \beta; \sigma)\rangle$$

Note: Let $G^*$ be the set of all intutionistic fuzzy valued functions $\tilde{t}, \tilde{k} \in G^*$. If there exist a intuitionistic fuzzy number, $\tilde{\xi}$ and satisfy the relation $\tilde{t} = \tilde{\xi} + \tilde{k}$, then $\tilde{\xi}$ is considered to be Hukuhara difference of $\tilde{t}$ and $\tilde{k}$, denoted by $\tilde{\xi} = \tilde{t} \ominus_g \tilde{k}$.

**Definition 2.6** (*Strong and Weak Solution of Intuitionistic Fuzzy Differential Equation (IFDE): [49]*)**.** Consider the differential equation $\frac{dx(t)}{dt} = kx(t)$, with the initial condition $x(t_0) = x_0$ is called intuitionistic fuzzy differential equation of any one or both of k and $x_0$ are intuitionistic fuzzy numbers.

Let the solution of the above intuitionistic differential equation be $x(t)$ and its $(\alpha, \beta)$ cut be

$\tilde{x}(t, \alpha, \beta) = \langle [x_{a1}(t, \alpha), x_{a2}(t, \alpha)], [x_{b1}(t, \beta), x_{b2}(t, \beta)]\rangle$

The solution is a strong solution if

$(i)\frac{dx_{a1}(t,\alpha)}{d\alpha} > 0$, $\frac{dx_{a2}(t,\alpha)}{d\alpha} < 0, \forall \alpha \in [0, 1]$, $x_{a1}(1) \le x_{a2}(1)$

and, $(ii)\frac{dx_{b1}(t,\beta)}{d\beta} < 0$, $\frac{dx_{b2}(t,\beta)}{d\beta} > 0, \forall \beta \in [0, 1]$, $x_{b1}(0) \le x_{b2}(0)$

Otherwise the solution is weak solution.

### 2.7 Properties on intuitionistic fuzzy number: [47]

Let, $\tilde{S}^i = \langle (b_1, b_2, b_3, b_4; \rho_1), (b_1', b_2, b_3, b_4'; \kappa_1)\rangle$ and $\tilde{T}^i = \langle (r_1, r_2, r_3, r_4; \rho_2), (r_1', r_2, r_3, r_4'; \kappa_2)\rangle$ be two GtrIFN then,

(i) $\tilde{S}^i \oplus \tilde{T}^i =< (b_1 + r_1, b_2 + r_2, b_3 + r_3, b_4 + r_4; \rho), (b_1' + r_1', b_2 + r_2, b_3 + r_3, b_4' + r_4'; \kappa)$ where, $\rho = min\{\rho_1, \rho_2\}, \kappa = min\{\kappa_1, \kappa_2\}$

(ii) $\tilde{S}^i \ominus \tilde{T}^i =< (b_1 - r_1, b_2 - r_2, b_3 - r_3, b_4 - r_4; \rho), (b_1' - r_1', b_2 - r_2, b_3 - r_3, b_4' - r_4'; \kappa)$ where, $\rho = min\{\rho_1, \rho_2\}, \kappa = min\{\kappa_1, \kappa_2\}$

(iii) $\lambda.\tilde{S}^i = \langle (\lambda b_1, \lambda b_2, \lambda b_3, \lambda b_4; \rho_1), (\lambda b_1', \lambda b_2, \lambda b_3, \lambda b_4'; \rho_1)\rangle, \lambda \ne 0$

(iv) $\tilde{S}^i \otimes \tilde{T}^i =< (b_1 r_1, b_2 r_2, b_3 r_3, b_4 r_4; \rho), (b_1' r_1', b_2 r_2, b_3 r_3, b_4' r_4'; \kappa)$ where, $\rho = min\{\rho_1, \rho_2\}, \kappa = min\{\kappa_1, \kappa_2\}$

(v) $\tilde{S}^i / \tilde{T}^i =< (\frac{b_1}{r_1}, \frac{b_2}{r_2}, \frac{b_3}{r_3}, \frac{b_4}{r_4}; \rho), (\frac{b_1'}{r_1'}, \frac{b_2}{r_2}, \frac{b_3}{r_3}, \frac{b_4'}{r_4'}; \kappa)$ where, $\rho = min\{\rho_1, \rho_2\}, \kappa = min\{\kappa_1, \kappa_2\}$

**Example 2.** Consider the two GrTIFN $\tilde{S}^i = \langle (5, 6, 7, 8; 0.3), (4, 6, 7, 11; 0.6)\rangle$ and $\tilde{T}^i =< (9, 11, 13, 16; 0.3), (8, 11, 13, 17; 0.6) >$, then the addition, subtraction, multiplication and division properties on IFN is defined by,

(i) $\tilde{S}^i \oplus \tilde{T}^i = \langle (14, 17, 20, 24; 0.3), (12, 17, 20, 28; 0.6)\rangle$

(ii) $\tilde{S}^i \ominus \tilde{T}^i = \langle (4, 5, 6, 8; 0.3), (4, 5, 6, 6; 0.6)\rangle$

(iii) $\lambda.\tilde{S}^i = \langle (10, 12, 14, 16; 0.3), (8, 12, 14, 22; 0.6)\rangle$, where $\Lambda = 2$ (iv) $\tilde{S}^i \otimes \tilde{T}^i = \langle (45, 66, 91, 108; 0.6), (32, 66, 91, 187; 0.3)\rangle$

(v) $\tilde{S}^i / \tilde{T}^i = \langle (\frac{5}{9}, \frac{6}{11}, \frac{7}{13}, \frac{8}{16}; 0.3), (\frac{4}{8}, \frac{6}{11}, \frac{7}{13}, \frac{11}{17}; 0.3)\rangle$

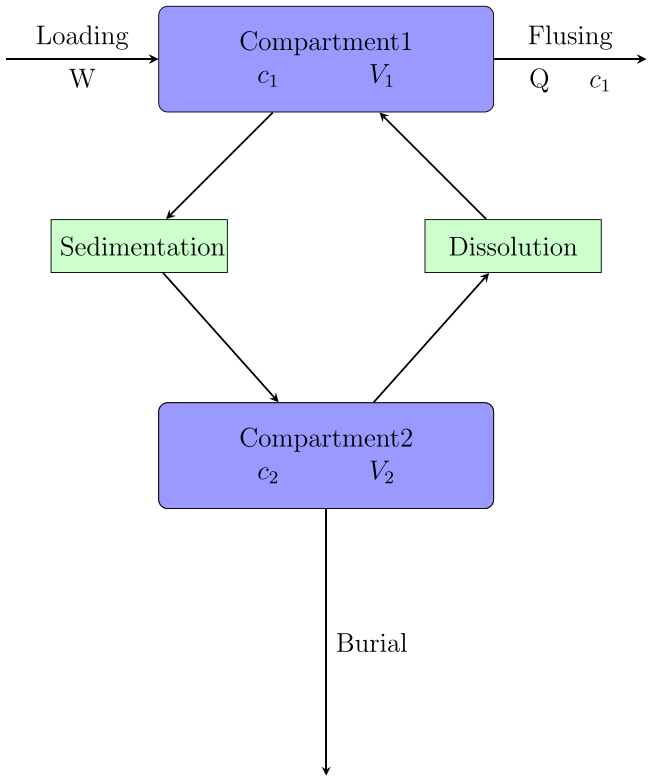


**Fig. 2.** Schematic diagram of proposed system (1).

## 3. Model formulation

Loading of phosphorus through the influent water occurs at a rate of W kg/year. Flushing of the lake occurs at a rate of Q ($cm^3$/year) and some phosphorus loss occurs in the flush water. Transport of phosphorus compartment 1 to the surface sediment is quantified by a setting velocity $V_s$ (m/year) and the area of the sediment is A. Recycling of phosphorus from the surface sediment to the water occurs with a mass transfer coefficient $K_s$(m/year) and the area of mass transfer remains the same i.e. A $m^2$. Burial of phosphorus occurs at the deep sediment characterized by a burial mass transfer coefficient $K_b$.

Two compartment phosphorus model [50] can be written as follows:

$$\begin{aligned} v_1\frac{dc_1(t)}{dt} &= W - Qc_1(t) - V_sAc_1(t) + K_sAc_2(t), \\ v_2\frac{dc_2(t)}{dt} &= V_sAc_1(t) - K_sAc_2(t) - K_bAc_2(t), \end{aligned} \tag{1}$$

With the initial condition, $c_1(t_0) = c_{01}, c_2(t_0) = c_{02}$

Compartment 1 contains a volume $V_1$ of water having a phosphorus concentration of $c_1$. The 'surface Sediment' constitutes compartment 2. It has a volume $V_2$ and a 'lumped' phosphorus concentration $c_2$. The above system (1) can be rewritten as follows:

$$\begin{aligned} \frac{dc_1(t)}{dt} &= \frac{W}{v_1} - \frac{Q}{v_1}c_1(t) - \frac{V_sA}{v_1}c_1(t) + \frac{K_sA}{v_1}c_2(t), \\ \frac{dc_2(t)}{dt} &= \frac{V_sA}{v_2}c_1(t) - \frac{K_sA}{v_2}c_2(t) - \frac{K_bA}{v_2}c_2(t), \end{aligned} \tag{2}$$

with the initial condition, $c_1(t_0) = c_{01}, c_2(t_0) = c_{02}$

The above crisp model converted in intuitionistic fuzzy environment given as follows:

$$\begin{aligned} \frac{d\tilde{c_1}(t)}{dt} &= \frac{W}{v_1} - \frac{Q}{v_1}\tilde{c_1}(t) - \frac{V_sA}{v_1}\tilde{c_1}(t) + \frac{K_sA}{v_1}\tilde{c_2}(t), \\ \frac{d\tilde{c_2}(t)}{dt} &= \frac{V_sA}{v_2}\tilde{c_1}(t) - \frac{K_sA}{v_2}\tilde{c_2}(t) - \frac{K_bA}{v_2}\tilde{c_2}(t), \end{aligned} \tag{3}$$

with the initial condition, $\tilde{c_1}(t_0) = \tilde{c_{01}}, \tilde{c_2}(t_0) = \tilde{c_{02}}$

## 4. Phosphorus compartment model in intuitionistic fuzzy environment

If we apply generalized Hukuhara intuitionistic fuzzy (GHIF) derivative to the proposed intuitionistic phosphorus model, then the following different cases arise as

(i) $\tilde{c_1}(t)$, $\tilde{c_2}(t)$ both are GHIF derivative of type 1
(ii) $\tilde{c_1}(t)$, $\tilde{c_2}(t)$ both are GHIF derivative of type 2
(iii) $\tilde{c_1}(t)$, $\tilde{c_2}(t)$ both are GHIF derivative of type 3
(iv) $\tilde{c_1}(t)$, $\tilde{c_2}(t)$ both are GHIF derivative of type 4
(v) $\tilde{c_1}(t)$ is a GHIF derivative of type 1 and $\tilde{c_2}(t)$ is GHIF derivative of type 2
(vi) $\tilde{c_1}(t)$ is a GHIF derivative of type 1 and $\tilde{c_2}(t)$ is GHIF derivative of type 3
(vii) $\tilde{c_1}(t)$ is a GHIF derivative of type 1 and $\tilde{c_2}(t)$ is GHIF derivative of type 4
(viii) $\tilde{c_1}(t)$ is a GHIF derivative of type 2 and $\tilde{c_2}(t)$ is GHIF derivative of type 1
(ix) $\tilde{c_1}(t)$ is a GHIF derivative of type 2and $\tilde{c_2}(t)$ is GHIF derivative of type 3
(x) $\tilde{c_1}(t)$ is a GHIF derivative of type 2 and $\tilde{c_2}(t)$ is GHIF derivative of type 4
(xi) $\tilde{c_1}(t)$ is a GHIF derivative of type 3 and $\tilde{c_2}(t)$ is GHIF derivative of type 1
(xii) $\tilde{c_1}(t)$ is a GHIF derivative of type 3 and $\tilde{c_2}(t)$ is GHIF derivative of type 2
(xiii) $\tilde{c_1}(t)$ is a GHIF derivative of type 3 and $\tilde{c_2}(t)$ is GHIF derivative of type 4
(xiv) $\tilde{c_1}(t)$ is a GHIF derivative of type 4 and $\tilde{c_2}(t)$ is GHIF derivative of type 1
(xv) $\tilde{c_1}(t)$ is a GHIF derivative of type 4 and $\tilde{c_2}(t)$ is GHIF derivative of type 2
(xvi) $\tilde{c_1}(t)$ is a GHIF derivative of type 4 and $\tilde{c_2}(t)$ is GHIF derivative of type 3

It is not important to show all the cases. If anyone can understand the techniques for any one of the cases then he can simply find the other cases result. For this paper we take only three cases as follows-

### *4.1. Two compartment phosphorus model with initial condition are intuitionistic fuzzy numbers*

#### *4.1.1. Case 1: When $\tilde{c_1}(t)$ and $\tilde{c_2}(t)$ both are GHIF derivative of type-1*

The two compartment phosphorus model (3) converted into following system of IFDE as follows:

$$\begin{aligned} \frac{dc_{1p}(t,\alpha)}{dt} &= \frac{W}{v_1} - \frac{Q}{v_1}c_{1q}(t,\alpha) - \frac{V_sA}{v_1}c_{1q}(t,\alpha) + \frac{K_sA}{v_1}c_{2p}(t,\alpha) \\ \frac{dc_{1q}(t,\alpha)}{dt} &= \frac{W}{v_1} - \frac{Q}{v_1}c_{1p}(t,\alpha) - \frac{V_sA}{v_1}c_{1p}(t,\alpha) + \frac{K_sA}{v_1}c_{2q}(t,\alpha) \\ \frac{dc_{1r}(t,\beta)}{dt} &= \frac{W}{v_1} - \frac{Q}{v_1}c_{1u}(t,\beta) - \frac{V_sA}{v_1}c_{1u}(t,\beta) + \frac{K_sA}{v_1}c_{2r}(t,\beta) \\ \frac{dc_{1u}(t,\beta)}{dt} &= \frac{W}{v_1} - \frac{Q}{v_1}c_{1r}(t,\beta) - \frac{V_sA}{v_1}c_{1r}(t,\beta) + \frac{K_sA}{v_1}c_{2u}(t,\beta) \\ \frac{dc_{2p}(t,\alpha)}{dt} &= \frac{V_sA}{v_2}c_{1p}(t,\alpha) - \frac{K_sA}{v_2}c_{2q}(t,\alpha) - \frac{K_bA}{v_2}c_{2q}(t,\alpha) \\ \frac{dc_{2q}(t,\alpha)}{dt} &= \frac{V_sA}{v_2}c_{1q}(t,\alpha) - \frac{K_sA}{v_2}c_{2p}(t,\alpha) - \frac{K_bA}{v_2}c_{2p}(t,\alpha) \\ \frac{dc_{2r}(t,\beta)}{dt} &= \frac{V_sA}{v_2}c_{1r}(t,\beta) - \frac{K_sA}{v_2}c_{2u}(t,\beta) - \frac{K_bA}{v_2}c_{2u}(t,\beta) \\ \frac{dc_{2u}(t,\beta)}{dt} &= \frac{V_sA}{v_2}c_{1u}(t,\beta) - \frac{K_sA}{v_2}c_{2r}(t,\beta) - \frac{K_bA}{v_2}c_{2r}(t,\beta) \end{aligned} \tag{4}$$

with the initial condition,

$$c_{1p}(t_0,\alpha) = c_{01p}(\alpha), c_{1q}(t_0,\alpha) = c_{01q}(\alpha), c_{1r}(t_0,\beta) = c_{01r}(\beta), c_{1u}(t_0,\beta) = c_{01u}(\beta)$$
$$c_{2p}(t_0,\alpha) = c_{02p}(\alpha), c_{2q}(t_0,\alpha) = c_{02q}(\alpha), c_{2r}(t_0,\beta) = c_{02r}(\beta), c_{2u}(t_0,\beta) = c_{02u}(\beta)$$

The $(\alpha,\beta)$-cut of $\tilde{c_1}(t), \tilde{c_2}(t)$ is given by,

$$\tilde{c_1}(t,\alpha,\beta) = \langle c_{1p}(t,\alpha), c_{1q}(t,\alpha), c_{1r}(t,\beta), c_{1u}(t,\beta)\rangle$$
$$\tilde{c_2}(t,\alpha,\beta) = \langle c_{2p}(t,\alpha), c_{2q}(t,\alpha), c_{2r}(t,\beta), c_{2u}(t,\beta)\rangle$$

*4.1.1.1 Existence of equilibrium point:* The transformed model (4) have coexistence of equilibrium point which is $E_p^1(c_{1p}^*(t,\alpha), c_{1q}^*(t,\alpha), c_{1r}^*(t,\beta), c_{1u}^*(t,\beta) c_{2p}^*(t,\alpha), c_{2q}^*(t,\alpha), c_{2r}^*(t,\beta), c_{2u}^*(t,\beta))$ where, $c_{1p}^*(t,\alpha) = c_{1q}^*(t,\alpha) = c_{1r}^*(t,\beta) = c_{1u}^*(t,\beta) = \frac{W(K_b+K_s)}{Q(K_b+K_s)+V_sK_bA}, (K_b+K_s) > 0, V_s > 0, K_b > 0$ $c_{2p}^*(t,\alpha) = c_{2q}^*(t,\alpha) = c_{2r}^*(t,\beta) = c_{2u}^*(t,\beta) = \frac{W.V_s}{Q(K_b+K_s)+V_sK_bA}, (K_b+K_s) > 0, V_s > 0, K_b > 0$

*4.1.1.2 Stability analysis:*

**Theorem 1.** *The transformed model (4) is unstable at* $E_p^1$.

**Proof.** The variational matrix at $E_p^1$ is given by,

$$V_{p_1}^* = \begin{pmatrix} 0 & x_1 & 0 & 0 & \frac{V_sA}{V_2} & 0 & 0 & 0 \\ x_1 & 0 & 0 & 0 & 0 & \frac{V_sA}{V_2} & 0 & 0 \\ 0 & 0 & 0 & x_1 & 0 & 0 & \frac{V_sA}{V_2} & 0 \\ 0 & 0 & x_1 & 0 & 0 & 0 & 0 & \frac{V_sA}{V_2} \\ \frac{K_sA}{V_1} & 0 & 0 & 0 & 0 & x_2 & 0 & 0 \\ 0 & \frac{K_sA}{V_1} & 0 & 0 & x_2 & 0 & 0 & 0 \\ 0 & 0 & \frac{K_sA}{v_1} & 0 & 0 & 0 & 0 & x_2 \\ 0 & 0 & 0 & \frac{K_sA}{V_1} & 0 & 0 & x_2 & 0 \end{pmatrix}.$$

where, $x_1 = -\frac{(Q+V_sA)}{v_1}, x_2 = -\frac{A(K_s+K_b)}{v_2}$

If $\rho_1$ is the eigenvalue of $V_{p_1}^*$, then the characteristic equation of $V_{p_1}^*$ becomes

$$(\rho_1^2 - (\tfrac{Q+V_sA}{v_1})^2)^2(\rho_1^2 - l_1^2)^2 = 0$$

where, $l_1 = \frac{A}{v_2}[\frac{Q(K_b+K_s)+V_sK_sA}{(Q+V_sA)}]$

The eigenvalues of $V_{p_1}^*$ are, $\frac{Q+V_sA}{v_1}, -\frac{Q+V_sA}{v_1}, \frac{Q+V_sA}{v_1}, -\frac{Q+V_sA}{v_1}, l_1, -l_1, l_1, -l_1$. Since 1st, 3rd, 5th and 7th eigenvalues are positive. Therefore, the coexistence of equilibrium point $E_p^1$ of the system (4) is unstable.

*4.1.2 Case 2: When $\tilde{c_1}(t)$ and $\tilde{c_2}(t)$ both are GHIF derivative of type-2*

The two compartment phosphorus model (3) transformed into system of IFDE as follows:

$$\begin{aligned}
\frac{dc_{1p}(t,\alpha)}{dt} &= \frac{W}{v_1} - \frac{Q}{v_1}c_{1p}(t,\alpha) - \frac{V_sA}{v_1}c_{1p}(t,\alpha) + \frac{K_sA}{v_1}c_{2q}(t,\alpha) \\
\frac{dc_{1q}(t,\alpha)}{dt} &= \frac{W}{v_1} - \frac{Q}{v_1}c_{1p}(t,\alpha) - \frac{V_sA}{v_1}c_{1p}(t,\alpha) + \frac{K_sA}{v_1}c_{2q}(t,\alpha) \\
\frac{dc_{1r}(t,\beta)}{dt} &= \frac{W}{v_1} - \frac{Q}{v_1}c_{1r}(t,\beta) - \frac{V_sA}{v_1}c_{1r}(t,\beta) + \frac{K_sA}{v_1}c_{2r}(t,\beta) \\
\frac{dc_{1u}(t,\beta)}{dt} &= \frac{W}{v_1} - \frac{Q}{v_1}c_{1r}(t,\beta) - \frac{V_sA}{v_1}c_{1r}(t,\beta) + \frac{K_sA}{v_1}c_{2u}(t,\beta) \\
\frac{dc_{2p}(t,\alpha)}{dt} &= \frac{V_sA}{v_2}c_{1q}(t,\alpha) - \frac{K_sA}{v_1}c_{2p}(t,\alpha) - \frac{K_bA}{v_2}c_{2p}(t,\alpha) \\
\frac{dc_{2q}(t,\alpha)}{dt} &= \frac{V_sA}{v_2}c_{1p}(t,\alpha) - \frac{K_sA}{v_2}c_{2q}(t,\alpha) - \frac{K_bA}{v_2}c_{2q}(t,\alpha) \\
\frac{dc_{2r}(t,\beta)}{dt} &= \frac{V_sA}{v_2}c_{1u}(t,\beta) - \frac{K_sA}{v_2}c_{2r}(t,\beta) - \frac{K_bA}{v_2}c_{2r}(t,\beta) \\
\frac{dc_{2u}(t,\beta)}{dt} &= \frac{V_sA}{v_2}c_{1r}(t,\beta) - \frac{K_sA}{v_2}c_{2u}(t,\beta) - \frac{K_bA}{v_2}c_{2u}(t,\beta)
\end{aligned} \tag{5}$$

with the initial condition,

$$c_{1p}(t_0,\alpha) = c_{01p}(\alpha), c_{1q}(t_0,\alpha) = c_{01q}(\alpha), c_{1r}(t_0,\beta) = c_{01r}(\beta), c_{1u}(t_0,\beta) = c_{01u}(\beta)$$
$$c_{2p}(t_0,\alpha) = c_{02p}(\alpha), c_{2q}(t_0,\alpha) = c_{02q}(\alpha), c_{2r}(t_0,\beta) = c_{02r}(\beta), c_{2u}(t_0,\beta) = c_{02u}(\beta)$$

The $(\alpha,\beta)$-cut of $\tilde{c_1}(t), \tilde{c_2}(t)$ is given by,

$$\tilde{c_1}(t,\alpha,\beta) = \langle c_{1p}(t,\alpha), c_{1q}(t,\alpha), c_{1r}(t,\beta), c_{1u}(t,\beta)\rangle$$
$$\tilde{c_2}(t,\alpha,\beta) = \langle c_{2p}(t,\alpha), c_{2q}(t,\alpha), c_{2r}(t,\beta), c_{2u}(t,\beta)\rangle$$

*4.1.2.1 Existence of equilibrium point:* The transformed model (5) have coexistence of equilibrium point which is $E_p^2(c_{1p}^*(t,\alpha), c_{1q}^*(t,\alpha), c_{1r}^*(t,\beta), c_{1u}^*(t,\beta), c_{2p}^*(t,\alpha), c_{2q}^*(t,\alpha), c_{2r}^*(t,\beta), c_{2u}^*(t,\beta))$ where,

$$c_{1p}^*(t,\alpha) = c_{1q}^*(t,\alpha) = c_{1r}^*(t,\beta) = c_{1u}^*(t,\beta) = \frac{W(K_b+K_s)}{Q(K_b+K_s)+V_sK_bA},$$
$$(K_b+K_s) > 0, V_s > 0, K_b > 0$$
$$c_{2p}^*(t,\alpha) = c_{2q}^*(t,\alpha) = c_{2r}^*(t,\beta) = c_{2u}^*(t,\beta) = \frac{W.V_s}{Q(K_b+K_s)+V_sK_bA},$$
$$(K_b+K_s) > 0, V_s > 0, K_b > 0$$

*4.1.2.2 Stability analysis:*

**Theorem 2.** *The transformed system (5) is locally asymptotically stable (LAS) at* $E_p^2$ *when* $(Q+V_sA) > 0, (K_s+K_b) > 0$.

**Proof.** The variational matrix at $E_p^2$ is given by,

$$V_{p_2}^* = \begin{pmatrix} -y_1 & 0 & 0 & 0 & 0 & \frac{V_sA}{v_2} & 0 & 0 \\ 0 & -y_1 & 0 & 0 & \frac{V_sA}{v_2} & 0 & 0 & 0 \\ 0 & 0 & -y_1 & 0 & 0 & 0 & 0 & \frac{V_sA}{v_2} \\ 0 & 0 & 0 & -y_1 & 0 & 0 & \frac{V_sA}{v_2} & 0 \\ 0 & \frac{K_sA}{v_1} & 0 & 0 & -y_2 & 0 & 0 & 0 \\ \frac{K_sA}{v_1} & 0 & 0 & 0 & 0 & -y_2 & 0 & 0 \\ 0 & 0 & 0 & \frac{K_sA}{v_1} & 0 & 0 & -y_2 & 0 \\ 0 & 0 & \frac{K_sA}{v_1} & 0 & 0 & 0 & 0 & -y_2 \end{pmatrix}.$$

where, $y_1 = \frac{(Q+V_sA)}{v_1}, y_2 = -\frac{(K_s+K_b)A}{v_2}$

Let, $\rho_2$ be the eigenvalue of $V_{p_2}^*$, then the characteristic equation of $V_{p_2}^*$ becomes,

$$[\rho_2 + \tfrac{(Q+V_sA)}{v_1}]^4[\rho_2 + l_2]^4 = 0$$

where, $l_2 = \frac{A}{v_2}[\frac{Q(K_s+K_b)+V_sK_bA}{(Q+V_sA)}]$

The eigenvalues of $V_{p_2}^*$ are $-(\frac{Q+V_sA}{v_1}), -(\frac{Q+V_sA}{v_1}), -(\frac{Q+V_sA}{v_1}), -(\frac{Q+V_sA}{v_1}), -y_1, -y_1, -y_1, -y_1$. Here, all the eigenvalues are negative when $(Q+V_sA) > 0, (K_s+K_b) > 0$. Therefore, the system (5) is locally asymptotically stable(LAS) at coexistence equilibrium point $E_p^2$.

## 5 Numerical simulation

In this section, we have been discussed of the system (4) and (5) rigorous numerical simulation to checked and validate all theoretical calculation by using MATLAB 2018 software. Here, we performed the dynamical behavior of two compartment phosphorus model (2) in the presence of intuitionistic fuzzy environment. To check the effect of fuzzy intuitionistic parameter of the proposed model (2) using the initial condition generalized trapezoidal intuitionistic fuzzy number(GTrIFN) and set all the parameter value mentioned in case 1 and case 2 as follows-

**Case 1: When $\tilde{c_1}(t), \tilde{c_2}(t)$ both are GHIF derivative of type 1:** In this section we considering all the parameter value used in the proposed system (4) are reported in Table 1, Table 2 and rate of two concentration of phosphorus in water at $t = 0$ i.e initial condition of $\tilde{c_1}(t_0), \tilde{c_2}(t_0)$ of the system (4) is taken GrTIFN as

$$\tilde{C}_1(t_0) = \langle(360, 370, 390, 400; 0.6), (350, 370, 390.410; 0.3)\rangle$$
$$\tilde{C}_2(t_0) = \langle(400, 410, 430, 440; 0.6), (390, 410, 430, 460; 0.3)\rangle$$

For the transformed model (4) we set the parameter as follows, $A = 1.5 \times 10^3, V_s = 0.005, K_b = 8.03 \times 10^{-4}, K_s = 0.0031, W = 11410, Q = 1928, v_1 = 53 \times 10^6, v_2 = 8 \times 10^3$

The $(\alpha,\beta)-$ cut of initial condition is given by,

$$\begin{aligned}
\tilde{c_1}_{\alpha,\beta} &= \langle 360 + \tfrac{50\alpha}{3}, 400 - \tfrac{100\alpha}{3}; 370 - 20\beta, 390 + 20\beta\rangle \\
\tilde{c_2}_{\alpha,\beta} &= \langle 400 + \tfrac{50\alpha}{3}, 440 - \tfrac{100\alpha}{3}; 410 - 20\beta, 430 + 30\beta\rangle
\end{aligned} \tag{6}$$

Fig. 3 depicts using the values of Table 2, Table 3 and the above initial condition of $(\alpha,\beta)$-cut of $\tilde{c_1}(t), \tilde{c_2}(t)$ for $\alpha = 0, \beta = 0.3; \alpha = 0.2, \beta =$

**Table 1**
The parameters value.

| Parameters | $A$ | $V_s$ | $K_b$ | $K_s$ | $W$ | $Q$ | $\upsilon_1$ | $\upsilon_2$ |
|---|---|---|---|---|---|---|---|---|
| Value | $1.5\times10^3$ | 0.005 | $8.03\times10^{-4}$ | 0.0031 | 11 410 | 1928 | $53\times10^6$ | $8\times10^3$ |
| Source | [51] | [52] | [51] | [*assumed*] | [51] | [51] | [52] | [51] |

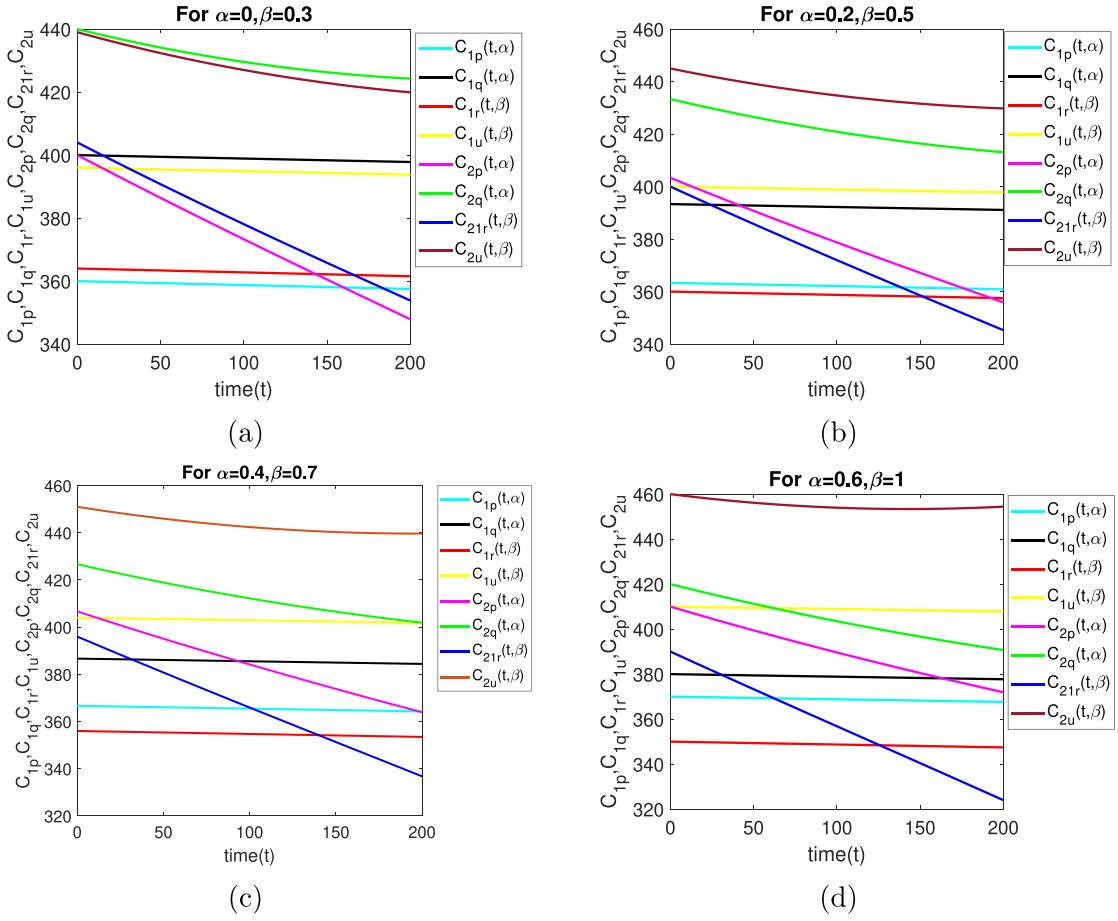


**Fig. 3.** Time series solution of the system (4) in Fig. 3(a) for $\alpha = 0, \beta = 0.3$; in Fig. 3(b) for $\alpha = 0.2, \beta = 0.5$; in Fig. 3(c) for $\alpha = 0.4, \beta = 0.7$; in Fig. 3(d) for $\alpha = 0.6, \beta = 1$ for $t \in [0, 200]$.

**Table 2**
Intuitionistic fuzzy solution of $c_{1_p}(t,\alpha), c_{1_q}(t,\alpha), c_{1_r}(t,\beta), c_{1_u}(t,\beta)$ the system (4) for $t = 100$.

| $\alpha$ | $c_{1_p}(t,\alpha)$ | $c_{1_q}(t,\alpha)$ | $\beta$ | $c_{1_r}(t,\beta)$ | $c_{1_u}(t,\beta)$ |
|---|---|---|---|---|---|
| 0 | 358.7523 | 398.8992 | | | |
| 0.1 | 360.4312 | 395.5597 | | | |
| 0.2 | 362.1101 | 392.2203 | | | |
| 0.3 | 363.7890 | 388.8808 | 0.3 | 362.7670 | 394.8845 |
| 0.4 | 365.4679 | 385.5413 | 0.4 | 360.7597 | 396.8919 |
| 0.5 | 367.1468 | 382.2019 | 0.5 | 358.7523 | 398.8992 |
| 0.6 | 368.8257 | 378.8624 | 0.6 | 356.7450 | 400.9066 |
| | | | 0.7 | 354.7377 | 402.9139 |
| | | | 0.8 | 352.7303 | 404.9212 |
| | | | 0.9 | 350.7230 | 406.9286 |
| | | | 1 | 348.7156 | 408.9359 |

**Table 3**
Intuitionistic fuzzy solution of $c_{2_p}(t,\alpha), c_{2_q}(t,\alpha), c_{2_r}(t,\beta), c_{2_u}(t,\beta)$ of the system (4) for $t = 100$.

| $\alpha$ | $c_{2_p}(t,\alpha)$ | $c_{2_q}(t,\alpha)$ | $\beta$ | $c_{2_r}(t,\beta)$ | $c_{2_u}(t,\beta)$ |
|---|---|---|---|---|---|
| 0 | 373.2740 | 429.5792 | | | |
| 0.1 | 375.9994 | 425.2335 | | | |
| 0.2 | 378.7248 | 420.8878 | | | |
| 0.3 | 381.4501 | 416.5421 | 0.3 | 378.0533 | 427.0096 |
| 0.4 | 384.1755 | 412.1964 | 0.4 | 375.0186 | 430.8604 |
| 0.5 | 386.9008 | 407.8507 | 0.5 | 371.9839 | 434.7111 |
| 0.6 | 389.6262 | 403.5051 | 0.6 | 368.9492 | 438.5618 |
| | | | 0.7 | 365.9145 | 442.4126 |
| | | | 0.8 | 362.8798 | 446.2633 |
| | | | 0.9 | 359.8451 | 450.1140 |
| | | | 1 | 356.8104 | 453.9648 |

$0.5; \alpha = 0.4, \beta = 0.7; \alpha = 0.6, \beta = 1$. Time series solution of the system (4) in intuitionistic fuzzy environment,is reflected in Fig. 3. Here in Figs. 3(a), 3(b), 3(c) and 3(d) we see that $c_{1_p}(t,\alpha) \le c_{1_q}(t,\alpha), c_{1_r}(t,\beta) \le c_{1_u}(t,\beta); c_{2_p}(t,\alpha) \le c_{2_q}(t,\alpha), c_{2_r}(t,\beta) \le c_{2_u}(t,\beta)$ where $t \in [0, 200]$. Hence, all the solution of the system (4) verify intuitionistic fuzzy solution where $\alpha \in [0, 0.6], \beta \in [0.3, 1]$ at $t = 100$. From Fig. 2 clearly states that the system (4) is unstable at coexistence equilibrium point.

Table 2 reflects $c_{1_p}(t,\alpha)$ is increasing, $c_{1_q}(t,\alpha)$ is decreasing; $c_{1_r}(t,\beta)$ is decreasing, $c_{1_u}(t,\beta)$ is increasing for $\alpha \in [0, 0.6], \beta \in [0.3, 1]$, for $t = 100$. Hence, $\tilde{c_1}(t)$ gives strong intuitionistic fuzzy solution of the transformed model (4).

Table 3 reflects that $c_{2_p}(t,\alpha)$ is increasing, $c_{2_q}(t,\alpha)$ is decreasing; $c_{2_r}(t,\beta)$ is decreasing, $c_{2_u}(t,\beta)$ is increasing for $\alpha \in [0, 0.6], \beta \in [0.3, 1]$,

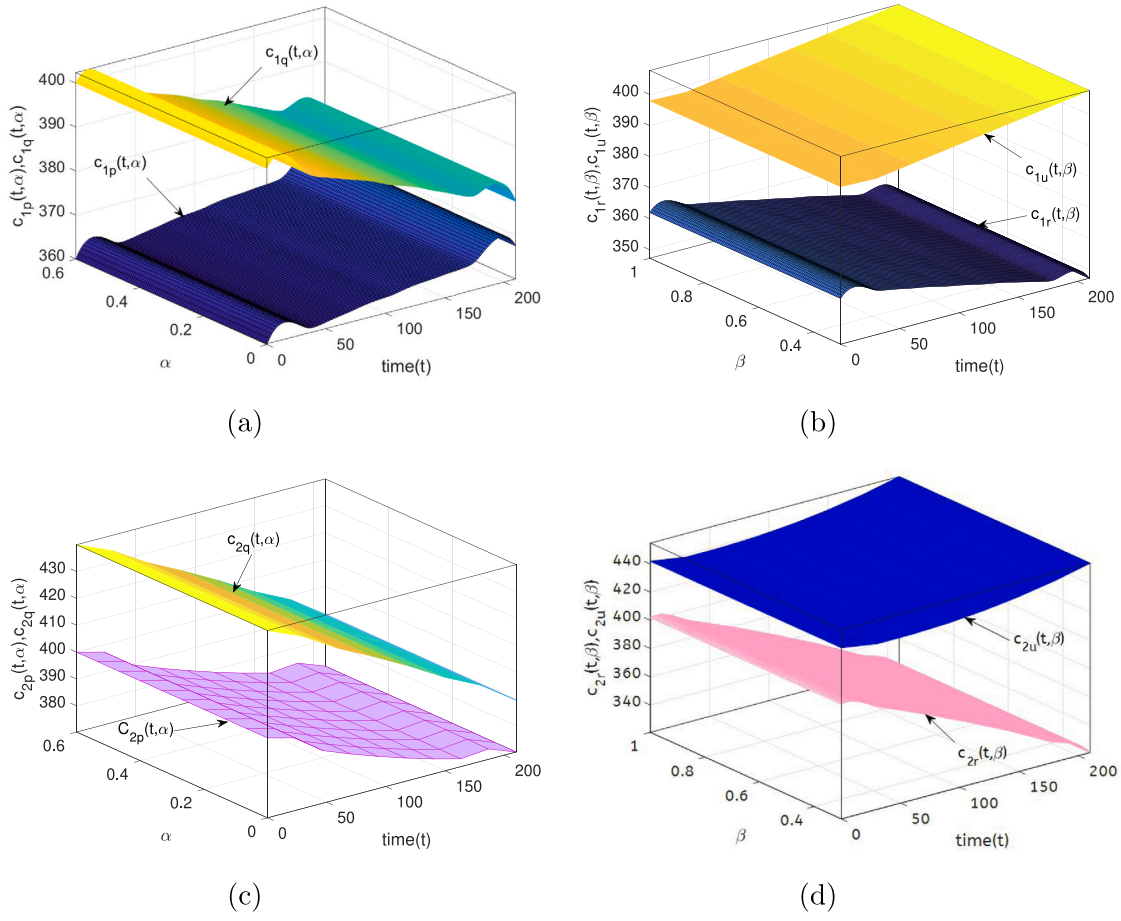


**Fig. 4.** 3D plot in Fig. 4(a) $c_{1_p}(t,\alpha), c_{1_q}(t,\alpha)$ vs. time(t) vs. $\alpha$ where $t \in [0,200], \alpha \in [0,0.6]$; in Fig. 4(b) $c_{1_r}(t,\beta), c_{1_u}(t,\beta)$ vs. time (t) vs. $\beta$ where $t \in [0,200], \beta \in [0.3,1]$; in Fig. 4(c) $c_{2_p}(t,\alpha), c_{2_q}(t,\alpha)$ vs. time(t) vs. $\alpha$ where $t \in [0,200], \alpha \in [0,0.6]$; in Fig. 4(d) $c_{2_r}(t,\beta), c_{2_u}(t,\beta)$ vs. time(t) vs $\beta$ where $t \in [0,200], \beta \in [0.3,1]$.

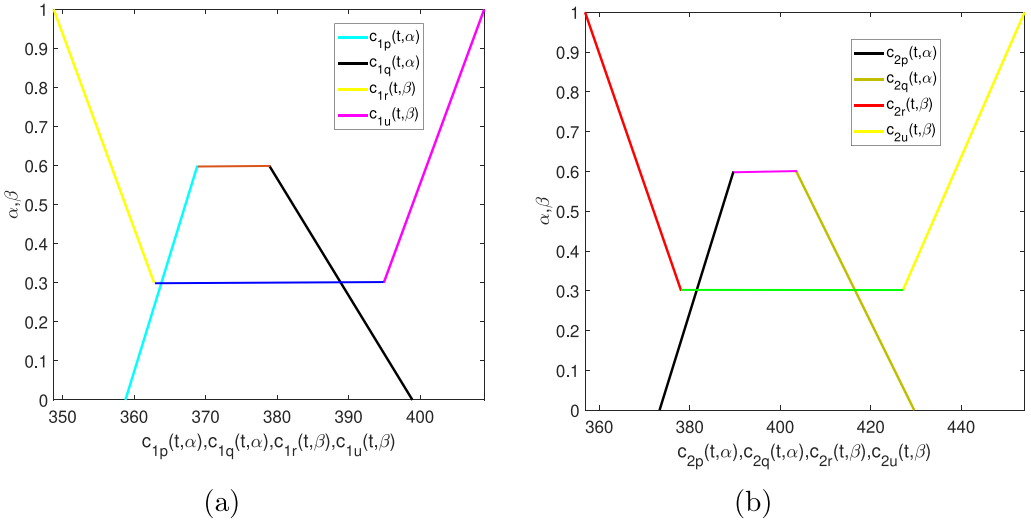


**Fig. 5.** Graph of membership function in Fig. 5(a) for $c_{1_p}(t,\alpha), c_{1_q}(t,\alpha), c_{1_r}(t,\beta), c_{1_u}(t,\beta)$ vs. $\alpha,\beta$ for $t = 100$; in Fig. 5(b) for $c_{2_p}(t,\alpha), c_{2_q}(t,\alpha), c_{2_r}(t,\beta), c_{2_u}(t,\beta)$ vs. $\alpha,\beta$ for $t = 100$ presents GTrIFN.

for $t = 100$. Hence, $\tilde{c_2}(t)$ gives strong intuitionistic fuzzy solution of the transformed model (4).

**Case 2: When $\tilde{c_1}(t), \tilde{c_2}(t)$ both are GHIF derivative of type 2:**

Using the values of $A, K_b, Q, v_1, v_2$ from the above case-1 with the values of $V_s = 0.0035, K_s = 0.00311, W = 114130$ and the $(\alpha,\beta)$-cut reported in (6), the values of $c_{1_p}(t,\alpha), c_{1_q}(t,\alpha), c_{1_r}(t,\beta), c_{1_u}(t,\beta)$ are tabulated in Table 4 and $c_{2_p}(t,\alpha), c_{2_q}(t,\alpha), c_{2_r}(t,\beta), c_{2_u}(t,\beta)$ are also tabulated in Table 5 for different scale of $\alpha \in [0,0.3], \beta \in [0.3,1]$

Fig. 6 depicts using the values in Table 4, Table 5 and taking parametric value $\alpha,\beta$-cut in GTrIFN from (7) of $\tilde{c_1}(t_0)$, $\tilde{c_2}(t_0)$ for $\alpha = 0, \beta = 0.3$; $\alpha = 0.2, \beta = 0.5; \alpha = 0.4, \beta = 0.7; \alpha = 0.6, \beta = 1$ where $t \in [0,2]$. Time series solution of the system (5) in intuitionistic

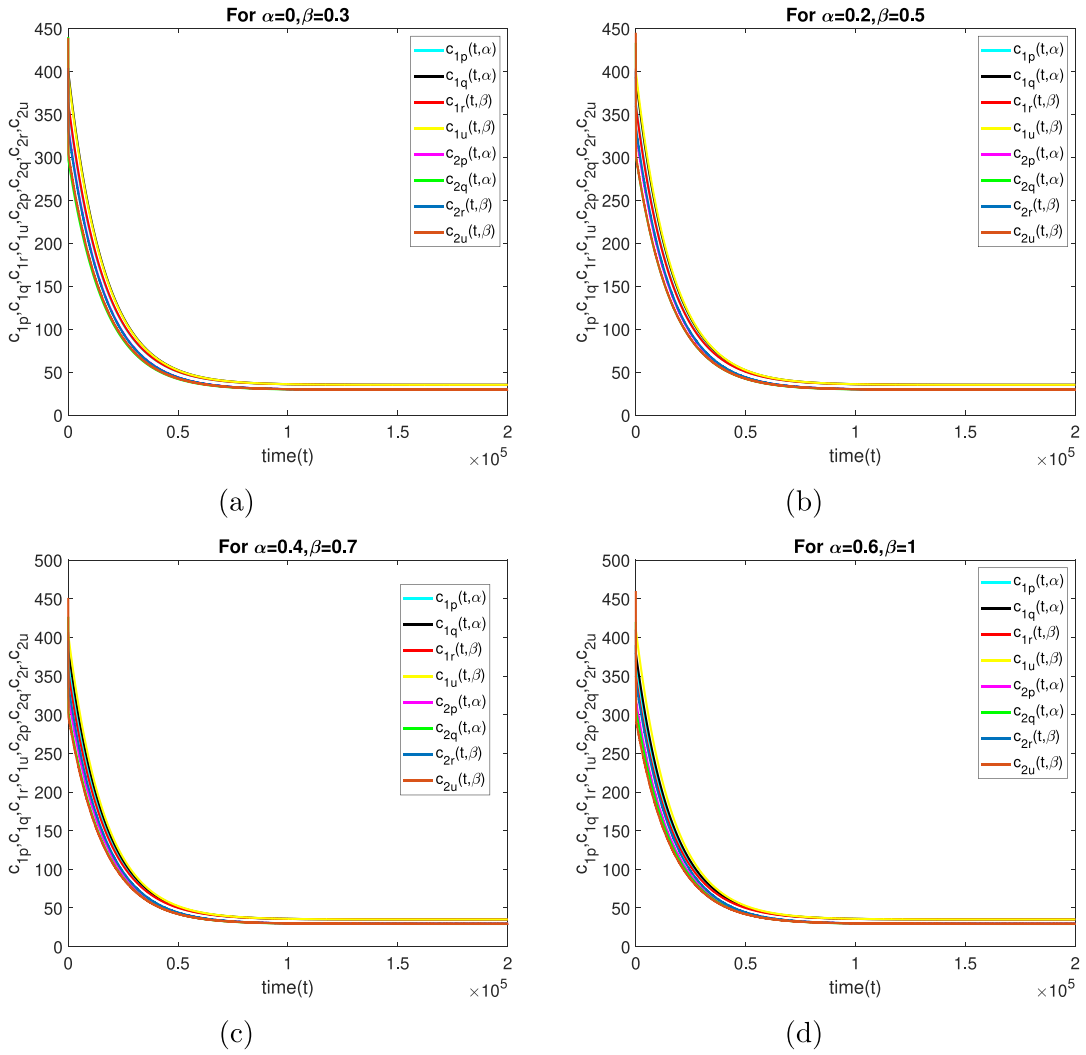


**Fig. 6.** Time series solution of the system (5) in Fig. 6(a) for $\alpha = 0, \beta = 0.3$; in Fig. 6(b) for $\alpha = 0.2, \beta = 0.5$;in Fig. 6(c) for $\alpha = 0.4, \beta = 0.7$; in Fig. 6(d) for $\alpha = 0.6, \beta = 1$ for $t \in [0, 2]$.

**Table 4**
Intuitionistic fuzzy solution of $c_{1_p}(t,\alpha), c_{1_q}(t,\alpha), c_{1_r}(t,\beta), c_{1_u}(t,\beta)$ of the system (5) for $t = 2$.

| $\alpha$ | $c_{1_p}(t,\alpha)$ | $c_{1_q}(t,\alpha)$ | $\beta$ | $c_{1_r}(t,\beta)$ | $c_{1_u}(t,\beta)$ |
|---|---|---|---|---|---|
| 0 | 358.9080 | 398.7620 | | | |
| 0.1 | 360.2292 | 395.4409 | | | |
| 0.2 | 362.2292 | 392..1197 | | | |
| 0.3 | 363.8897 | 388.7985 | 0.3 | 362.8934 | 394.7766 |
| 0.4 | 365.5503 | 385.4773 | 0.4 | 360.9008 | 396.7693 |
| 0.5 | 367.2109 | 382.1561 | 0.5 | 358.9081 | 398.7620 |
| 0.6 | 368.8715 | 378.8349 | 0.6 | 356.9154 | 400.7548 |
| | | | 0.7 | 354.9227 | 402.7475 |
| | | | 0.8 | 352.9300 | 404.7402 |
| | | | 0.9 | 350.9373 | 406.7329 |
| | | | 1 | 348.9446 | 408.7256 |

**Table 5**
Intuitionistic fuzzy solution of $c_{2_p}(t,\alpha), c_{2_q}(t,\alpha), c_{2_r}(t,\beta), c_{2_u}(t,\beta)$ of the system (5) for $t = 2$.

| $\alpha$ | $c_{2_p}(t,\alpha)$ | $c_{2_q}(t,\alpha)$ | $\beta$ | $c_{2_r}(t,\beta)$ | $c_{2_u}(t,\beta)$ |
|---|---|---|---|---|---|
| 0 | 396.9737 | 433.7229 | | | |
| 0.1 | 398.3120 | 430.7403 | | | |
| 0.2 | 399.6502 | 427.7577 | | | |
| 0.3 | 400.9884 | 424.7751 | 0.3 | 400.4381 | 430.9411 |
| 0.4 | 402.3267 | 421.7925 | 0.4 | 398.7059 | 433.6026 |
| 0.5 | 403.6649 | 418.8099 | 0.5 | 396.9737 | 436.2640 |
| 0.6 | 405.0031 | 415.8273 | 0.6 | 395.2415 | 438.9255 |
| | | | 0.7 | 393.5093 | 441.5869 |
| | | | 0.8 | 391.7771 | 444.2484 |
| | | | 0.9 | 390.1449 | 446.9098 |
| | | | 1 | 388.3127 | 449.5713 |

fuzzy environment is reflected in Fig. 6. From Figs. 6(a), 6(b), 6(c) and 6(d) we see that $c_{1_p}(t,\alpha) \le c_{1_q}(t,\alpha), c_{1_r}(t,\beta) \le c_{1_u}(t,\beta); c_{2_p}(t,\alpha) \le c_{2_q}(t,\alpha), c_{2_r}(t,\beta) \le c_{2_u}(t,\beta)$. Hence, all the solution of the system (5) verify intuitionistic fuzzy solution where $\alpha \in [0, 0.6], \beta \in [0.3, 1]$ at $t = 2$. From Fig. 6 we can say that the system (5) is stable at coexistence equilibrium point.

Table 4 reflects $c_{1_p}(t,\alpha)$ is increasing, $c_{1_q}(t,\alpha)$ is decreasing; $c_{1_r}(t,\beta)$ is decreasing, $c_{1_u}(t,\beta)$ is increasing; for $\alpha \in [0, 0.6], \beta \in [0.3, 1]$, for $t = 2$. Hence, $\tilde{c_1}(t)$ gives strong intuitionistic fuzzy solution of the transformed model (5).

Table 5 reflects that $c_{2_p}(t,\alpha)$ is increasing, $c_{2_q}(t,\alpha)$ is decreasing; $c_{2_r}(t,\beta)$ is decreasing, $c_{2_u}(t,\beta)$ is increasing; for $\alpha \in [0, 0.6], \beta \in [0.3, 1]$, for $t = 2$. Hence, $\tilde{c_2}(t)$ gives strong intuitionistic fuzzy solution of the transformed model (5).

### *5.1 Flowchart of two compartment phosphorus model in intutionistic fuzzy environment*

The entire scenario in this paper are describe in flow chart for the proposed algorithm and the diagram given in Fig. 9:

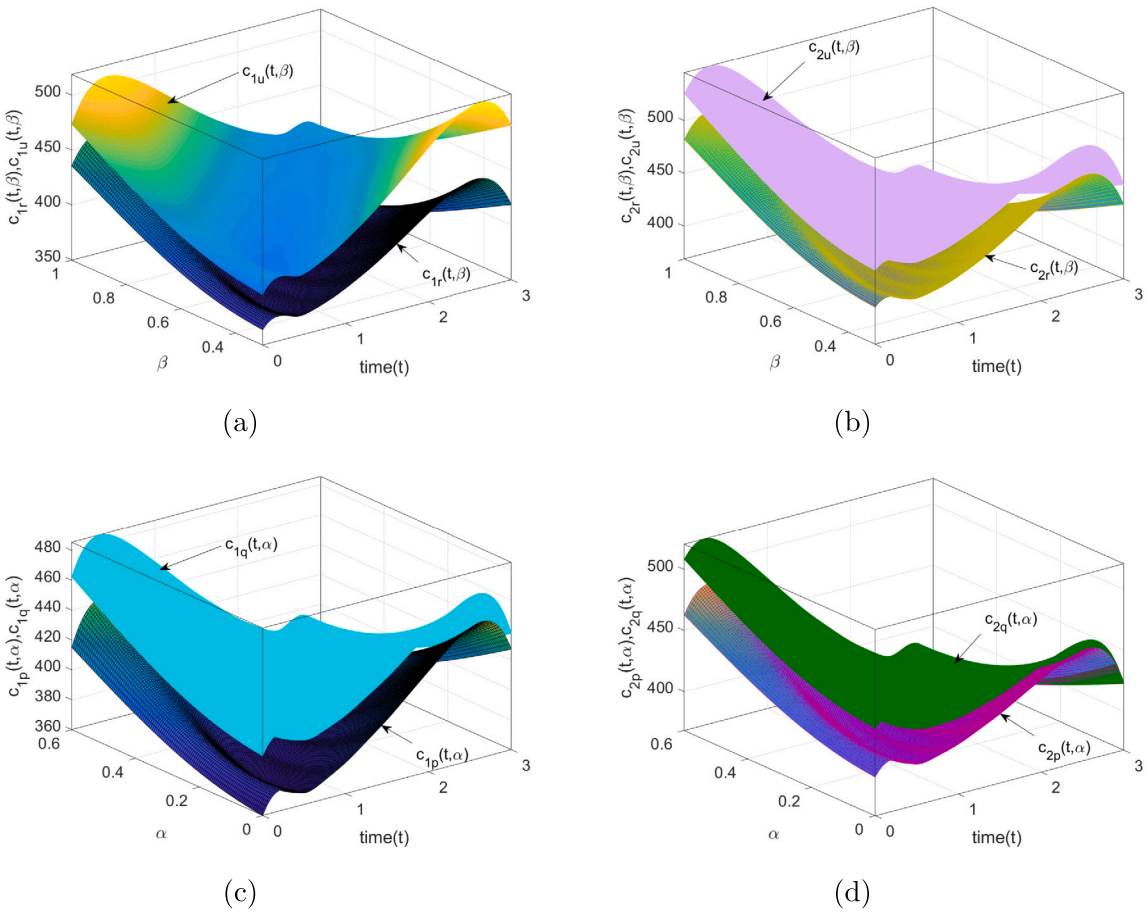


**Fig. 7.** 3D plot in Fig. 7(a) $c_{1r}(t,\beta), c_{1u}(t,\beta)$ vs. time(t) vs $\beta$ where $t \in [0,3], \beta \in [0.3,1]$; in Fig. 7(b) $c_{2r}(t,\beta), c_{2u}(t,\beta)$ vs. time(t) vs. $\beta$ where $t \in [0,3], \beta \in [0.3,1]$; in Fig. 7(c) $c_{1p}(t,\alpha), c_{1q}(t,\alpha)$ vs. time(t) vs. $\alpha$ where $t \in [0,3], \alpha \in [0,0.6]$; in Fig. 7(d) $c_{2p}(t,\alpha), c_{2q}(t,\alpha)$ vs. time(t) vs. $\alpha$ where $t \in [0,3], \alpha \in [0,0.6]$.

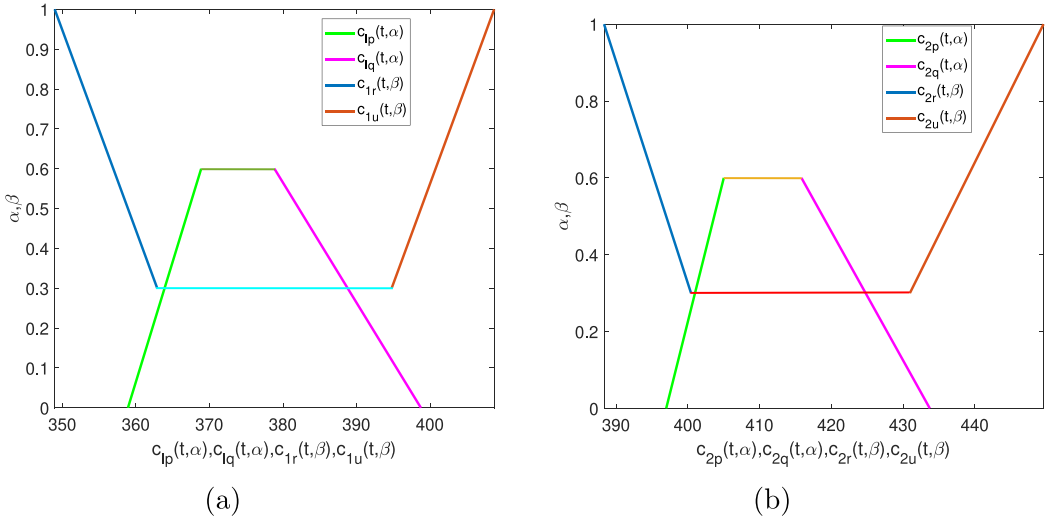


**Fig. 8.** Graph of membership function in Fig. 8(a) for $c_{1p}(t,\alpha), c_{1q}(t,\alpha), c_{1r}(t,\beta), c_{1u}(t,\beta)$ vs. $\alpha,\beta$ for $t = 2$; in Fig. 8(b) for $c_{2p}(t,\alpha), c_{2q}(t,\alpha), c_{2r}(t,\beta), c_{2u}(t,\beta)$ vs. $\alpha,\beta$ for $t = 2$ presents GTrIFN.

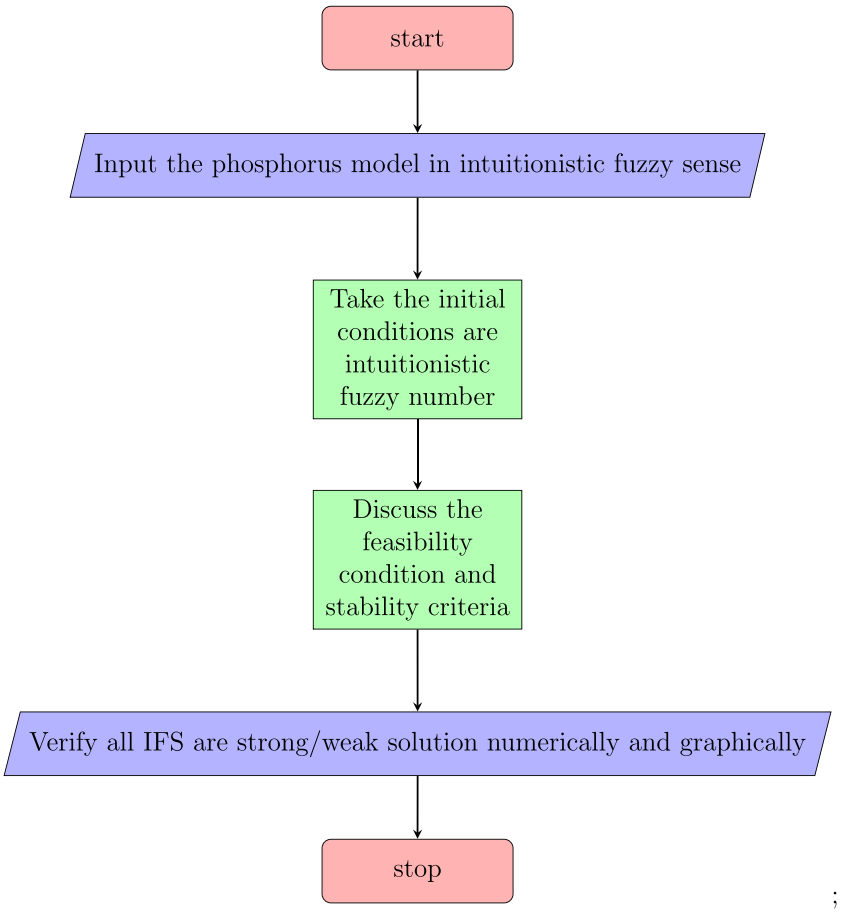


**Fig. 9.** Flow chart of two compartment phosphorus model.

To demonstrate the entire work which is presented in the following way:

S1: Input the two compartment phosphorus model with parameter $W, Q, V_s, K_s, K_b, A$.
S2: Formulate the two compartment phosphorus model (TCPM) taking with initial condition are IFN.
S3: Convert TCPM into system of DE by Hukuhara differentiability on intuitionistic fuzzy equation.
S4: Obtain the existence of equilibrium points and discuss the stability criteria for each cases.
S5: Calculate all the results and verify the results numerically.
S6: Verify all intuitionistic fuzzy solution are strong/weak TIFN solution with respective input.
S7: Stop

## 6 Conclusion and discussion

Recently mathematical modeling plays a very crucial role for different kinds of biochemical modeling. In this paper we introduced a phosphorus model subjected to the phosphorus concentrate in lake water and sediment in intuitionistic fuzzy environment. We apply the concept of different generalized Hukuhara intuitionistic fuzzy derivative elucidate to find the intuitionistic fuzzy solution of the proposed model. The biological system's set of differential equations is represented using diverse functional responses, with a majority of parameters considered as constants. However, when uncertainty affects the system, arising from factors such as environmental conditions and the collective impact of human activities, the parameters that were initially fixed may become variable. To address these phenomena, we have conceptualized the model within an intuitionistic fuzzy environment. In this work, the initial conditions of the proposed model is taken as generalized trapezoidal intuitionistic fuzzy number. To discuss the qualitative behavior of the suggested intuitionistic fuzzy model,we convert it into the system of differential equation with $(\alpha, \beta)$-cut form using the technique of GHIF derivative of type-1 and type-2. Equilibrium points and stability criteria are performed in different cases. The values of all solutions of both system follow membership function of generalized trapezoidal intuitionistic fuzzy number at $t = 100$ (see Tables 1 and 2) and $t = 2$ (see Tables 3 and 4). Strong intuitionistic fuzzy solution are obtained from both system. Thus in future research work we seek to apply these concept of different types of generalized Hukuhara neutrosophic derivative in this proposed model.

## Declaration of competing interest

The authors declare that they have no known competing financial interests or personal relationships that could have appeared to influence the work reported in this paper.

## Data availability

Data will be made available on request.

## Acknowledgments

The authors are grateful to the reviewers and Editor-in-chief, for valuable comments and suggestions.

## References


[1] S.C. Chapra, R.P. Canale, Long-term phenomenological model of phosphorus and oxygen for stratified lakes, Water Res. 25 (6) (1991) 707–715.

[2] J. Garnier, J. Nemery, G. Billen, S. Théry, Nutrient dynamics and control of eutrophication in the marne river system: modelling the role of exchangeable phosphorus, J. Hydrol. 304 (1–4) (2005) 397–412.

[3] R. Paudel, J.H. Min, J.W. Jawitz, Management scenario evaluation for a large treatment wetland using a spatio-temporal phosphorus transport and cycling model, Ecol. Eng. 36 (12) (2010) 1627–1638.

[4] X. Wang, S. Shang, Z. Qu, T. Liu, A.M. Melesse, W. Yang, Simulated wetland conservation-restoration effects on water quantity and quality at watershed scale, J. Environ. Manag. 91 (7) (2010) 1511–1525.

[5] K. Wild-Allen, M. Herzfeld, P.A. Thompson, U. Rosebrock, J. Parslow, J.K. Volkman, Applied coastal biogeochemical modelling to quantify the environmental impact of fish farm nutrients and inform managers, J. Mar. Syst. 81 (1–2) (2010) 134–147.

[6] J.I. Allen, K.R. Clarke, Effects of demersal trawling on ecosystem functioning in the North Sea: a modelling study, Mar. Ecol. Prog. Ser. 336 (2007) 63–75.

[7] A.N. Blauw, H.F. Los, M. Bokhorst, P.L. Erftemeijer, GEM: a generic ecological model for estuaries and coastal waters, Hydrobiologia 618 (2009) 175–198.

[8] L.C. Bruce, J. Imberger, The role of zooplankton in the ecological succession of plankton and benthic algae across a salinity gradient in the Shark Bay solar salt ponds, Hydrobiologia 626 (2009) 111–128.

[9] W. Gentleman, A chronology of plankton dynamics in silico: how computer models have been used to study marine ecosystems, Hydrobiologia 480 (2002) 69–85.

[10] R. Chaudhary, M. Mittal, M.K. Jayaswal, A sustainable inventory model for defective items under fuzzy environment, Decis. Anal. J. 7 (2023) 100207.

[11] S. Chakraborty, R.D. Raut, T.M. Rofin, S. Chatterjee, S. Chakraborty, A comparative analysis of Multi-Attributive Border Approximation Area Comparison (MABAC) model for healthcare supplier selection in fuzzy environments, Decis. Anal. J. 8 (2023) 100290.

[12] A. Das, A. Dutta, U.K. Bera, A pentagonal type-2 fuzzy variable defuzzification model with application in humanitarian supply chains, Decis. Anal. J. 8 (2023) 100303.

[13] N. Sil, A. Mahata, B. Roy, Dynamical behavior of HIV infection in fuzzy environment, Results Control Optim. 10 (2023) 100209.

[14] Y.C. Wang, T.C.T. Chen, Analyzing the impact of COVID-19 vaccination requirements on travelers' selection of hotels using a fuzzy multi-criteria decision-making approach, Healthc. Anal. 2 (2022) 100064.

[15] S.A. Suha, M. Akhtaruzzaman, T.F. Sanam, A fuzzy model for predicting burn patients' intravenous fluid resuscitation rate, Healthc. Anal. 2 (2022) 100070.

[16] A. Wilinski, R. Tadeusiewicz, A. Piegat, G. Bocewicz, A. Skorzak, K. Dabkowski, A. Smereczynski, T. Starzynska, A fuzzy interval model for assessing patient status and treatment effectiveness using blood morphology, Healthc. Anal. 4 (2023) 100234.

[17] E.K. Mohammadi, H.R. Talaie, M. Azizi, A healthcare service quality assessment model usinga fuzzy best–worst method with application to hospitals within-patient services, Healthc. Anal. 4 (2023) 100241.

[18] D.D. Patil, M.P. Lokhande, N.M. Mule, An intelligent system with fuzzy-based inference engine for secured tele-robotic surgery, Healthc. Anal. 4 (2023) 100264.

[19] P. Dubey, S. Kumar, S.K. Behera, S.K. Mishra, A Takagi–Sugeno fuzzy controller for minimizing cancer cells with application to androgen deprivation therapy, Healthc. Anal. 4 (2023) 100277.

[20] S.N. Matia, A. Mahata, S. Paul, S. Mukherjee, S. Alam, B. Roy, A study on imprecise mathematical model for optimal management and utilization of renewable resource by population, Results Control Optim. (2023) 100252.

[21] P. Singh, B. Gor, K.H. Gazi, S. Mukherjee, A. Mahata, S.P. Mondal, Analysis and interpretation of malaria disease model in crisp and fuzzy environment, Results Control Optim. (2023) 100257.

[22] A. Mahata, S.P. Mondal, B. Roy, S. Alam, Study of two species prey-predator model in imprecise environment with MSY policy under different harvesting scenario, Environ. Dev. Sustain. 23 (2021) 14908–14932.

[23] L.A. Zadeh, Fuzzy sets, Inf. Control 8 (3) (1965) 338–353.

[24] D. Dubois, H. Prade, Operations on fuzzy numbers, Int. J. Syst. Sci. 9 (6) (1978) 613–626.

[25] K.T. Atanassov, K.T. Atanassov, Intuitionistic Fuzzy Sets, Physica-Verlag HD, 1999, pp. 1–137.

[26] K.T. Atanassov, Intuitionistic fuzzy sets VII ITKR's session, in: Sofia, June, 1, 1983, p. 983.

[27] K.T. Atanassov, Operators over interval valued intuitionistic fuzzy sets, Fuzzy Sets and Systems 64 (2) (1994) 159–174.

[28] K. Atanassov, Intuitionistic fuzzy sets, Fuzzy Sets Syst. (1986).

[29] S. Melliani, M. Elomari, L.S. Chadli, R. Ettoussi, Intuitionistic fuzzy metric space, Notes Intuitionistic Fuzzy Sets 21 (1) (2015) 43–53.

[30] S. Melliani, M. Elomari, M. Atraoui, L.S. Chadli, Intuitionistic fuzzy differential equation with nonlocal condition, Notes Intuitionistic Fuzzy Sets 21 (4) (2015) 58–68.

[31] T. Allahviranloo, N.A. Kiani, N. Motamedi, Solving fuzzy differential equations by differential transformation method, Inform. Sci. 179 (7) (2009) 956–966.

[32] S.A. Altaie, A.F. Jameel, A. Saaban, Homotopy perturbation method approximate analytical solution of fuzzy partial differential equation, IAENG Int. J. Appl. Math. 49 (1) (2019) 22–28.

[33] A.F. Jameel, S.G. Amen, A. Saaban, N.H. Man, F.M. Alipiah, Homotopy perturbation method for solving linear fuzzy delay differential equations using double parametric approach, Stat 8 (2020) 551–558.

[34] R. Ettoussi, S. Melliani, M. Elomari, L.S. Chadli, Solution of intuitionistic fuzzy differential equations by successive approximations method, Notes Intuitionistic Fuzzy Sets 21 (2) (2015) 51–62.

[35] S. Wan, J. Dong, Decision Making Theories and Methods Based on Interval-Valued Intuitionistic Fuzzy Sets, Springer Nature, 2020.

[36] S.P. Wan, F. Wang, J.Y. Dong, Theory and method of intuitionistic fuzzy preference relation group decision making, 2019.

[37] J. Xu, J.Y. Dong, S.P. Wan, J. Gao, Multiple attribute decision making with triangular intuitionistic fuzzy numbers based on zero-sum game approach, Iran. J. Fuzzy Syst. 16 (3) (2019) 97–112.

[38] S.P. Wan, L.L. Lin, J.Y. Dong, MAGDM based on triangular atanassov's intuitionistic fuzzy information aggregation, Neural Comput. Appl. 28 (2017) 2687–2702.

[39] A. Acharya, A. Mahata, N. Sil, S. Mahato, S. Mukherjee, S.K. Mahato, B. Roy, A prey-refuge harvesting model using intuitionistic fuzzy sets, Decis. Anal. J. 8 (2023) 100308.

[40] R. Krishankumar, K.S. Ravichandran, M. Aggarwal, D. Pamucar, An improved entropy function for the intuitionistic fuzzy sets with application to cloud vendor selection, Decis. Anal. J. 7 (2023) 100262.

[41] Y. Yener, G.F. Can, A FMEA based novel intuitionistic fuzzy approach proposal: Intuitionistic fuzzy advance MCDM and mathematical modeling integration, Expert Syst. Appl. 183 (2021) 115413.

[42] A. Acharya, A. Mahata, S. Mukherjee, M.A. Biswas, K.P. Das, S.P. Mondal, B. Roy, A neutrosophic differential equation approach for modeling glucose distribution in the bloodstream using neutrosophic sets, Decis. Anal. J. (2023) 100264.

[43] R. Imran, K. Ullah, Z. Ali, M. Akram, T. Senapati, The theory of prioritized muirhead mean operators under the presence of complex single-valued neutrosophic values, Decis. Anal. J. 7 (2023) 100214.

[44] F. Yiğit, A three-stage fuzzy neutrosophic decision support system for human resources decisions in organizations, Decis. Anal. J. (2023) 100259.

[45] S. Moi, S. Biswas, S.P. Sarkar, A novel romberg integration method for neutrosophic valued functions, Decis. Anal. J. 9 (2023) 100338.

[46] S.P. Mondal, T.K. Roy, Generalised intutionistic fuzzy Laplace transformation and its application in electrical circuit, TWMS J. Appl. Eng. Math. 5 (1) (2015) 30–45.

[47] A.K. Shaw, T.K. Roy, Trapezoidal intuitionistic fuzzy number with some arithmetic operations and its application on reliability evaluation, Int. J. Math. Oper. Res. 5 (1) (2013) 55–73.

[48] A. Shabani, E.B. Jamkhananeh, A new generalized intuitionistic fuzzy number, Int. Sci. Publ. Consult. Serv. 2014 (2014) 1–10.

[49] S.P. Mondal, T.K. Roy, System of differential equation with initial value as triangular intuitionistic fuzzy number and its application, Int. J. Appl. Comput. Math. 1 (2015) 449–474.

[50] B.K. Dutta, Mathematical Methods in Chemical and Biological Engineering, CRC Press, ISBN: 978-1-4822-1038-5, 2017.

[51] D.S. Moura, I.E.L. Neto, A. Clemente, S. Oliveira, C.J. Pestana, M.A.D. Melo, J.S. Neto, Modeling phosphorus exchange between bottom sediment and water in topical semiarid reservoirs, Chemosphere 246 (2020) 125686.

[52] W.S. Lung, R.P. Canale, P.L. Freedman, Phosphorus models for eutrophic lakes, Water Res. 10 (1976) 1101–1114.

Decision Analytics Journal 10 (2024) 100386

Contents lists available at ScienceDirect

Decision Analytics Journal

journal homepage: www.elsevier.com/locate/dajour

# A two-compartment drug concentration model using intuitionistic fuzzy sets

Pramodh Bharati [a,b,1], Ashish Acharya [c,1], Animesh Mahata [d,*,1], Subrata Paul [e,1], Manajat Ali Biswas [f,1], Supriya Mukherjee [g,1], Nikhilesh Sil [h,1], Banamali Roy [i,1]

[a] Department of Mathematics, Swami Vivekananda University, Barrackpore 700121, West Bengal, India
[b] Department of Mathematics, Ramnagar College, Depal, Purba Medinipur, West Bengal 721453, India
[c] Department of Mathematics, Swami Vivakananda Institute of Modern Science, Karbala More, Kolkata 700103, West Bengal, India
[d] Department of Mathematics, Sri Ramkrishna Sarada Vidya Mahapitha, Kamarpukur, Hooghly 712612, West Bengal, India
[e] Department of Mathematics, Arambagh Government Polytechnic, Arambagh, West Bengal, 712601, India
[f] Department of Mathematics, Gobardanga Hindu College, Gobardanga, North 24 Pargona, West Bengal 743252, India
[g] Department of Mathematics, Gurudas College, 1/1 Suren Sarkar Road, Kolkata 700054, West Bengal, India
[h] Department of Mathematics, Narula Institute of Technology, 81, Nilgunj Road, Agarpara, Kolkata 700109, West Bengal, India
[i] Department of Mathematics, Bangabasi Evening, Kolkata 700009, West Bengal, India

ARTICLE INFO

*Keywords:*
Two-compartment drug concentration model
Generalized Hukuhara derivative
Intuitionistic fuzzy valued function (IFDE)
Strong and weak IFDE solutions
Triangular intuitionistic fuzzy number special type
Numerical simulation

ABSTRACT

The intuitionistic fuzzy differential equation (IFDE) is a robust mathematical tool that can deal with problems arising from model uncertainties. Intuitionistic sets are generalized sets of fuzzy sets. They establish that IFDE comprises an intuitionistic number characterized by membership and non-membership functions. This paper deals with generalized Hukuhara derivatives for intuitionistic fuzzy-valued functions. A compartment drug concentration system has been described in a fuzzy, intuitionistic setting to get a more accurate mathematical model. The initial conditions of the proposed drug system are considered triangular intuitionistic fuzzy numbers. The proposed model's critical points of stability analysis have been explored in an intuitionistic environment. All intuitionistic fuzzy solutions of the proposed system support robust solutions. All results and formulas are confirmed graphically and numerically by MATLAB software.

## 1. Introduction

Nowadays the compartmental model of drug concentration is a serious concern due to its importance. Drug dose, drug inflow and drug outflow in the human body through various compartments have both complimentary and unfavorable effects. So many researchers devoted their time to study the compartmental behavior of administering drug in the human body over a time period and establish a suitable drug therapeutic approach. Mathematical model is an essential tool to know the behavior of drug diffusion. In the field drug diffusion so many research work have been done by using mathematical model and numerical simulation. In pharmacokinetics compartmental model plays a crucial role to study physiological or pharmacological kinetic of the body. There are so many compartments in the human body, they are in series or parallel interrelation to transport material such as drugs or any chemical. Compartmental model plays a crucial role to understand the pharmacokinetics behavior of a drug concentration in the body. The body behaves as a single or more compartment system on the basis of drug. The body act as a homogeneous system in one compartmental model and the induced drug diffuses within the body very easily, whereas the body act as two but different connected compartment such as central compartment and peripheral in two compartmental model. Probably Widmark in 1920s [1], done the pioneering work on propagation of alcohol in to the body through compartmental model.

So many researchers devoted their time to developing two compartmental model to describe drug diffusion in the field of anti-cancer agents [2], pharmacokinetics [3], cholesterol transport [4], bolus injection [5], skin-like membrane [6], TDD systems [7,8], oxygen transport in biological tissues [9,10]. Moreover Khanday et al. [11] studied the drug diffusion in blood, tissue and observed the concentration of drug in the human body. In the field of drug diffusion uncertainty plays a crucial role. Due to the lack of data, insufficient supply of data, technical fault and environmental fluctuation, uncertainty comes into the human body. To handle these type of noise into the human body, nowadays the researcher are eager to frame there model of drug concentration and diffusion through fuzzy differential equations (FDEs) approach to get realistic scenario.

Nowadays fuzzy differential equation is a promising tools in various fields such as engineering, biology, physics etc. Fuzzy set theory plays an crucial role to model different type of real scenario. The

* Corresponding author.
*E-mail address:* animeshmahata8@gmail.com (A. Mahata).
[1] All authors contributed equally in this manuscript.

https://doi.org/10.1016/j.dajour.2023.100386
Received 1 October 2023; Received in revised form 8 December 2023; Accepted 12 December 2023
Available online 15 December 2023

concept of fuzzy number and fuzzy set is a major concern today. Zadeh [12] and Dubois and Parade [13] are the pioneer of fuzzy set theory. Atanassov [14–16] introduced the intuitionistic fuzzy set theory (IFST) which is nothing but the extended version of fuzzy set theory developed by Zadeh [12] and Dubois and Parade [13]. In fuzzy set theory degree of belongingness and non belongingness is considered but that of the membership and non-membership function are not defined whereas intuitionistic fuzzy set theory (IFST) is free from this ambiguity [17].

In the last few years intuitionistic fuzzy set theory (IFST) becomes more demandable. It is used in several industries, robotics, to control the complex process, in transmission of energy, in audiovisual systems etc. Nowadays so many researchers are interested and develop intuitionistic fuzzy set theory. Atanassov mention the notion of intuitionistic fuzzy set theory (IFST) [14–16]. The conception of intuitionistic fuzzy metric space was given by Melliani et al. [18]. The existence and uniqueness theorem of the solution of intuitionistic fuzzy differential equation with nonlocal condition is described in Melliani et al. [19]. So many researchers devoted their time to study intuitionistic fuzzy differential equation numerically [20–24]. The interval valued intuitionistic fuzzy set theory (IFST) and its application are described in [25–27]. Triangular Atanassov intuitionistic fuzzy set theory are described in [28]. So nowadays intuitionistic fuzzy set theory (IFST) is a well defined theory, which is nothing but the extended version of fuzzy set theory. Unfortunately it is not widely used to describe the dynamical behavior of drug diffusion model. In this research article we want to apply the theory of IFST to analyze the drug diffusion from peripheral to kidney in the human body.

Acharya et al. [29] studied a prey-refuge harvesting model using intuitionistic fuzzy sets. Mahata et al. [30] designed a neutrosophic differential equation approach for modeling glucose distribution in the bloodstream using neutrsophic sets. In [31], the authors presented a FMEA based novel intuitionistic fuzzy approach proposal: Intuitionistic fuzzy advance MCDM and mathematical modeling integration. Chaudhury et al. [32] presented a sustainable inventory model for defective items under fuzzy environment. Authors [33] proposed the theory of prioritized murihead mean operators under the presence of complex single-valued neutrosophic values. In [34], the authors introduced an inventory control model in the framework of COVID-19 disruptions considering overage items with neutrosophic fuzzy uncertainty. The reader is referred to [35–44] and its references for more information.

### 1.1. Motivation and novelty

Nowadays, researchers are much more interested in devoting their time to real-life problems in a crisp environment. Human pharmacokinetics are simulated, and bacterial cultures are exposed in two compartmental models [45]. A two-compartmental pharmacokinetic model presents an effective numerical solution for oral drug concentration [46]. The methods of two-compartment kinetic analysis are given in [47]. Recirculatory pharmacokinetic concepts are elaborated in a two-compartment recirculatory model [48]. Our literature review discovered that many research articles have been published on two-compartmental drug concentration models in a crisp environment. Still, till now research work on two-compartmental drug concentration models has yet to be done in a fuzzy environment. Due to the several environmental fluctuations, uncertainty plays an important role. Fuzzy differential equations are one of the most efficient methods for handling this situation. Fuzzy set theory is a vital tool to model different uncertain real-life scenarios. This idea is becoming more and more significant as fuzzy number theories and applications become more popular. Only the degree of belongingness and non-belongingness is considered by the fuzzy set. Fuzzy set theory does not look at the level of uncertainty or non-determinacy, which is equal to the sum of the membership function and the non-membership function times one. The intuitionistic fuzzy sets (IFS) are a generalization of fuzzy sets. Through IFS theory, Atanassov investigated the idea of fuzzy set theory to deal with such circumstances. IFS is characterized by membership and non-membership functions, so the total of both values might be less than one. In contrast, the degree of acceptance in fuzzy sets is the only factor considered [14–16]. IFSs are now the subject of much research and application across several scientific and technological domains. Using different generalized Hukuhara derivatives made for intuitionistic fuzzy-valued functions, this paper is seen as a model that shows how concentrated drugs are in two areas. Generalized Hukuhara intuitionistic fuzzy derivatives of type 1 and type 2 formulate a model describing drug concentration in two compartments. Stability criteria are analyzed along with strong and weak solutions for the model. So, to get a more realistic scenario of the given system of differential equations, one can study the given system of differential equations with the help of intuitionistic fuzzy set theory instead of fuzzy set theory.

### 1.2. Structure of the paper

Necessary preliminary ideas are included in Section 2. Section 3 we discussed the model formulation of two compartment drug concentration model in intuitionistic fuzzy environment. Stability analysis of the proposed model are considered in Section 4. Section 5 discuss the numerical simulation for various values of $(\alpha, \beta)$-cut of the triangular intuitionistic fuzzy number (special type). Section 6 consists of the conclusion.

## 2. Pre-requisite concept

**Definition 2.1** (*Intuitionistic Fuzzy Set (IFS) [49,50]*)**.** Let U be a set which is fixed. An IFS $\tilde{B}^i$ in U is considered by a set $\tilde{B}^i = \{\langle y, \chi_{\tilde{B}^i}(y), \rho_{\tilde{B}^i}(y)\rangle : y \in U\}$ where $\chi_{\tilde{B}^i}(y) : U \to [0,1]$ and $\rho_{\tilde{B}^i}(y) : U \to [0,1]$ represents the degree of membership and degree of non-membership function respectively, for every element $y \in U$ of the set $\tilde{B}^i$ such that $0 \le \chi_{\tilde{B}^i}(y) + \rho_{\tilde{B}^i}(y) \le 1$.

**Definition 2.2** (*Intuitionistic Fuzzy Number (IFN) [50]*)**.** An IFN $\tilde{B}^i$ is defined as follows:
$(i)$ An intuitionistic fuzzy subject of real line.
$(ii)$ Normal i.e. there exist $y_0 \in R$ such that $\chi_{\tilde{B}^i}(y) = 1$ (so $\rho_{\tilde{B}^i}(y) = 1$).
$(iii)$ A convex set for the membership function $\chi_{\tilde{B}^i}(y)$, i.e.
$\chi_{\tilde{B}^i}(\xi y_1 + (1-\xi)y_2) \ge min(\chi_{\tilde{B}^i}(y_1), \chi_{\tilde{B}^i}(y_2))$ for all $y_1, y_2 \in R, \xi \in [0,1]$.
$(iv)$ A concave set for the non-membership function $\rho_{\tilde{B}^i}(y)$, i.e.
$\rho_{\tilde{B}^i}(\xi y_1 + (1-\xi)y_2) \ge min(\rho_{\tilde{B}^i}(y_1), \rho_{\tilde{B}^i}(y_2))$ for all $y_1, y_2 \in R, \xi \in [0,1]$.

**Definition 2.3** (*$(\alpha, \beta)$-cut of Intuitionistic Fuzzy Number (IFN) [50]*)**.** A set of $(\alpha, \beta)-$cut, generalized by IFS $\tilde{B}^i$, where $(\alpha, \beta) \in [0,1]$, is a fixed number such that $\alpha + \beta \le 1$ is defined as $\tilde{B}^i_{(\alpha,\beta)} = \{\langle y, u_{\tilde{B}^i}(y), v_{\tilde{B}^i}(y)\rangle : y \in X, u_{\tilde{B}^i}(y) \ge \alpha, v_{\tilde{B}^i}(y) \le \beta; \alpha, \beta \in [0,1]\}$.

$(\alpha, \beta)$-cut represented by $\tilde{B}^i_{(\alpha,\beta)}$, the crisp set of elements $y$ belong to $\tilde{B}^i$ at least to the degree $\alpha$, which is belong to $\tilde{B}^i$ at most to the degree $\beta$.

**Definition 2.4** (*Triangular Intuitionistic Fuzzy Number (TIFN) [51]*)**.** A special type of triangular intuitionistic fuzzy number (special type) $\tilde{d}^i = \langle s_1, s_2, s_3; \nu_{\tilde{d}^i}, \kappa_{\tilde{d}^i}\rangle$ of IFN on set of real number R, whose membership and non-membership function of $\tilde{d}^i$ is defined as,

$$
\begin{aligned}
u_{\tilde{d}^i}(y) &= \frac{y-s_1}{s_2-s_1}\nu_{\tilde{d}^i}, && if\ s_1 \le y < s_2,\\
&= \nu_{\tilde{d}^i}, && if\ y = s_2,\\
&= \frac{s_3-y}{s_3-s_2}\nu_{\tilde{d}^i}, && if\ s_2 < y \le s_3,\\
&= 0, && otherwise.
\end{aligned}
$$

$$= \frac{s_2 - y + \kappa_{\tilde{d}^i}(y - s_1)}{s_2 - s_1}, \quad if\ s_1 \le y < s_2,$$

$$v_{\tilde{d}^i}(y) = \kappa_{\tilde{d}^i}, \quad if\ y = s_2,$$

$$= \frac{y - s_2 + \kappa_{\tilde{d}^i}(s_3 - y)}{s_3 - s_2}, \quad if\ s_2 < y \le s_3,$$

$$= 1, \quad otherwise.$$

The values of $v_{\tilde{d}^i}, \kappa_{\tilde{d}^i}$ represents the degree of maximum membership and minimum non-membership respectively and satisfy the condition $0 \le v_{\tilde{d}^i} \le 1$, $0 \le \kappa_{\tilde{d}^i} \le 1$, $0 \le v_{\tilde{d}^i} + \kappa_{\tilde{d}^i} \le 1$.

A $(\alpha, \beta)$-cut of TIFN $\tilde{d}^i = \langle s_1, s_2, s_3; v_{\tilde{d}^i}, \kappa_{\tilde{d}^i} \rangle$ is a subset of $R$ with its $(\alpha, \beta)$-cut can be defined as,

$$\tilde{d}^i_\alpha = \{y : u_{\tilde{d}^i}(y) \ge \alpha\} = [L_{\tilde{d}^i}(\alpha), R_{\tilde{d}^i}(\alpha)] = [s_1 + \frac{\alpha(s_2 - s_1)}{v_{\tilde{d}^i}}, s_3 - \frac{\alpha(s_3 - s_2)}{v_{\tilde{d}^i}}],$$

$$\tilde{d}^i_\beta = \{y : v_{\tilde{d}^i}(y) \le \beta\} = [L_{\tilde{d}^i}(\beta), R_{\tilde{d}^i}(\beta)]$$
$$= [\frac{(1-\beta)s_2 + (\beta - \kappa_{\tilde{d}^i})s_1}{1 - \kappa_{\tilde{d}^i}}, \frac{(1-\beta)s_2 + (\beta - \kappa_{\tilde{d}^i})s_3}{1 - \kappa_{\tilde{d}^i}}],$$

where $0 \le \alpha \le v_{\tilde{d}^i}$, $\kappa_{\tilde{d}^i} \le \beta \le 1$.

**Definition 2.5** (*Generalized Hukuhara Derivative for Intuitionistic Fuzzy Valued (GHIF) Function [50]*)**.** Let $f_{gI} : (a, b) \to R_I$ be a IFV function and $y_0 \in (a, b)$. We mention the function $f_{gI}$ is Hukuhara differentiable at $y_0$ if there exist an element $f'_{gI}(y_0) \in R_I$, such that $\forall h > 0$ sufficiently small

$$f'_{gI}(y_0) = \lim_{l_1 \to 0} \frac{f_{gI}(y_0 + l_1) \Theta_g f_{gI}(y_0)}{l_1} = \lim_{l_1 \to 0} \frac{f_{gI}(y_0) \Theta_g f_{gI}(y_0 - l_1)}{l_1}.$$

Note: Let, $f_{gI} : (a, b) \to R_I$ be a IFV function and $f_{gI}(y)$ is generalized Hukuhara intuitionistic fuzzy (GHIF) derivative at $y_0$ is denoted by $f'_{gI}(y_0)$ and defined by,

$$\tilde{f}'_{gI}(y_0) = \langle f'_1(y_0, \alpha; \omega_1), f'_2(y_0, \alpha; \omega_1), h'_1(y_0, \beta; \sigma_1), h'_2(y_0, \beta; \sigma_1) \rangle,$$

for each $\alpha \in [0, \omega_1], \beta \in [\sigma_1, 1], 0 < \omega_1, \sigma_1 \le 1$.

(i) If $\tilde{f}_{gI}(y)$ is GHIF derivative of type-1 then $f_1(y, \alpha; \omega_1), f_2(y, \alpha; \omega_1), h_1(y, \beta; \sigma_1), h_2(y, \beta; \sigma_1)$ are all differentiable functions and

$$[\tilde{f}'_{gI}(y_0)]_{\alpha,\beta} = \langle f'_1(y_0, \alpha; \omega_1), f'_2(y_0, \alpha; \omega_1), h'_1(y_0, \beta; \sigma_1), h'_2(y_0, \beta; \sigma_1) \rangle.$$

(ii) If $\tilde{f}_{gI}(y)$ is GHIF derivative of type-2 then $f_1(y, \alpha; \omega_1), f_2(y, \alpha; \omega_1), h_2(y, \beta; \sigma_1), h_1(y, \beta; \sigma_1)$ are all differentiable function and

$$[\tilde{f}'_{gI}(y_0)]_{\alpha,\beta} = \langle f'_1(y_0, \alpha; \omega_1), f'_2(y_0, \alpha; \omega_1), h'_1(y_0, \beta; \sigma_1), h'_2(y_0, \beta; \sigma_1) \rangle.$$

(iii) If $\tilde{f}_{gI}(y)$ is GHIF derivative of type-3 then $f_1(y, \alpha; \omega_1), f_2(y, \alpha; \omega_1), h_1(y, \beta; \sigma_1), h_2(y, \beta; \sigma_1)$ are all differentiable functions and

$$[\tilde{f}'_{gI}(y_0)]_{\alpha,\beta} = \langle f'_2(y, \alpha; \omega_1), f'_1(y_0, \alpha; \omega_1), h'_1(y_0, \beta; \sigma_1), h'_2(y_0, \beta; \sigma_1) \rangle.$$

(iv) If $\tilde{f}_{gI}(y)$ is GHIF derivative of type-4 then $f_1(y, \alpha; \omega_1), f_2(y, \alpha; \omega_1), h_1(y, \beta; \sigma_1), h_2(y, \beta; \sigma_1)$ are all differentiable functions and

$$[\tilde{f}'_{gI}(y_0)]_{\alpha,\beta} = \langle f'_1(y_0, \alpha; \omega_1), f'_2(y_0, \alpha; \omega_1), h'_2(y_0, \beta; \sigma_1), h'_1(y_0, \beta; \sigma_1) \rangle.$$

**Definition 2.6** (*Strong and Weak Solution of Intuitionistic Fuzzy Differential Equation (IFDE) [49]*)**.** Let us consider the differential equation (DE) $\frac{dy(t)}{dt} = ky(t)$, with the initial condition $y(t_0) = y_0$ is called IFDE of any one or both of k and $y_0$ are intuitionistic fuzzy numbers.

Let the solution of the above IFDE be $y(t)$ with its $(\alpha, \beta)$-cut be,

$$\tilde{y}(t, \alpha, \beta) = \langle [y_{a1}(t, \alpha), y_{a2}(t, \alpha)], [y_{b1}(t, \beta), y_{b2}(t, \beta)] \rangle.$$

The solution is a strong solution if
$(i) \frac{dy_{a1}(t,\alpha)}{d\alpha} > 0$, $\frac{dy_{a2}(t,\alpha)}{d\alpha} < 0, \forall \alpha \in [0, 1]$, $y_{a1}(1) \le y_{a2}(1)$
and, $(ii) \frac{dy_{b1}(t,\beta)}{d\beta} < 0$, $\frac{dy_{b2}(t,\beta)}{d\beta} > 0, \forall \beta \in [0, 1]$, $y_{b1}(0) \le y_{b2}(0)$,
otherwise the solution is weak solution.

## 3. Model formulation

In this section we introduce the formulation of the two compartmental drug diffusion model. Here $c_1$ and $c_2$ are the drug concentration and the two compartment are denoted by $v_1, v_2$ respectively. Initially plasma known as compartment 1, receives the drug and release the drug. It is well known that kidney eliminates the drug. $k_{12}$ and $k_{21}$ are the exchange rate constant of the drug from central compartment to peripheral compartment and the clearance rate of the drug from kidney is denoted by $k'$. The exchange rate of the drug depends upon the concentration of the drug as well as the volume of the compartment. The corresponding mathematical model of the drug concentration [52] are given below

$$\begin{aligned} \frac{dc_1(t)}{dt} &= k_{21} v c_2(t) - (k_{12} + k')c_1(t), \\ \frac{dc_2(t)}{dt} &= (\frac{k_{12}}{v})c_1(t) - k_{21}c_2(t), \end{aligned} \quad (1)$$

where, $v = \frac{v_2}{v_1}$,
with the initial condition,

$$c_1(t_0) = c_{1i}, c_2(t_0) = c_{02}, \quad (2)$$

where, $c_{1i}$ represent the drug concentration in blood immediate after injection.

The corresponding schematic diagram of the drug exchange from central compartment to peripheral is given in Fig. 1

In an intuitionistic fuzzy environment, the proposed model is formulated as:

$$\begin{aligned} \frac{d\tilde{c_1}(t)}{dt} &= k_{21} v \tilde{c_2}(t) - (k_{12} + k')\tilde{c_1}(t), \\ \frac{d\tilde{c_2}(t)}{dt} &= (\frac{k_{12}}{v})\tilde{c_1}(t) - k_{21}\tilde{c_2}(t), \end{aligned} \quad (3)$$

with the initial condition,

$$\tilde{c_1}(t_0) = \tilde{c_{1i}}, \tilde{c_2}(t_0) = \tilde{c_{02}}. \quad (4)$$

## 4. Two compartment drug concentration model in intuitionistic fuzzy environment

In this section we consider $\tilde{c_1}(t)$ and $\tilde{c_2}(t)$ as intuitionistic fuzzy number in the system of Eq. (3). Then the following different cases arise as

(i) $\tilde{c_1}(t)$, $\tilde{c_2}(t)$ both are GHIF derivative of type 1,
(ii) $\tilde{c_1}(t)$, $\tilde{c_2}(t)$ both are GHIF derivative of type 2,
(iii) $\tilde{c_1}(t)$, $\tilde{c_2}(t)$ both are GHIF derivative of type 3,
(iv) $\tilde{c_1}(t)$, $\tilde{c_2}(t)$ both are GHIF derivative of type 4,
(v) $\tilde{c_1}(t)$ is GHIF derivative of type 1 and $\tilde{c_2}(t)$ is GHIF derivative of type 2,
(vi) $\tilde{c_1}(t)$ is GHIF derivative of type 1 and $\tilde{c_2}(t)$ is GHIF derivative of type 3,
(vii) $\tilde{c_1}(t)$ is GHIF derivative of type 1 and $\tilde{c_2}(t)$ is GHIF derivative of type 4,
(viii) $\tilde{c_1}(t)$ is GHIF derivative of type 2 and $\tilde{c_2}(t)$ is GHIF derivative of type 1,
(ix) $\tilde{c_1}(t)$ is GHIF derivative of type 2 and $\tilde{c_2}(t)$ is GHIF derivative of type 3,
(x) $\tilde{c_1}(t)$ is GHIF derivative of type 2 and $\tilde{c_2}(t)$ is GHIF derivative of type 4,
(xi) $\tilde{c_1}(t)$ is GHIF derivative of type 3 and $\tilde{c_2}(t)$ is GHIF derivative of type 1,
(xii) $\tilde{c_1}(t)$ is GHIF derivative of type 3 and $\tilde{c_2}(t)$ is GHIF derivative of type 2,
(xiii) $\tilde{c_1}(t)$ is GHIF derivative of type 3 and $\tilde{c_2}(t)$ is GHIF derivative of type 4,
(xiv) $\tilde{c_1}(t)$ is GHIF derivative of type 4 and $\tilde{c_2}(t)$ is GHIF derivative of type 1,
(xv) $\tilde{c_1}(t)$ is GHIF derivative of type 4 and $\tilde{c_2}(t)$ is GHIF derivative of type 2,

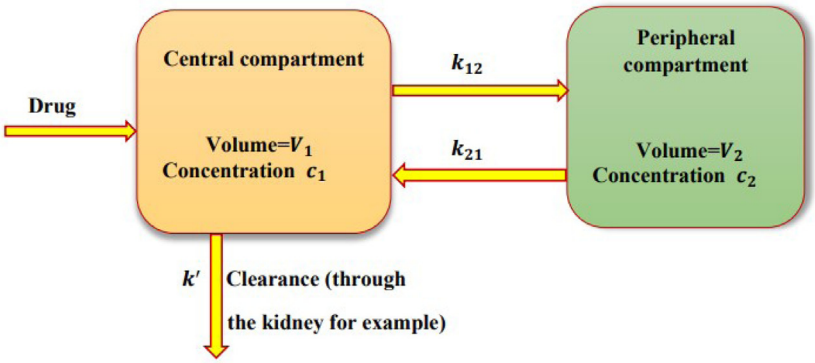


**Fig. 1.** Flow diagram of two compartment drug concentration model.

(xvi) $\tilde{c_1}(t)$ is GHIF derivative of type 4 and $\tilde{c_2}(t)$ is GHIF derivative of type 3.

In this research article, to understand the kinetics of the drug concentration system in human body, we consider only two cases as follows: (a) $\tilde{c_1}(t)$ and $\tilde{c_2}$(t) both are GHIF derivative of type-1; (b) $\tilde{c_1}(t)$ and $\tilde{c_2}(t)$ both are GHIF derivative of type-2.

### 4.1. Case 1: When $\tilde{c_1}(t)$, $\tilde{c_2}(t)$ both are GHIF derivative of type-1

The two compartment drug concentration model converted into system of IFDE as follows:

$$\begin{aligned}
\frac{dc_{11L}(t,\alpha)}{dt} &= k_{21}vc_{21L}(t,\alpha) - (k_{12}+k')c_{11R}(t,\alpha)\\
\frac{dc_{11R}(t,\alpha)}{dt} &= k_{21}vc_{21R}(t,\alpha) - (k_{12}+k')c_{11L}(t,\alpha)\\
\frac{dc_{12L}(t,\beta)}{dt} &= k_{21}vc_{22L}(t,\beta) - (k_{12}+k')c_{12R}(t,\beta)\\
\frac{dc_{12R}(t,\beta)}{dt} &= k_{21}vc_{22R}(t,\beta) - (k_{12}+k')c_{12L}(t,\beta)\\
\frac{dc_{21L}(t,\alpha)}{dt} &= \frac{k_{12}}{v}c_{11L}(t,\alpha) - k_{21}c_{21R}(t,\alpha)\\
\frac{c_{21R}(t,\alpha)}{dt} &= \frac{k_{12}}{v}c_{11R}(t,\alpha) - k_{21}c_{21L}(t,\alpha)\\
\frac{dc_{22L}(t,\beta)}{dt} &= \frac{k_{12}}{v}c_{12L}(t,\beta) - k_{21}c_{22R}(t,\beta)\\
\frac{c_{22R}(t,\beta)}{dt} &= \frac{k_{12}}{v}c_{12R}(t,\beta) - k_{21}c_{22L}(t,\beta)
\end{aligned} \tag{5}$$

The initial condition as follows,

$c_{11L}(0,\alpha) = c_{11Li}(\alpha), c_{11R}(0,\alpha) = c_{11Ri}(\alpha), c_{12L}(0,\beta) = c_{12Li}(\beta), c_{12R}(0,\beta) = c_{12Ri}(\beta), c_{21L}(0,\alpha) = c_{021L}(\alpha), c_{21R}(0,\alpha) = c_{021R}(\alpha), c_{22L}(0,\beta) = c_{022L}(\beta), c_{22R}(0,\beta) = c_{022R}(\beta)$

The $(\alpha,\beta)$ cut of $\tilde{c_1}$(t), $\tilde{c_2}(t)$ is given by,

$$\tilde{c_1}(t) = \langle c_{11L}(t,\alpha), c_{11R}(t,\alpha), c_{12L}(t,\beta), c_{12R}(t,\beta)\rangle,$$
$$\tilde{c_2}(t) = \langle c_{21L}(t,\alpha), c_{21R}(t,\alpha), c_{22L}(t,\beta), c_{22R}(t,\beta)\rangle.$$

#### 4.1.1. Stability analysis

*4.1.1.1. Existence of equilibrium point.* The transformed model (5) has only trivial equilibrium point which is $E^*_{0e}(c^*_{11L}(t,\alpha), c^*_{11R}(t,\alpha), c^*_{12L}(t,\beta), c^*_{12R}(t,\beta), c^*_{21L}(t,\alpha), c^*_{21R}(t,\alpha), c^*_{22L}(t,\beta), c^*_{22R}(t,\beta))$, where $c^*_{11L}(t,\alpha) = c^*_{11R}(t,\alpha) = c^*_{12L}(t,\beta) = c^*_{12R}(t,\beta) = c^*_{21L}(t,\alpha) = c^*_{21R}(t,\alpha) = c^*_{22L}(t,\beta) = c^*_{22R}(t,\beta) = 0$.

**Theorem 1.** *The transformed system (5) is unstable at* $E^*_{0e}$.

**Proof.** The variational matrix $V^*_{01}$ at $E^*_{0e}$ is given by, $V^*_{01}$ is given in Box I.

The characteristics equation of $V^*_{01}$ becomes,

$\mu_1^8 - 2[(k_{21})^2 + (k_{12}+k')^2]\mu_1^6 + [(k_{12}+k')^4 + (k_{21})^4 + 4(k_{21})^2(k_{12}+k')^2]\mu_1^4 - 2[(k_{21})^4(k_{12}+k')^4 + (k_{21})^2(k_{12}+k')^4]\mu_1^2 - (k_{12})^4(k_{21})^4 = 0$ where, $\mu_1$ is the root of the characteristic equation. The above equation has the coefficient of $\mu_1^7, \mu_1^5, \mu_1^3, \mu_1$ is zero. From the stability criteria, the transformed system (5) is unstable at trivial equilibrium point $E^*_{0e}$.

### 4.2. Case 2: When $\tilde{c_1}(t)$ and $\tilde{c_2}(t)$ both are GHIF derivative of type-2

The two compartment drug concentration model converted into system of IFDE as follows:

$$\begin{aligned}
\frac{dc_{11L}(t,\alpha)}{dt} &= k_{21}vc_{21R}(t,\alpha) - (k_{12}+k')c_{11L}(t,\alpha)\\
\frac{dc_{11R}(t,\alpha)}{dt} &= k_{21}vc_{21L}(t,\alpha) - (k_{12}+k')c_{11R}(t,\alpha)\\
\frac{dc_{12L}(t,\beta)}{dt} &= k_{21}vc_{22R}(t,\beta) - (k_{12}+k')c_{12L}(t,\beta)\\
\frac{dc_{12R}(t,\beta)}{dt} &= k_{21}vc_{22L}(t,\beta) - (k_{12}+k')c_{12R}(t,\beta)\\
\frac{c_{21L}(t,\alpha)}{dt} &= \frac{k_{12}}{v}c_{11R}(t,\alpha) - k_{21}c_{21L}(t,\alpha)\\
\frac{c_{21R}(t,\alpha)}{dt} &= \frac{k_{12}}{v}c_{11L}(t,\alpha) - k_{21}c_{21R}(t,\alpha)\\
\frac{c_{22L}(t,\beta)}{dt} &= \frac{k_{12}}{v}c_{12R}(t,\beta) - k_{21}c_{22L}(t,\beta)\\
\frac{c_{22R}(t,\beta)}{dt} &= \frac{k_{12}}{v}c_{12L}(t,\beta) - k_{21}c_{22R}(t,\beta)
\end{aligned} \tag{6}$$

The initial condition as follows,

$c_{11L}(0,\alpha) = c_{11Li}(\alpha), c_{11R}(0,\alpha) = c_{11Ri}(\alpha), c_{12L}(0,\beta) = c_{12Li}(\beta), c_{12R}(0,\beta) = c_{12Ri}(\beta), c_{21L}(0,\alpha) = c_{021L}(\alpha), c_{21R}(0,\alpha) = c_{021R}(\alpha), c_{22L}(0,\beta) = c_{022L}(\beta), c_{22R}(0,\beta) = c_{022R}(\beta)$.

The $(\alpha,\beta)$ cut of $\tilde{c_1}$(t), $\tilde{c_2}(t)$ is given by,

$$\tilde{c_1}(t) = \langle c_{11L}(t,\alpha), c_{11R}(t,\alpha), c_{12L}(t,\beta), c_{12R}(t,\beta)\rangle,$$

$$\tilde{c_2}(t) = \langle c_{21L}(t,\alpha), c_{21R}(t,\alpha), c_{22L}(t,\beta), c_{22R}(t,\beta)\rangle.$$

#### 4.2.1. Stability analysis

*4.2.1.1. Existence of equilibrium point.* The transformed model (6) has only trivial equilibrium point which is $E^{**}_{0e}(c^*_{11L}(t,\alpha), c^*_{11R}(t,\alpha), c^*_{12L}(t,\beta), c^*_{12R}(t,\beta), c^*_{21L}(t,\alpha), c^*_{21R}(t,\alpha), c^*_{22L}(t,\beta), c^*_{22R}(t,\beta))$, where $c^*_{11L}(t,\alpha) = c^*_{11R}(t,\alpha) = c^*_{12L}(t,\beta) = c^*_{12R}(t,\beta) = c^*_{21L}(t,\alpha) = c^*_{21R}(t,\alpha) = c^*_{22L}(t,\beta) = c^*_{22R}(t,\beta) = 0$.

**Theorem 2.** *The transformed system (6) is locally asymptotically stable (LAS) at* $E^{**}_{0e}$ *when* $k_{21} > 0, k_{12} > 0, (k_{12}+k') > \frac{k_{12}}{v}, v > 1$.

**Proof.** The variational matrix $V^*_{02}$ at $E^{**}_{0e}$ is given by, $V^*_{02}$ is given in Box II.

Let $\mu_2$ is the eigenvalue of $V^*_{02}$, then the characteristics equation of $V^*_{02}$ becomes,

$[\mu_2 - (\frac{k_{12}}{v} - (k_{12}+k'))]^4[\mu_2 + k_{21}v]^4 = 0.$

$$V_{01}^{*}=\begin{pmatrix} 0 & (k_{12}+k') & 0 & 0 & -\frac{k_{12}}{\nu} & 0 & 0 & 0 \\ (k_{12}+k') & 0 & 0 & 0 & 0 & -\frac{k_{12}}{\nu} & 0 & 0 \\ 0 & 0 & 0 & (k_{12}+k') & 0 & 0 & -\frac{k_{12}}{\nu} & 0 \\ 0 & 0 & (k_{12}+k') & 0 & 0 & 0 & 0 & -\frac{k_{12}}{\nu} \\ -k_{21}\nu & 0 & 0 & 0 & 0 & k_{21} & 0 & 0 \\ 0 & -k_{21}\nu & 0 & 0 & k_{21} & 0 & 0 & 0 \\ 0 & 0 & -k_{21}\nu & 0 & 0 & 0 & 0 & k_{21} \\ 0 & 0 & 0 & -k_{21}\nu & 0 & 0 & k_{21} & 0 \end{pmatrix}.$$

**Box I.**

$$V_{02}^{*}=\begin{pmatrix} -(k_{12}+k') & 0 & 0 & 0 & 0 & \frac{k_{12}}{\nu} & 0 & 0 \\ 0 & -(k_{12}+k') & 0 & 0 & \frac{k_{12}}{\nu} & 0 & 0 & 0 \\ 0 & 0 & -(k_{12}+k') & 0 & 0 & 0 & 0 & \frac{k_{12}}{\nu} \\ 0 & 0 & 0 & -(k_{12}+k') & 0 & 0 & \frac{k_{12}}{\nu} & 0 \\ 0 & k_{21}\nu & 0 & 0 & -k_{21}\nu & 0 & 0 & 0 \\ k_{21}\nu & 0 & 0 & 0 & 0 & -k_{21}\nu & 0 & 0 \\ 0 & 0 & 0 & k_{21}\nu & 0 & 0 & -k_{21}\nu & 0 \\ 0 & 0 & k_{21}\nu & 0 & 0 & 0 & 0 & -k_{21}\nu \end{pmatrix}.$$

**Box II.**

**Table 1**
The parameters value.

| Parameters | $\nu$ | $k_{12}$ | $k_{21}$ | $k'$ |
|---|---|---|---|---|
| Value | 3.5 | 0.003 | 0.25 | 0.5 |
| Source | [*assumed*] | [53] | [53] | [53] |

All eigenvalues of the above characteristic equation are $-k_{21}\nu, -k_{21}\nu, -k_{21}\nu, -k_{21}\nu, [(\frac{k_{12}}{\nu}-(k_{12}+k'))], [(\frac{k_{12}}{\nu}-(k_{12}+k'))], [(\frac{k_{12}}{\nu}-(k_{12}+k'))], [(\frac{k_{12}}{\nu}-(k_{12}+k'))]$. Hence, the model system (6) is LAS at trivial equilibrium point $E_{0e}^{**}$ when $k_{21}>0, k_{12}>0, (k_{12}+k')>\frac{k_{12}}{\nu}, \nu>1$.

## 5. Numerical studies

In this section, we have been discussed of the system (5) and (6) rigorous numerical simulation to checked and validate all theoretical calculation by using MATLAB 2018 software. Here, we performed the dynamical behavior of two compartment drug concentration model (1) in the presence of intuitionistic fuzzy environment. To check the effect of fuzzy intuitionistic parameter of the proposed model (1) using the initial condition are triangular intuitionistic fuzzy number(special type) and set all the parameter value mentioned in case 1 and case 2 as follows-

**Case 1: When $\tilde{c_1}(t), \tilde{c_2}(t)$ are GHIF derivative of type-1:**

Consider all parameter values used in the proposed system (5) are reported in Table 1 as follows:

The initial drug concentration are taken as TIFN (special type) as $\tilde{c_1}(t_0)=\langle 40,50,60;0.5,0.4\rangle$, $\tilde{c_2}(t_0)=\langle 50,60,70;0.5,0.4\rangle$. The $(\alpha,\beta)-$ cut of initial condition is given by,

$$\begin{aligned}\tilde{c_1}_{\alpha,\beta}&=\langle 40+20\alpha, 60-20\alpha; \tfrac{34-10\beta}{0.6}, \tfrac{26+10\beta}{0.6}\rangle,\\ \tilde{c_2}_{\alpha,\beta}&=\langle 50+20\alpha, 70-20\alpha; \tfrac{40-10\beta}{0.6}, \tfrac{32+10\beta}{0.6}\rangle.\end{aligned} \tag{7}$$

The values of $c_{11L}(t,\alpha), c_{11R}(t,\alpha), c_{12L}(t,\beta), c_{12R}(t,\beta)$ are tabulated in Table 2, and $c_{21L}(t,\alpha), c_{21R}(t,\alpha), c_{22L}(t,\beta), c_{22R}(t,\beta)$ are also tabulated in Table 3 respectively at different levels of $\alpha(=0,0.1,0.2,0.3,0.4,0.5)$ and $\beta(=0.4,0.5,0.6,0.7,0.8,0.9,1)$ using the values of Table 1, and

**Table 2**
Intuitionistic fuzzy solution of $c_{11L}(t,\alpha), c_{11R}(t,\alpha), c_{12L}(t,\beta), c_{12R}(t,\beta)$ the system (5) for $t=1$.

| $\alpha$ | $c_{11L}(t,\alpha)$ | $c_{11R}(t,\alpha)$ | $\beta$ | $c_{12L}(t,\beta)$ | $c_{12R}(t,\beta)$ |
|---|---|---|---|---|---|
| 0 | 37.0490 | 95.7057 | | | |
| 0.1 | 42.9146 | 89.8400 | | | |
| 0.2 | 48.7803 | 83.9744 | | | |
| 0.3 | 54.6460 | 78.1087 | | | |
| 0.4 | 60.5117 | 72.2430 | 0.4 | 66.3773 | 66.3773 |
| 0.5 | 66.3773 | 66.3773 | 0.5 | 61.4893 | 71.2654 |
| 0.6 | | | 0.6 | 56.6012 | 76.1535 |
| 0.7 | | | 0.7 | 51.7131 | 81.0415 |
| 0.8 | | | 0.8 | 46.8251 | 85.9296 |
| 0.9 | | | 0.9 | 41.9370 | 90.8176 |
| 1 | | | 1 | 37.0490 | 95.7057 |

the $(\alpha,\beta)$-cut of $\tilde{c_1}(t_0), \tilde{c_2}(t_0)$. Fig. 2 depicts the kinetics of two compartment drug concentration relative to time beginning with initial concentrations $(\tilde{c_1}(t_0), \tilde{c_2}(t_0))$ for various value $\alpha(=0,0.2,0.4,0.5)$ and $\beta(=0.4,0.6,0.8,1)$ when $t\in[0,2]$. Here in Fig. 2(a), (b), (c) and (d) we notice that $c_{11L}(t,\alpha)\le c_{11R}(t,\alpha), c_{12L}(t,\beta)\le c_{12R}(t,\beta); c_{21L}(t,\alpha)\le c_{21R}(t,\alpha), c_{22L}(t,\beta)\le c_{22R}(t,\beta)$ where $t\in[0,2]$ that lead to verify all the solution of the system (5) are intuitionistic fuzzy solution where $\alpha\in[0,0.5], \beta\in[0.4,1]$ for $t=1$. From the Tables 2, 3 and the membership function at $t=1$ togetherly shows strong intuitionistic fuzzy solution of the transformed system (5).

From Tables 2 and 3 we see that, the values of $c_{11L}(t,\alpha)$ is increasing whereas the values of $c_{11R}(t,\alpha)$ is decreasing, the values of $c_{12L}(t,\beta)$ is decreasing whereas the values of $c_{12R}(t,\beta)$ is increasing for $\alpha\in[0,0.5], \beta\in[0.4,1]$, for $t=1$; the values of $c_{21L}(t,\alpha)$ is increasing whereas the values of $c_{21R}(t,\alpha)$ is decreasing, the values of $c_{22L}(t,\beta)$ is decreasing whereas the values of $c_{22R}(t,\beta)$ is increasing for $\alpha\in[0,0.5], \beta\in[0.4,1]$ for $t=1$. Hence $\tilde{c_1}(t), \tilde{c_2}(t)$ give strong intuitionistic fuzzy solution of the system (5).

**Case 2: When $\tilde{c_1}(t), \tilde{c_2}(t)$ both are GHIF derivative of type 2:**

Consider that all parameter values employed in the proposed system (6) are listed as follows in Table 4:

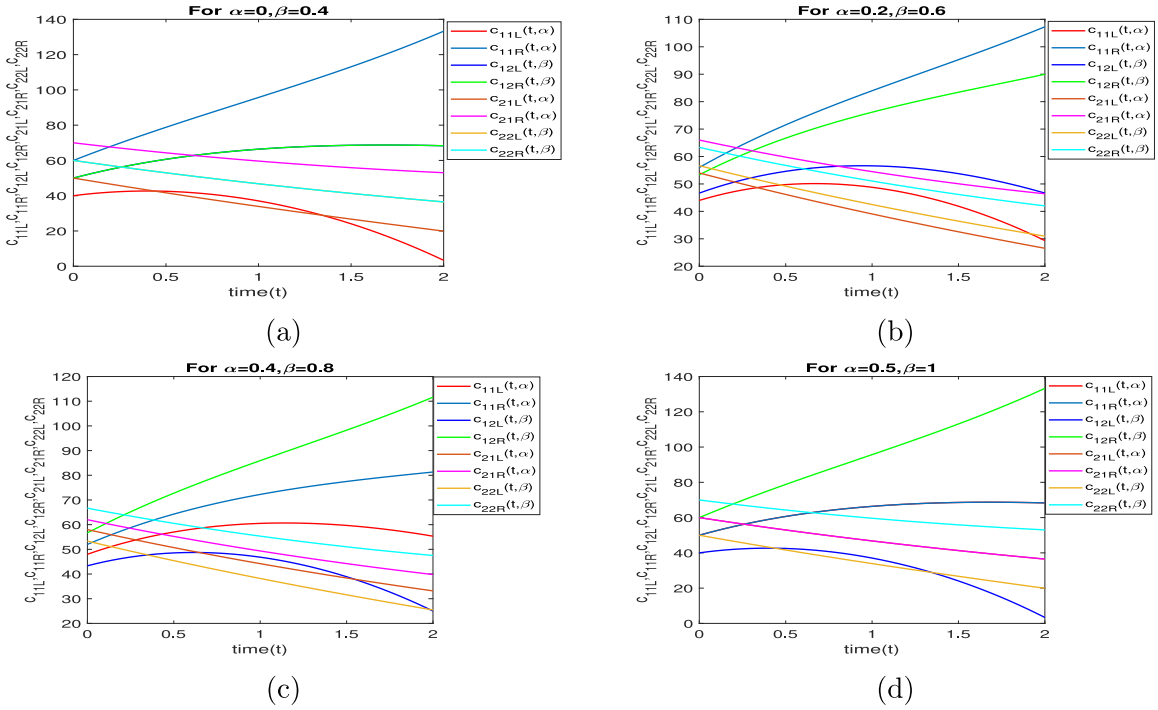


**Fig. 2.** Time series solution in Fig. 2(a) for $\alpha = 0, \beta = 0.4$; in Fig. 2(b) for $\alpha = 0.2, \beta = 0.6$; in Fig. 2(c) for $\alpha = 0.4, \beta = 0.8$; in Fig. 2(d) for $\alpha = 0.5, \beta = 1$ for $t \in [0, 2]$ of the system (5).

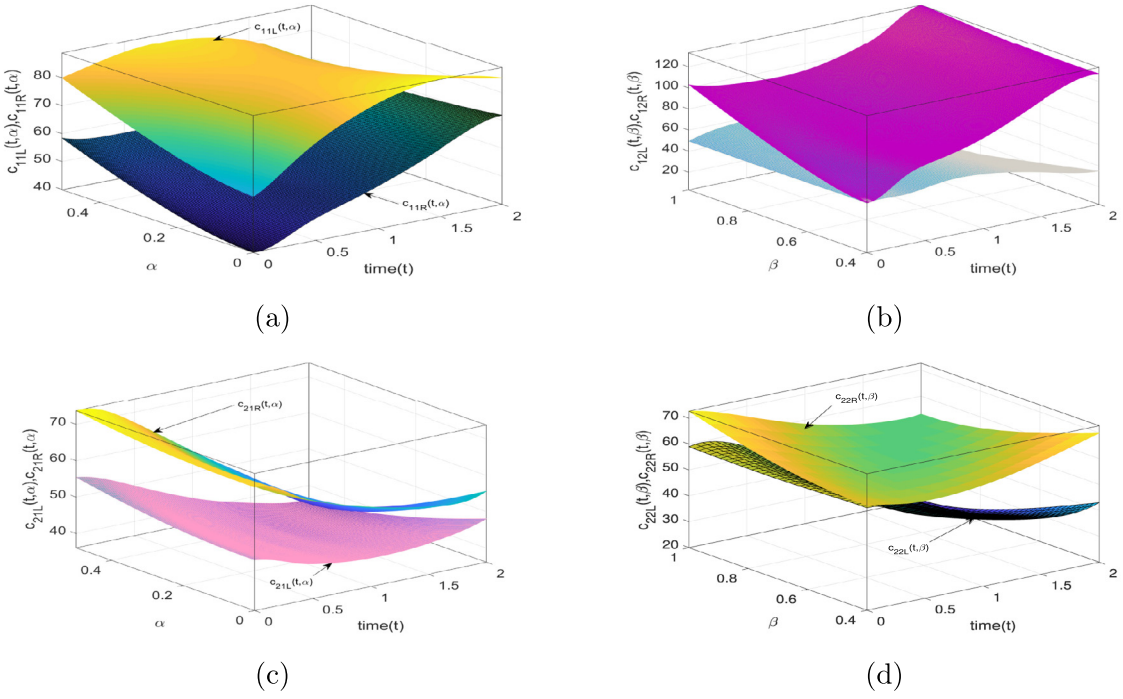


**Fig. 3.** 3D plot in Fig. 3(a) $c_{11L}(t,\alpha), c_{11R}(t,\alpha)$ vs. time(t) vs. $\alpha$ where $t \in [0,2], \alpha \in [0,0.5]$; in Fig. 3(b) $c_{12L}(t,\beta), c_{12R}(t,\beta)$ vs. time(t) vs. $\beta$ where $t \in [0,2], \beta \in [0.4,1]$;in Fig. 3(c) $c_{21L}(t,\alpha), c_{21R}(t,\alpha)$ vs. time(t) vs. $\alpha$ where $t \in [0,2], \alpha \in [0,0.5]$; in Fig. 3(d) $c_{22L}(t,\beta), c_{22R}(t,\beta)$ vs. time(t) vs. $\beta$ where $t \in [0,2], \beta \in [0.4,1]$.

Using the values from Table 4 the $(\alpha,\beta)$-cut of $\tilde{c_1}(t_0)$, $\tilde{c_2}(t_0)$ mentioned in (7), the values of $c_{11L}(t,\alpha), c_{11R}(t,\alpha), c_{12L}(t,\beta), c_{12R}(t,\beta)$ are tabulated in Table 5, and $c_{21L}(t,\alpha), c_{21R}(t,\alpha), c_{22L}(t,\beta), c_{22R}(t,\beta)$ are also tabulated in Table 6 respectively at $t = 3$ for different levels of $\alpha(= 0, 0.1, 0.2, 0.3, 0.4, 0.5)$ and $\beta(= 0.4, 0.5, 0.6, 0.7, 0.8, 0.9, 1)$. The dynamics of the two compartment drug concentration with respect to time are shown in Fig. 5 starting with the initial populations $(\tilde{c_1}(t_0), \tilde{c_2}(t_0))$ for a range of $\alpha(= 0, 0.2, 0.4, 0.5)$ and $\beta(= 0.4, 0.6, 0.8, 1)$ when $t$ in $[0, 250]$. From the Fig. 5(a), (b), (c) and (d), we notice that $c_{11L}(t,\alpha) \leq c_{11R}(t,\alpha)$, $c_{12L}(t,\beta) \leq c_{12R}(t,\beta)$; $c_{21L}(t,\alpha) \leq c_{21R}(t,\alpha)$, $c_{22L}(t,\beta) \leq c_{22R}(t,\beta)$ where $t \in [0, 250]$ that leads to verify all the solution of the system (6) are intuitionistic fuzzy solutions for $\alpha \in [0, 0.5], \beta \in [0.4, 1]$ for $t = 3$. The Fig. 5 depicts the system (6) is locally asymptotically stable at $E^{**}_{0e}$. From the Tables 5, 6 and the membership function at $t = 3$ togetherly

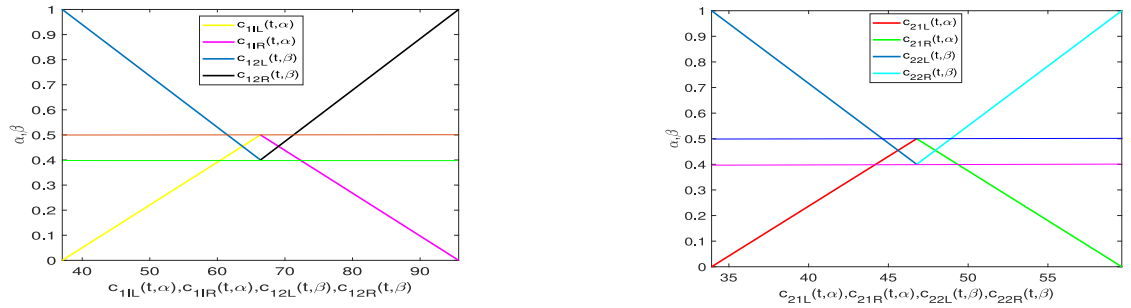


**Fig. 4.** Pictorial presentation of membership function in Fig. 4(a) for $c_{11L}(t,\alpha), c_{11R}(t,\alpha), c_{12L}(t,\beta), c_{12R}(t,\beta)$ vs. $(\alpha,\beta)$ at $t=1$ and in Fig. 4(b) for $c_{21L}(t,\alpha), c_{21R}(t,\alpha), c_{22L}(t,\beta), c_{22R}(t,\beta)$ vs. $(\alpha,\beta)$ at $t=1$ presents triangular intuitionistic fuzzy number.

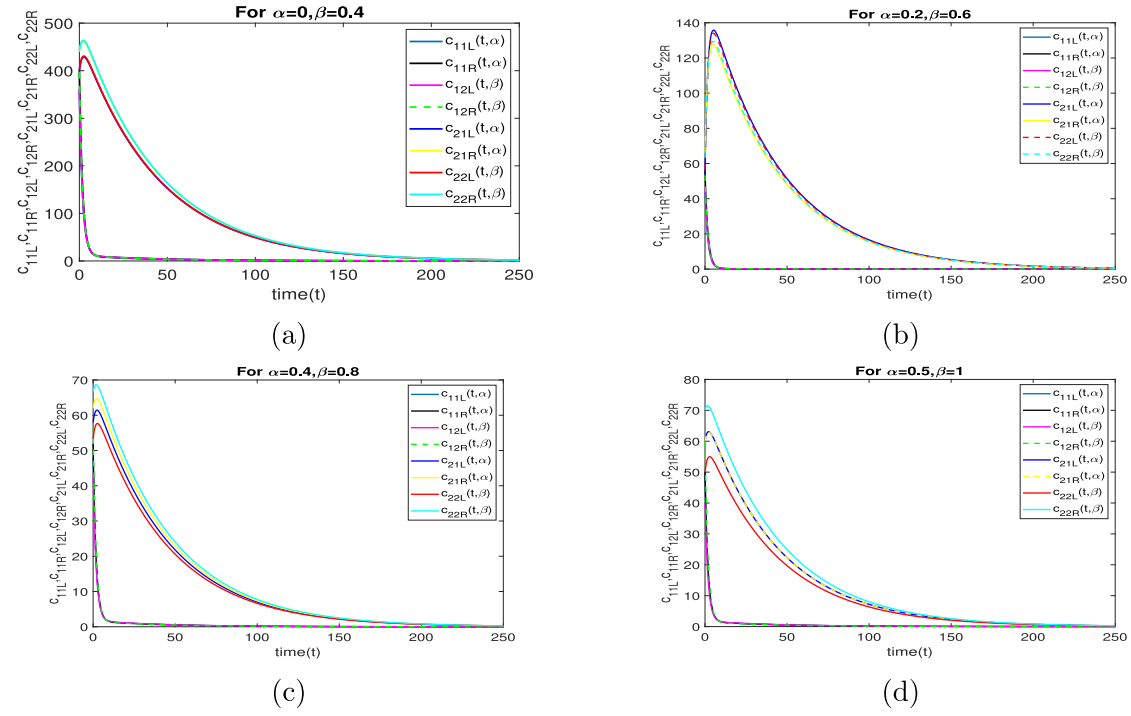


**Fig. 5.** Time series solution in Fig. 5(a) for $\alpha=0,\beta=0.4$; in Fig. 5(b) for $\alpha=0.2,\beta=0.6$; in Fig. 5(c) for $\alpha=0.4,\beta=0.8$; in Fig. 5(d) for $\alpha=0.5,\beta=1$ for $t\in[0,250]$ of the system (6).

**Table 3**
Intuitionistic fuzzy solution of $c_{21L}(t,\alpha), c_{21R}(t,\alpha), c_{22L}(t,\beta), c_{22R}(t,\beta)$ of the system (5) for $t=1$.

| $\alpha$ | $c_{21L}(t,\alpha)$ | $c_{21R}(t,\alpha)$ | $\beta$ | $c_{22L}(t,\beta)$ | $c_{22R}(t,\beta)$ |
|---|---|---|---|---|---|
| 0 | 33.9156 | 59.6317 | | | |
| 0.1 | 36.4873 | 57.0601 | | | |
| 0.2 | 39.0589 | 54.4885 | | | |
| 0.3 | 41.6305 | 51.9169 | | | |
| 0.4 | 44.2021 | 49.3453 | 0.4 | 46.7737 | 46.7737 |
| 0.5 | 46.7737 | 46.7737 | 0.5 | 44.6307 | 48.9167 |
| 0.6 | | | 0.6 | 42.4877 | 51.0597 |
| 0.7 | | | 0.7 | 40.3447 | 53.2027 |
| 0.8 | | | 0.8 | 38.2017 | 55.3457 |
| 0.9 | | | 0.9 | 36.0587 | 57.4887 |
| 1 | | | 1 | 33.9156 | 59.6317 |

depicts strong intuitionistic fuzzy solution of the transformed system (6).

From Tables 5 and 6 we see that, the values of $c_{11L}(t,\alpha)$ is increasing whereas the values of $c_{11R}(t,\alpha)$ is decreasing, the values of $c_{12L}(t,\beta)$ is decreasing whereas the values of $c_{12R}(t,\beta)$ is increasing for $\alpha\in[0,0.5],\beta\in[0.4,1]$, for $t=3$; the values of $c_{21L}(t,\alpha)$ is increasing whereas the values of $c_{21R}(t,\alpha)$ is decreasing, the values of $c_{22L}(t,\beta)$ is decreasing whereas the values of $c_{22R}(t,\beta)$ is increasing for $\alpha\in[0,0.5],\beta\in[0.4,1]$, for $t=3$. Hence, $\tilde{c_1}(t)$, $\tilde{c_2}(t)$ give strong intuitionistic fuzzy solution of the transformed system (6).

**Table 4**
The parameters value.

| Parameters | $\nu$ | $k_{12}$ | $k_{21}$ | $k'$ |
|---|---|---|---|---|
| Value | 1.5 | 0.005 | 0.025 | 0.5 |
| Source | [53] | [assumed] | [assumed] | [53] |

## 6. Discussion and conclusion

Mathematical modeling on intuitionistic fuzzy sets has been essential for decades. The generalized Hukuhara derivatives for intuitionistic fuzzy-valued functions are the subject of this study. A compartment drug concentration system has been articulated in an intuitionistic

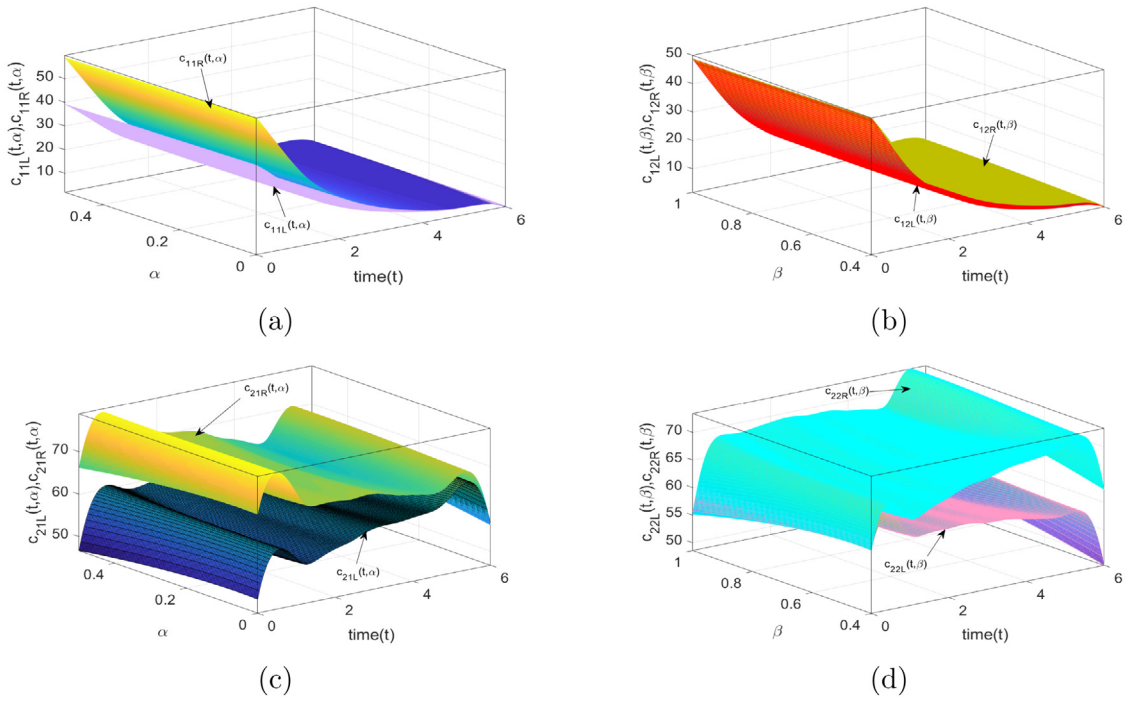


**Fig. 6.** 3D plot in Fig. 6(a) $c_{11L}(t,\alpha), c_{11R}(t,\alpha)$ vs. time(t) vs. $\alpha$ where $t \in [0,6], \alpha \in [0,0.5]$; in Fig. 6(b) $c_{12L}(t,\beta), c_{12R}(t,\beta)$ vs. time(t) vs. $\beta$ where $t \in [0,6], \beta \in [0.4,1]$; in Fig. 6(c) $c_{21L}(t,\alpha), c_{21R}(t,\alpha)$ vs. time(t) vs. $\alpha$ where $t \in [0,6], \alpha \in [0,0.5]$; in Fig. 6(d) $c_{22L}(t,\beta), c_{22R}(t,\beta)$ vs. time(t) vs. $\beta$ where $t \in [0,6], \beta \in [0.4,1]$.

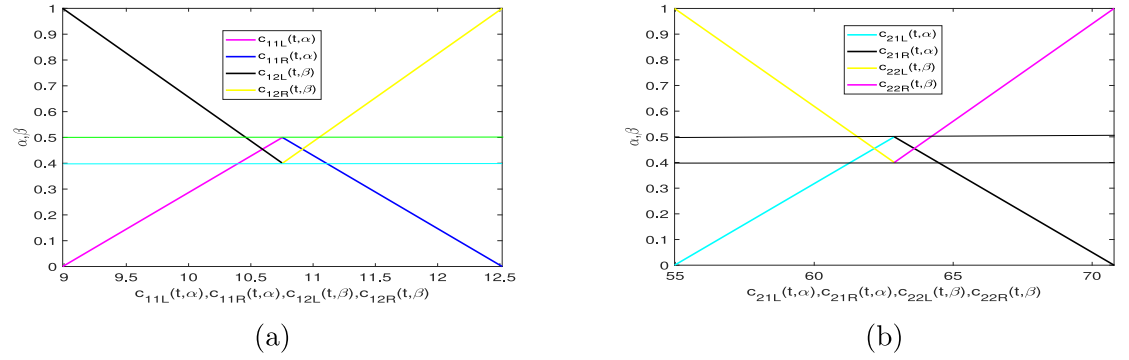


**Fig. 7.** Pictorial presentation of membership function in Fig. 7(a) for $c_{11L}(t,\alpha), c_{11R}(t,\alpha), c_{12L}(t,\beta), c_{12R}(t,\beta)$ vs. $(\alpha,\beta)$ at $t=3$ and in Fig. 7(b) for $c_{21L}(t,\alpha), c_{21R}(t,\alpha), c_{22L}(t,\beta), c_{22R}(t,\beta)$ vs. $(\alpha,\beta)$ at $t=3$ presents triangular intuitionistic fuzzy number.

**Table 5**
Intuitionistic fuzzy solution of $c_{11L}(t,\alpha), c_{11R}(t,\alpha), c_{12L}(t,\beta), c_{12R}(t,\beta)$ of the system (6) for $t=3$.

| $\alpha$ | $c_{11L}(t,\alpha)$ | $c_{11R}(t,\alpha)$ | $\beta$ | $c_{12L}(t,\beta)$ | $c_{12R}(t,\beta)$ |
|---|---|---|---|---|---|
| 0 | 8.9890 | 12.5184 | | | |
| 0.1 | 9.3420 | 12.1655 | | | |
| 0.2 | 9.6949 | 11.8125 | | | |
| 0.3 | 10.0478 | 11.4596 | | | |
| 0.4 | 10.4008 | 11.1067 | 0.4 | 10.7537 | 10.7537 |
| 0.5 | 10.7537 | 10.7537 | 0.5 | 10.4596 | 11.0478 |
| 0.6 | | | 0.6 | 10.1655 | 11.3419 |
| 0.7 | | | 0.7 | 9.8714 | 11.6361 |
| 0.8 | | | 0.8 | 9.5773 | 11.9302 |
| 0.9 | | | 0.9 | 9.2831 | 12.2243 |
| 1 | | | 1 | 8.9890 | 12.5184 |

**Table 6**
Intuitionistic fuzzy solution of $c_{21L}(t,\alpha), c_{21R}(t,\alpha), c_{22L}(t,\beta), c_{22R}(t,\beta)$ of the system (6) for $t=3$.

| $\alpha$ | $c_{21L}(t,\alpha)$ | $c_{21R}(t,\alpha)$ | $\beta$ | $c_{22L}(t,\beta)$ | $c_{22R}(t,\beta)$ |
|---|---|---|---|---|---|
| 0 | 54.9749 | 70.7879 | | | |
| 0.1 | 56.5562 | 69.2066 | | | |
| 0.2 | 58.1375 | 67.6253 | | | |
| 0.3 | 59.7188 | 66.0440 | | | |
| 0.4 | 61.3001 | 64.4627 | 0.4 | 62.8814 | 62.8814 |
| 0.5 | 62.8814 | 62.8814 | 0.5 | 61.5637 | 64.1992 |
| 0.6 | | | 0.6 | 60.2459 | 65.5169 |
| 0.7 | | | 0.7 | 58.9282 | 66.8347 |
| 0.8 | | | 0.8 | 57.6104 | 68.1524 |
| 0.9 | | | 0.9 | 56.2927 | 69.4702 |
| 1 | | | 1 | 54.9749 | 70.7879 |

fuzzy environment to get a more precise mathematical model. The suggested drug system's beginning conditions are regarded as fuzzy triangular intuitionistic numbers. The proposed model's critical point stability analysis has been investigated intuitively. The application of different types of generalized Hukuhara derivatives for intuitionistic fuzzy-valued functions is evangelized in this article. We have applied this concept to the two-compartment drug concentration model in an uncertain environment. In this work, the initial conditions of the proposed model are taken as a triangular intuitionistic fuzzy number. To talk about the suggested intuitionistic fuzzy model's qualitative

behavior, we turn it into a differential equation system with a $(\alpha, \beta)$-cut form. This is done using the GHIF derivative of type-1 and type-2 techniques. Critical points and stability analysis are performed. The values of all solutions in both systems follow the membership function of a triangular intuitionistic fuzzy number at $t = 1$ (see Tables 2 and 3) and $t = 3$ (see Tables 5 and 6). Robust intuitionistic fuzzy solutions are obtained from both systems. We may conclude that the intuitionistic fuzzy models are better than the original, classical, deterministic model. In future studies, the authors want to look into more ecological modeling using neutrosophic environments and different functional responses. They also want to use mathematical modeling techniques to develop ideas for medical research models.

## Declaration of competing interest

The authors declare that they have no known competing financial interests or personal relationships that could have appeared to influence the work reported in this paper.

## Data availability

Data will be made available on request.

## Acknowledgments

The authors are grateful to the anonymous referees and Dr. Madjid Tavana, Editor-in-Chief, for their careful reading, valuable comments and helpful suggestions.

## References

[1] E.M.P. Widmark, Principles and Applications of Medicolegal Alcohol Determination, Vol. 12, Biomedical Publication, 1981, p. 163.
[2] M.S. Feizabadi, C. Volk, S. Hirschbeck, A two-compartment model interacting with dynamic drugs, Appl. Math. Lett. 22 (8) (2009) 1205–1209.
[3] G.A. Koch-Noble, Drugs in the classroom: Using pharmacokinetics to introduce biomathematical modeling, Math. Model. Nat. Phenom. 6 (6) (2011) 227–244.
[4] O. Hrydziuszko, A. Wrona, J. Balbus, K. Kubica, Mathematical two-compartment model of human cholesterol transport in application to high blood cholesterol diagnosis and treatment, Electron. Notes Theor. Comput. Sci. 306 (2014) 19–30.
[5] A.W. El-Kareh, T.W. Secomb, A mathematical model for comparison of bolus injection, continuous infusion, and liposomal delivery of doxorubicin to tumor cells, Neoplasia 2 (4) (2000) 325–338.
[6] M.B. Abd-el Malek, M.M. Kassem, M.L. Meky, Group theoretic approach for solving the problem of diffusion of a drug through a thin membrane, J. Comput. Appl. Math. 140 (1–2) (2002) 1–11.
[7] M.A. Khanday, A. Rafiq, Variational finite element method to study the absorption rate of drug at various compartments through transdermal drug delivery system, Alex. J. Med. 51 (3) (2015) 219–223.
[8] M.A. Khanday, A. Rafiq, Numerical estimation of drug diffusion at dermal regions of human body in transdermal drug delivery system, J. Mech. Med. Biol. 16 (03) (2016) 1650022.
[9] M.A. Khanday, A. Najar, Maclaurin's series approach for the analytical solution of oxygen transport to the biological tissues through capillary bed, J. Med. Imag. Health Inform. 5 (5) (2015) 959–963.
[10] M.A. Khanday, A. Najar, Mathematical model for the transport of oxygen in the living tissue through capillary bed, J. Mech. Med. Biol. 15 (04) (2015) 1550055.
[11] M.A. Khanday, A. Rafiq, K. Nazir, Mathematical models for drug diffusion through the compartments of blood and tissue medium, Alex. J. Med. 53 (3) (2017) 245–249.
[12] L.A. Zadeh, Fuzzy sets, Inf. Control 8 (3) (1965) 338–353.
[13] D. Dubois, H. Prade, Operations on fuzzy numbers, Internat. J. Systems Sci. 9 (6) (1978) 613–626.
[14] K.T. Atanassov, Intuitionistic Fuzzy Sets, Vol. 35, Physica, Heidelberg, 1999, pp. 1–137.
[15] K.T. Atanassov, Intuitionistic Fuzzy Sets VII ITKR's Session. Sofia, Vol. 1, 1983, p. 983.
[16] K.T. Atanassov, Operators over interval valued intuitionistic fuzzy sets, Fuzzy Sets and Systems 64 (2) (1994) 159–174.
[17] K.T. Atanassov, Intuitionistic fuzzy sets, Fuzzy Sets and Systems 20 (1986) 87–96.
[18] S. Melliani, M. Elomari, L.S. Chadli, R. Ettoussi, Intuitionistic fuzzy metric space, Notes Intuitionistic Fuzzy Sets 21 (1) (2015) 43–53.
[19] S. Melliani, M. Elomari, M. Atraoui, L.S. Chadli, Intuitionistic fuzzy differential equation with nonlocal condition, Notes Intuitionistic Fuzzy Sets 21 (4) (2015) 58–68.
[20] T. Allahviranloo, N.A. Kiani, N. Motamedi, Solving fuzzy differential equations by differential transformation method, Inform. Sci. 179 (7) (2009) 956–966.
[21] S.A. Altaie, A.F. Jameel, A. Saaban, Homotopy perturbation method approximate analytical solution of fuzzy partial differential equation, IAENG Int. J. Appl. Math. 49 (1) (2019) 22–28.
[22] A.F. Jameel, S.G. Amen, A. Saaban, N.H. Man, F.M. Alipiah, Homotopy perturbation method for solving linear fuzzy delay differential equations using double parametric approach, Mathematics 8 (2020) 551–558.
[23] R. Ettoussi, S. Melliani, M. Elomari, L.S. Chadli, Solution of intuitionistic fuzzy differential equations by successive approximations method, Notes Intuitionistic Fuzzy Sets 21 (2) (2015) 51–62.
[24] M. Friedman, M. Ma, A. Kandel, Numerical solutions of fuzzy differential and integral equations, Fuzzy Sets and Systems 106 (1) (1999) 35–48.
[25] S. Wan, J. Dong, Decision Making Theories and Methods Based on Interval-Valued Intuitionistic Fuzzy Sets, Springer Nature, 2020.
[26] S.P. Wan, F. Wang, J.Y. Dong, Theory and method of intuitionistic fuzzy preference relation group decision making, Comput. Model. Eng. Sci. (2019) http://dx.doi.org/10.32604/cmes.2022.020598.
[27] J. Xu, J.Y. Dong, S.P. Wan, J. Gao, Multiple attribute decision making with triangular intuitionistic fuzzy numbers based on zero-sum game approach, Iran. J. Fuzzy Syst. 16 (3) (2019) 97–112.
[28] S.P. Wan, L.L. Lin, J.Y. Dong, MAGDM based on triangular Atanassov's intuitionistic fuzzy information aggregation, Neural Comput. Appl. 28 (2017) (2017) 2687–2702.
[29] A. Acharya, A. Mahata, N. Sil, S. Mahato, S. Mukherjee, S.K. Mahato, B. Roy, A prey-refuge harvesting model using intuitionistic fuzzy sets, Decis. Anal. J. 8 (2023) 100308.
[30] A. Acharya, A. Mahata, S. Mukherjee, M.A. Biswas, K.P. Das, S.P. Mondal, B. Roy, A neutrosophic differential equation approach for modelling glucose distribution in the bloodstream using neutrsophic sets, Decis. Anal. J. 8 (2023) 100264.
[31] Y. Yener, G.F. Can, A FMEA based novel intuitionistic fuzzy approach proposal: Intuitionistic fuzzy advance MCDM and mathematical modelling integration, Expert Syst. Appl. 183 (2021) 115413.
[32] R. Chaudhury, M. Mittal, M.K. Jayaswal, A sustainable inventory model for defective items under fuzzy environment, Decis. Anal. J. 7 (2023) 100207.
[33] R. Imran, K. Ullah, Z. Ali, M. Akram, T. Senapati, The theory of prioritized muri-head mean operators under the presence of complex single-valued neutrosophic values, Decis. Anal. J. 7 (2023) 100214.
[34] S. Pattnaik, M.M. Nayak, P. Kumar, An inventory control model in the framework of COVID-19 disruptions considering overage items with neutrosophic fuzzy uncertainty, Neutrosophic Sets Syst. 56 (2023).
[35] F. Yiğit, A three-stage fuzzy neutrosophic decision support system for human resources decisions in organizations, Decis. Anal. J. 7 (2023) 100259.
[36] R. Krishankumar, K.S. Ravichandran, M. Aggarwal, D. Pamucar, An improved entropy function for the intuitionistic fuzzy sets with application to cloud vendor section, Decis. Anal. J. 7 (2023) 100262.
[37] F. Smarandache, Neutrosophy: Neutrosophic Probability, Set, and Logic: Analytic Synthesis & Synthetic Analysis, 1998.
[38] F. Smarandache, First International Conference on Neutrosophy, Neutrosophic Logic, Set, Probability and Statistics, Vol. 4, Florentin Smarandache, 2001.
[39] F. Smarandache, Neutrosophic set-a generalization of the intuitionistic fuzzy set, in: 2006 IEEE International Conference on Granular Computing, IEEE, 2006, pp. 38–42.
[40] S. Moi, S. Biswas, S. Sarkar(Pal), A novel Romberg integration method for neutrosophic valued functions, Decis. Anal. J. 9 (2023) 100338.
[41] S. Chakraborty, R.D. Raut, T.M. Rafin, S. Chatterjee, S. Chakraborty, A comparative analysis of multi-attributive border approximation area comparison (MABAC) model for healthcare supplier in fuzzy environments, Decis. Anal. J. 8 (2023) 100290.
[42] K. Kumar, S.M. Chen, Group decision making based on weighted distance measure of linguistic intuitionistic fuzzy sets and the TOPSIS method, Inform. Sci. 611 (2022) 660–676.
[43] A. Roushan, A. Das, A. Dutta, U.K. Bera, A pentagonal type-2 fuzzy variable defuzzification model with application in humanitarian supply chains, Decis. Anal. J. 8 (2023) 100303.
[44] S. Man, B.C. Saw, A. Bairagi, S.B. Hazra, Finite difference method for intuitionistic fuzzy partial differential equations, Comput. Sci. Math. Forum 7 (2023) 48.
[45] J. Blaser, B.B. Stone, S.H. Ziner, Two compartment kinetic model with multiple artificial capillary units, J. Antimicrob. Chemother. 15 (1985) 131–137.
[46] I. Petras, R.L. Magin, Simulation of drug uptake in a two compartmental fractional model for a biological system, Commun. Nonlinear Sci. Numer. Simul. 16 (12) (2011) 4588–4595.
[47] P.M. Loughnan, D.S. Sitar, R.I. Ogilvie, A.H. Neims, The two-compartment open-system kinetic model: A review of its clinical implications and applications, J. Pediatr. 88 (5) (1976) 869–873.
[48] R.N. Upton, The two-compartment recirculatory pharmacokinetic model: an introduction to recirculatory pharmacokinetic concepts, Br. J. Anaesth. 92 (4) (2004) 475–484.

[49] S.P. Mondal, T.K. Roy, System of differential equation with initial value as triangular intuitionistic fuzzy number and its application, Int. J. Appl. Comput. Math. 1 (2015) 449–474.

[50] S.P. Mondal, T.K. Roy, Generalised intuitionistic fuzzy Laplace transformation and its application in electrical circuit, TWMS J. Appl. Eng. Math. 5 (1) (2015) 30–45.

[51] D.F. Li, A ratio ranking of triangular intuitionistic fuzzy member and its application to MADM problems, Comput. Math. Appl. 60 (2010) 1557–1570.

[52] B.K. Dutta, Mathematical Methods in Chemical and Biological Engineering, CRC Press, ISBN: 978-1-4822-1038-5, 2017.

[53] M.A. Khanday, A. Rafiq, K. Nazir, Mathematical models for drug diffusion through the compartments of blood and tissue medium, Alex. J. Med. 53 (2016) 245–249.

International Journal of Humanities Social Science and Management (IJHSSM)
Volume 3, Issue 1, Jan.-Feb. 2023, pp: 523-527 www.ijhssm.org

# The Rural Development of West Bengal and Impact of Human Resource Management

Prof. Bivash Saha
*Assistant Professor, Department of Business Management*
*Swami Vivekananda Institute of Modern Science, MAKAUT*

Date of Submission: 07-02-2023 Date of Acceptance: 19-02-2023

**Abstract**
Present condition of rural development that needed immediate attention to the Human Resource Management (HRM) system at native self-determination establishments for effective and desired rural development in West Bengal. thanks to absence of forward planning, lack of responsibility, lack of morality, lack of higher cognitive process in the slightest degree levels, apply of recent methods, ineffective leadership, faulty staffing procedure and lack of motivation and co-ordination parallel and desired development had not been fulfilled. And here arose the necessity to train, to update and inspire the government functionaries through human resource management for higher results. A form was developed to gather information on operational a part of HRM and workers development. One district and eight local self- government establishments were selected for this study. The analysis study took a glance at HRM, vital} tool for institutional impassiveness. a lot of over, the results of the study disclosed that the HRM practices had an excellent impact and significant effect on institutional effectiveness and employee's performance. Therefore, the research study suggested and ended that the HRM practices were a vital tool to attain expected rural development in West Bengal.

**Keywords**
Human Resource Management, local self-help group, rural development, socio-economic transformation

## I. Introduction

Development is a wide concept than economic growth. Rural development has been a major issue inIndia and also in West Bengal. After independence, the institutions of the Panchayati Raj were involved and were to play a significant role in India's rural development. The commissions and planning committees set up by the Government of India gave special attention and importance to these rural development institutions.

Rural development in our state was an emerging factor in the challenging global scenario. Because what we understand by appropriate rural development was not yet possible in our federal state. During my field visit it was seen that most people live in villages and many people live below the poverty line (PPL). They suffered from malnutrition. There was a lagoon with food, clothing and shelter. Ignorance and illiteracy enveloped his life. Adequate infrastructure, drinking water, roads and communication facilities were one of the main problems.

In India, 1992 Constitutional Amendment which is known as 73rd amendment, decentralized Agriculture, Irrigation, Health, Education along with 23 other articles to the Panchayats, the local self-governing body. The three-tier panchayat system at district, block and village level should fulfil the rural development goal by decentralizing planning, various programs and their implementation. In West Bengal, a state in East India, the pre-constitutional panchayats were revived in and took great initiative as part of the local-level self-governing body to implement the three-tier panchayat system. Rural development is the main pillar of the nation's development. According to our constitution and political aspect the local self-government in India known as Panchayati Raj Institutions.

However, West Bengal pioneered the implementation of the three-tiered Panchayti Raj system for the socio-economic development and transformation of rural society. But what we mean by appropriate and desirable rural development has not yet been achieved. In West Bengal, unified rural development has yet to be realized due to lack of accountability, responsibility, proper and accurate planning, flawed recruitment procedures, ineffective

International Journal of Humanities Social Science and Management (IJHSSM)
Volume 3, Issue 1, Jan.-Feb. 2023, pp: 523-527 www.ijhssm.org

leadership, use of old methods, and motivation and coordination in the local self-government institutions.

In many different areas of India, the Panchayat stays as a susceptible frame with confined powers, and, very frequently, is ruled with the aid of using the socially and economically powerful. The Panchayat structure in West Bengal, all even though now no longer freed from all weaknesses, supplied a distinctive picture. Like the path of improvement itself, the overall performance of Panchayat establishments throughout the State turned into unequal, of course, as now no longer they all had been similarly ready to deal with their responsibilities. However, nicely-functioning Panchayats had been frequently capable of make a widespread distinction to making plans and implementation of improvement programmes, and, extra importantly, to the lives of the poor. The latest traits in West Bengal undermine this achievement, and might nicely usher in a shift in magnificence alliances and strength family members withinside the State.

Human resources are institution's finest strength due to the fact without them, features of Panchayat Institutions which includes managing, monitoring, implementation of programmes/projects, conversation and managing stakeholders couldn't be completed. Human resources and the potentials they possess are the important thing drivers for an institutional success. With globalization and technological advances, trendy establishments (PRIs) are constantly changing. In order to maximise institutional effectiveness, human potentials, individuals' capabilities, time, and capabilities should be controlled and developed. Hence, theexercise of human useful resource management (HRM) in Panchayati Raj Institutions met the goals of rural improvement in West Bengal.

Human assets of an organisation may be a supply of aggressive advantage, supplied that the regulations for dealing with human beings are included with strategic commercial enterprise making plans and organizational culture. Human assets or human capital of a company that represent the useful resource main to aggressive advantage. However, personnel are a more asset than bodily or economic assets, for the skills of personnel is what determines an organisation’s success. Development of human beings, their competencies, and the system improvement of the total organisation are the primary issues of human useful resource control.

This research study mainly focused on how human resource management practicescontributed to the overall performance of Panchayati Raj Institutions for powerful rural improvement. This article has a look at tested of Human Resource Management (HRM) from the perspective ofrural improvement in West Bengal. Thus, the paper diagnosed the importance of human resource and its control and effect on rural improvement.

## II. Problem of the Study

West Bengal is a state with a large population. There are so many villages scattered all over West Bengal. Agriculture is one of the pillars and a determining factor of the state economy. Rural villages are the heart and soul of the state's progress. If it were possible to properly develop every single village in the state, then the progress and prosperity of the people in the village and the economy of the state would develop at the same time. But how was that possible? This has only been possible through proper rural development.

According to 2011 census, the total population of West Bengal is about 9.13 billion people, and about 68% of the population lives in villages, and the majority of our total population remains deprived of basic needs. of life. Rural development in West Bengal did not bring the expected result. The lack of food, rural infrastructure, road infrastructure, drinking water, health and sanitation facilities was identified due to the ineffectiveness of local self-government institutions and their officials in relation to rural development.

After a detailed evaluation of the Panchayat-Level work, some clear deficiencies could be identified. These shortcomings were mainly negligence, lack of proper oversight, lack of accountability and responsibility, and gaps in capacity development, etc. There were also some other shortcomings such as quality of leadership, practice of old methods, ineffectiveness of Panchayati Raj institutions, the gap at resource mobilization etc. In addition, emphasis should be placed on transparency, implementation of an appropriate training system and management of.

The right idea and the promotion of responsibility were partially or completely missing. In some cases, the seriousness of the correct work goal was disregarded. Workers and supervisors had not received adequate training. Urgent and essential work was not selected after sampling. In many cases, the working hours were not respected. Some work was carried out beyond the project period. In

International Journal of Humanities Social Science and Management (IJHSSM)
Volume 3, Issue 1, Jan.-Feb. 2023, pp: 523-527 www.ijhssm.org

many cases, not much attention was paid to the work. As a result, villagers and stakeholders did not always receive adequate and accurate information and services. At one point, an obstacle stood in the way of the expected smooth development of rural areas in West Bengal.

All those quick comings and defects had made maximum initiatives and works omitted and incomplete. Above all human accountability, duty and moralities had been absent and those had been the principal limitations toward attainment of rural improvement aim in West Bengal.

## III. Objectives of the Study

The aim objective of the research paper is having a look at turned into focused its attention, to have a look at the human resource control practices at Panchayat Raj Institutions and its contribution to the overall performance of Panchayati Raj Institutions in the direction of powerful rural improvement in West Bengal.

- To decide courting among HRM and effectiveness of Panchayati Raj Institutions for rural improvement in West Bengal.
- To decide the position of staff/member of Panchayat group could end up more competent, efficient, responsible and accountable via human resource control in the direction of attainment of institutional effectiveness and rural improvement.

## IV. Methods

To conduct a research study to investigate the impact of human resources management in Panchayati Raj institutions on desired rural development in West Bengal. In this research process data mainly collected from published documents of govt, regulatory orders and reports, some recorded interviews of elected officials and beneficiaries from the reliable source of internet. In this research article most of the data are secondary and mainly collected from official records at different levels, such as districts, blocks and villages, through discussions, collecting views and opinions from officials of Panchayat Raj institutions and interest groups. The collected data were analysed using descriptive Analysis process.

## V. Literature Review and Conceptual Framework

Human Resources (HR), what's Management and what's the that means of HRM and the way its capabilities in organizational settings, why humans are critical and crucial as organizational assets and the way this asset may be effectively, efficaciously and nicely applied for person in addition to institutional fulfilment.

The literature at the topics of rural improvement in all fairness large, at the same time as it isn't so in the difficulty of rural improvement thru human aid control that's a developing place of research. A few seminal contributions with regards to take a look at have been reviewed to become aware of the fundamental developments and to project into a brand-new place of research. Government of India and Governments of West Bengal's Panchayat and Rural Development Programmes have been evaluated via way of means of diverse Government businesses viz. Programme Evaluation Organisation of the Planning Commission, Concurrent Evaluations performed via way of means of the Ministry of Rural Development with the assist of reputed establishments positioned on the nearby level, RBI, NABARD, IFMR, NIUA, NIRD, DFID, UNICEF and different country wide and international businesses like Universities, Research Institutes, NGOs, and Individuals. Their approaches, conceptualization and technique laid their consciousness at the fulfilment and shortfalls in phrases of performance, as measured via way of means of aid mobilization, poverty remedy or assets creation. But they have got infrequently tried to reinforce the Capacity, accountability, duty and effectiveness of nearby authorities' functionaries through human aid control.

## VI. Proposed Theoretical/Conceptual Framework

The examiner aimed to examine the interrelationship among the impartial variables and worker overall performance, efficiency, competency, effectiveness through undertaking studies on how those three variables have an effect on the overall performance of the functionaries of neighbourhoodself-authorities' institutions. Here the examiner illustrated and attempted to present a clean photo how human aid planning, education and improvement, overall performance and ability appraisal helped and assisted the staff to improve and replace their overall performance, skills, efficiency, competency and additionally institutional effectiveness toward attainment of rural improvement in West Bengal. In short, the proposed framework recommended how planning, education and improvement, overall performance and ability appraisal as part of human aid control facilitated the neighbourhoodself-authority's organization in attaining the aim of rural improvement thru effective usage of staff.

International Journal of Humanities Social Science and Management (IJHSSM)
Volume 3, Issue 1, Jan.-Feb. 2023, pp: 523-527 www.ijhssm.org

## VII. Findings of the Study

During field visits and at the time of data analysis, it was noted that in the panchayat-level planning system, infrastructure, agriculture, poverty alleviation, sanitation, health, education, etc. lack of interest and initiatives to improve and manage panchayat-level officials. Hardly any planning was found in human resources. It was also noted that there was no human resource planning strategy integrated with the institution's strategy to achieve institutional goals. A gap in training and development practices at Panchayat level was also identified during the field visit.

Maximum training program organized by the panchayat basically in projects, plans, accounts and related audits, but hardly any human resource training and development program was found. ultimately making the workforce ineffective and inefficient. It was also noted during field visits and at the time of data analysis that no system for performance appraisal existed at the panchayat level to ensure institutional effectiveness by correcting staff for standard and improved performance and suggesting changes in staff behaviour. The individual performance appraisal system for panchayat officials has hardly been found. Also, there was no reward system for good, responsible & amp; responsible employee/member at panchayat level.

## VIII. Discussion and Conclusion

In the technology of globalization and technological development the nature, extent and range of works of an agency have been converting fast. In the aggressive worldwide situation organizations have been going through such a lot of issues in opposition to their development and prosperity. To preserve up their development intact organizations had to expand and nurture their essential belongings i.e., human sources. If human sources of an agency have been competent, green and powerful then the overall performance of the agency might be accordingly. HRM is believed to have an effect on knowledge, skills, abilities (Schuler & Jackson 1995), attitudes and behaviour of personneland can consequently have an effect on the overall performance of an agency.

HRM is worried with the right and powerful makes use of personnel to gain organizational and character goals. Through human useful resource control, it's miles viable to make competent,green and powerful staff for the agency. Through which an agency enables to take right strategy, planning, programmes and might execute the equal also. By such an powerful staff organizations grow to be capable of produce in time carrier delivery. Therefore, the position of staff in an agency isn't always most effective essential however vital also. To inspire the staff and to extract the capability toward attainment of organizational goaland success, human useful resource control acts as a critical tool. The exercise of HRM isthat human beings are the organization’s key useful resource andorganizational overall performance largely relies upon on them.Under the above circumstances and after reviewing the panchayat system in West Bengal, it was found that the HRM policy was partially or totally absent. After analyzing the Panchayat system, it was found that infrastructure, agriculture, poverty alleviation, sanitation, health, education, etc. were important. employees, etc.

It was also noted that no such planning, training, development and performance appraisal practices have been found that would make Panchayat officials dynamic, effective and efficient to take an active and important role in rural development. If they were not competent, efficient, accountable, accountable, how would they approach adequate and effective planning, needs-based planning for rural development? Such a policy proved of little help, making the officials of the Panchayat effective and dynamic for the purpose. Only those panchayats that managed human resources better could achieve better rural development. If the human resources of a panchayat were good, responsible and efficient, rural development under that panchayat could be carried out accordingly.

For this it was necessary to create precise and efficient human resources for a perfect administration and institutionalist of the panchayat. Through proper planning, training and development of human resources and potential assessment system, it was possible to establish perfect management and efficient administration of Rural Development Panchayat. For this, there was an urgent need to develop the workforce and human potential through HRM.

In end Panchayats had been to be properly evolved and properly controlled alongside withcommunication, technological improvement, which turned into worrying responsibility,accountability, management first-rate and performance of workforce. It had to introduce newcontrol strategies to expand human assets for fast selection making, planning,right provider

transport and enhancement of capacity, right managing stakeholderssome of the team of workers/contributors of Panchayats to fulfil the demanding situations of recent millennium.

Therefore, the function of human assets at Panchayati Raj establishments turned into very critical and inevitable. Even simplest planning, programmes, projects, infrastructure and cash had been not capable of meet the motive of important rural improvement in West Bengal, without efficient, equipped and powerful Panchayat functionaries. Therefore, human useful resource turned into the core and critical problem for rural improvement in West Bengal. Through HRM it turned into viable to nurture, inspire and evolved the capacity, performance, competency of the team of workers and contributors of Panchayat establishments and which in the long run helped the Panchayat towards attainment of rural improvement.

## Bibliography

[1]. Armstrong, M 2006, A Handbook of Human Resource Management Practice, 10th ed., London, Kogan Page, P. 44-76.
[2]. Ann, G, Jerry, WG, Scott, AQ & Pamela, D 2009, The Praeger Handbook of Human Resource Management, Praeger Publishers, London, p. xvi-xvii.
[3]. Annual Report, 2008-2009, Panchayat and Rural Development Department, Government of West Bengal
[4]. Bakshi, A 2011, 'Weakening Panchayats in West Bengal', Field Report, Review of Agrarian Studies, vol. 1, no. 2, Review of Agrarian Studies, Bangalore, India, pp.203-205 available at www.ras.org.in.
[5]. Beer, M, Spector, B, Lawrence, P, Mills, DQ & Walton, R 1985, Human Resource Management: A General Managers Perspective, New York, Free Press.
[6]. Census Report, 2011, Government of India (Provisional).
[7]. Chakrabarti, B, Chattopadhyay, R & Nath, S 2011, 'Local Governments in Rural West Bengal, India and their Coordination with Line Departments', Commonwealth Journal of Local Governance, no 8/9: May-November 2011.
[8]. Den Hartog, DN, Boselie, P & Paauwe, J 2004, 'Performance Management: A model and research agenda', Applied Psychology: An International Review, vol. 53, no. 4, pp. 556-569.
[9]. Gupta R.K. 2004, Rural Development in India , Atlanta Publishers & Distributors (P) Ltd, New Delhi.
[10]. Guest, DE 1997, 'Human resource management and performance; a review of the research agenda', The International Journal of Human Resource Management, vol. 8, no. 3, pp. 263–76.
[11]. Megginson, Leon C. 1977, Personnel and Human Resource Administration, Richard D. Irwin, Illinois, Homewood, p. – 4
[12]. Pareek, U & Rao, T V 1992, Designing and managing human resource systems, New Delhi, Oxford & IBH Publishing Company.
[13]. Rensis Likert 1967, The Human Organisation : Its Management and Value, New York : MacGraw-Hill Book Co.) p.1.
[14]. Schuler, RS & Jackson, SE 1995, 'Understanding human resource management in the context of organizations and their environment', Annual Review of Psychology, no. 46, pp. 237-264.
[15]. Wright, PM, McMahan, GC & McWilliams, A 1994, 'Human resources and sustained competitive advantage: A resource-based perspective', International Journal of Human Resource Management, vol. 5, no. 2, p. 301.

*SVOA Microbiology*

ISSN: 2634-534X

ScienceVolks Open Access

Research

# Study of Comparison of Oral Fungal Flora of Smokers vs Non-Smokers in a Metropolitan City

**Shyam Sundar Tiwari[1], Atul Raj[2]*, Sayan Bhattacharyya[2] and Abhirup Ganguli[3]**

[1] *Swami Vivekananda Institute of Modern Science, Sonarpur, West Bengal, India.*

[2] *Department of Microbiology, All India Institute of Hygiene and Public Health, Kolkata, India.*

[3] *Department of Microbiology, Swami Vivekananda Institute of Modern Science, Kolkata, India.*

***Corresponding Author:** Atul Raj, Department of Microbiology, All India Institute of Hygiene and Public Health, Kolkata, India.*

DOI: https://doi.org/10.58624/SVOAMB.2023.04.036

***Received:** November 09, 2023* ***Published:** November 29, 2023*

## Abstract

There are some common fungi found in the oral cavity. Epidemiological studies indicate higher risk for periodontal disease in smokers vis a vis non-smokers. The increased risk is proportional to the length and frequency of smoking. This is an important area of public health research. In our study we found fungi to be present significantly more in oral cavity of smokers as compared to non-smokers.

***Keywords:** Oral Microbiome, Pathogenic microorganisms, Smokers, Non smokers*

**Abbreviations:** CSC: Cigarette smoke condensate

## 1. Introduction

Cigarette smoking is injurious to health, there are various types of microbes present in our oral flora, some are beneficial some are harmful, but when we smokes or chews tobacco these beneficial microbes starting decline and pathogenic microbes starts multiplying their number, which leads to different types of oral problem. Cigarette smoke concentrate (CSC) comprises in excess of 7000 known chemical molecules of which 6 are complex miture of oxidants and various free radicals. It can modify the oral microenvironment and lead to significant oxidative stress, which in turn can damage the oral epithelial barrier.[1]

Cigarette smoking is a cause to many abnormal alterations that can begin with an increase of *candida* colony count that causes oral diseases such as pseudomembranous candidiasis, acute atopic candidiasis, chronic hyperplastic candidiasis, chronic atopic candidiasis, and angular cheilitis [9]. Other factors such as long-term antibiotic consumption, HIV infection, diabetes mellitus, radiotherapy, bad oral hygiene, dental prostheses, and cigarette smoking can also contributes to an increase of candida colony count [9,10,11].

## 2. Materials and Methods

### 2.1. Timeline of study

This study was carried out in a span of 3 months from February 2023 to May 2023.

### 2.2. Place of study

Department of Microbiology, Bidhan Nagar campus, All India Institute of Hygiene and Public Health, Kolkata.

### 2.3 Type of study

Laboratory based observational study.

### 2.4 Sample size

Fifty four (54) subjects, representing both genders, ranging in age from 18 to 60. Fifty-four (54) samples were tested. This sample size had been calculated by method of convenience. In case of smokers the swabs were taken from those, who smoked from a minimum of 5 years. There were 27 swabs taken from smokers and 27 swabs from non-smokers. Two swabs were taken from each volunteer, one for culture and another for Gram stain and Albert's stain. Gram stain for seeing gram positive and gram negative bacteria while Albert stain for seeing bacteria containing Metachromatic Granules(MCG)16,17.

### 2.5 Methodology proper

These volunteers were from the below-mentioned campuses or worked there:-

a) Bidhannagar campus

b) Urban health unit and Training centre, All India Institute of Hygiene and Public health, Chetla

c) Central Avenue (main campus),

d) Sonarpur

e) Howrah

Samples from the following nine sites were analyzed for each subject: dorsum of the tongue, lateral sides of the tongue, buccal fold, hard palate, soft palate, labial gingiva and tonsils of soft tissue surfaces, and supragingival and subgingival plaques from tooth surfaces. samples were be collected by swab from the adjacent area and was brought to the laboratory. Then samples were transported to the laboratory in an ice-pack or within 4 hours of collection. Then the samples were processed for bacteria and Yeast. Samples were inoculated on the following media:

1. Mac Conkey agar with neutral red as pH indicator (Peptone, Neutral red, agar agar, Lactose, Sodium taurocholate, deionized water) for distinguish bacteria based on their lactose-fermenting properties into LF (Lactose-fermenting) and NLF (Non-Lactose-fermenting) colonies..

2. Sabouraud's dextrose agar (SDA) plate (pH 5.6-6) (containing D-glucose 2gm, Peptone 2 grams, Agar agar 2 grams, and deionized water 100 ml) for fungal isolation.

3. Robertson's cooked meat medium (RCM) for culturing anaerobes, made as per manufacturer's instruction .

4. Blood agar plate for differentiating bacteria based on their pattern of hemolysis.

5. Muller Hilton Agar for Antibiotic Susceptibility Test.

6. Nutrient Agar with 6.5% NaCl and Tellurite Agar for inoculation of Enterococcus spp.

7.Egg Yolk Agar for inoculation of Bacillus spp.

Gram's stain and Albert's stain were carried out from samples directly, to detect Gram positive or gram negative bacteria, and bacteria with metachromatic granules respectively, as another Add the fungal colony to the drop of LPCB using a sterile mounter an inoculation loop (from solid medium), depending on the sample of use part of the study.

Samples were inoculated on specific media and identification of microorganisms were done.

**Identification of fungus**

*A: LPCB mount showed budding yeast:*

Lactophenol Cotton Blue (LPCB) Staining is an easy method employed for the microscopic examination and subsequent identification of fungi. This method works on the principle of aiding the identification of the fungal cell walls.

1. On a clean & sterile microscopic glass slide, we added a drop of LPCB solution.
2. We added fungal colony on the drop of LPCB solution, using a sterile mounter or inoculation loop (from solid medium), depending on the sample of use.

3. Tease the fungal sample of the alcohol using a needle mounter, to ensure the sample mixes well with the alcohol.
4. Carefully cover the stain with a clean sterile coverslip without making air bubbles to the stain.
5. Examine the stain microscopically at 40X, to observe for fungal spores and other fungal structures.

*B. Germ tube test:*

Two to three colonies of yeasts were passed in 0.5 ml of pooled human serum in a small test tube and incubated aerobically at 37ºC for 2-4 hours. Then a wet mount was prepared from the suspension and observed under the 10X and 40X objectives of the light microscope.

Positive germ tube was declared when there was tube-like narrow elongated projection without constriction at base.

Germ tube positivity is found in *Candida albicans* and *Candida dubliniensis*..

*C. Sugar fermentation test:*

Sugar fermentation test was done in peptone water containing 2%(w/v) sugar (Lactose, Sucrose, Glucose , Maltose) and Andrade Indicator (contains Acid Fuchsin and NaOH). Colour change and pellicle formation were noted and interpreted as follows:

*Candida albicans*:- Glucose and Maltose fermented, sucrose variable, lactose not fermented.

*Candida tropicalis*:- Glucose , Maltose and sucrose fermented, lactose not fermented.

*Candida glabrata*:- Glucose fermented, Maltose, lactose and sucrose not fermented.

*Candida kefyr*:- Glucose, sucrose and lactose fermented, lactose not fermented.

Sugar fermentation test results are shown in figure 1 below.

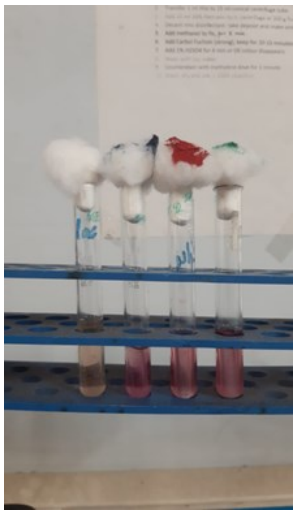

***Fig1:*** *Sugar Fermentation Test*

*D. Thermotolerance test:*

Germ tube test positive *Candida* isolates were inoculated on SDA tube and kept at 44.5ºC in the Water bath overnight. If growth shown in SDA tube the next day, then the isolate interpreted as Candida albicans, growth not shown in SDA tube then it was noted as Candida.

*E. Dalmau test:*

It was done on Corn Meal Agar. With the help of loop or straight wire, yeast colonies were taken, slit culture was done on the Corn meal Agar. It was incubated at room temperature for 2-3 days in a dark place. After 2-3 days of time, the inoculated Corn meal agar plate was observed under the 10X and 40X objectives of the compound microscope. If terminal chlamydospores were observed under the microscope then a confirmation test will be done. Terminal chlamydospores are seen by Dalmau test in *Candida albicans* as well as *Candida dubliniensis*. Dalmau test is shown in figure 2 below.

***Fig 2:*** *Dalmau Test.*

Scheme for yeast Identification (G= glucose, M=Maltose, S+ Sucrose, L= lactose) is shown in Table 1 below.

**Table 1:** Results of Dalmau, Germ tube test and sugar fermentation of yeasts.

| Sl. No | Name of yeast | Colony character | Germ tube test | Sugar fermentation test | Thermotol erance test at 44.5 Degree C | Dalmau test |
|---|---|---|---|---|---|---|
| 1 | *Candida albicans* | Moist pasty colonies on SDA. | Positive | G+ M+ S (Variable) L- | positive | Single Terminal chlamydospore |
| 2 | *Candida dubliniensis* | Moist pasty colonies on SDA. | Negative | G+, M+, S (VARIABLE), L -, | negative | Multiple Terminal chlamydospore |
| 3 | *Wickerhamomyces anomalus* | Moist pasty colonies on | Negative | G+, M+, S +, L-, | negative | Only yeasts |
| 4 | *Candida kefyr* | G+, M+, S (VARIABLE), L-, | Negative | G+, M-, S +, L+, | negative | Logs in stream appearance of yeasts and pseudo-hyphae |

We did a biofilm formation test for every *C.albicans* isolate by test tube method using 1% alcoholic Safranine.

## 3. Results

### 3.1 How many samples tested

In this study 54 samples were collected , out of which 14 were taken from females and 40 from males. Out of 14 females, 7 were smokers and 7 were non-smokers. Out of 40 males 20 were smokers and 20 were non-smokers. Out of 27 smokers 7 were occasional smokers while 20 were regular/chain smokers. Of all the subjects who were smokers, only 1 smoked bidi(handmade smoking stick) while others smoked cigarettes. Out of all the smokers, 4 individuals were also consuming oral tobacco.

The Biofilm formation test on every *C.albicans* isolation was positive.

The Fungal species we isolated in smokers was *Candida albicans* (14 out of 27) (51.85%), *Candida dubliniensis* (4 out of 27) (14.81%), *Wickerhamomyces anomalus* (5 out of 27) (18.51%), *Candida kefyr* (2 out of 27) (7.40%) and *Trichosporon* (2 out of 27) (7.40%). *Candida albicans* was the commonest fungus isolated from smokers.

We isolated no fungal species in Non smokers. (sample size of non-smokers was 27).

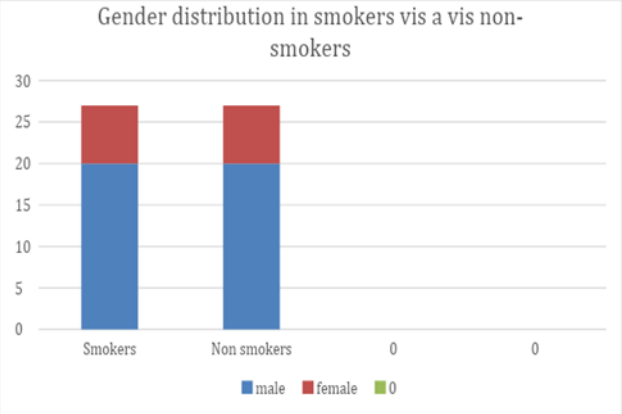


***Fig 3:*** *Gender distribution of Smokers vs nonsmokers*

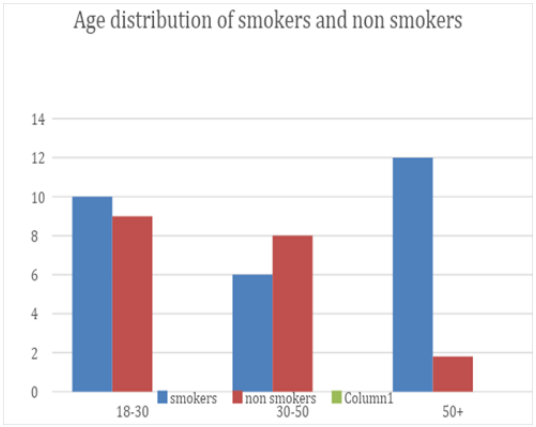


***Fig 4:*** *Age distribution of Smokers vs nonsmokers.*

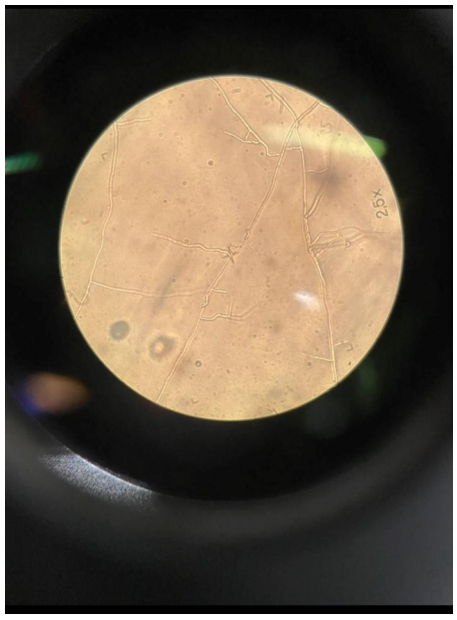


***Fig 5:*** *Microscopic image of Trichosporon spp.*

All the *Candida* isolates were susceptible to Fluconazole in vitro, by the disk diffusion test on Mueller Hinton Agar containing 2 gm/ 100 ml Glucose and 0.5 micrograms per ml Methylene blue.

## 4. Discussion

Smoking is one of the major factors affecting the pulmonary, cardiovascular and some infectious diseases. Smoking can influence both the innate and adaptive immune responses, both humoral and cell mediated immunity.[1]

In the present study we collected samples from male and females between the age range of 18-60 years. Though our sample size of Smokers and Non smokers was 54.

In this study we isolated fungus in smokers only. The most prevalent species was *Candida albicans.* [2]

The trend of cigarette smoking is on the rise in developing countries like India. Youth are attracted towards it, which is an alarming sign .[3]

Nicotine and other particles in tobacco smoke increase *C.albicans adhesion* and also biofilm formation[4].

One limitation of our study was that the sample size was small (54).

The present study can infer that smoking cigarettes can increase the risk of candidiasis. We also found *Candida* spp. in smokers. However, this study was carried out in a restricted geographical setting with a limited sample size. The habit of smoking is recognized as a very important predisposing factor for Oral candidiasis, because it can incite more keratinization in the oral epithelial cells. In addition to this, the smoke constituents increase fungal virulence. Many studies have documented that smoking can stimulate increase in carriage of oral candidiasis [5]. More such studies should be done in future for the sake of public health[6].

CSC (Cigarette smoke concentrate)- mediated induction of *C. albicans* adherence to cells, growth, and also biofilm formation may explain the increased persistence of this pathogen in smokers. These findings may also be relevant in case of other oral diseases where biofilms are found.[7] Exposure to cigarette smoke increases fungal growth and biofilm production. Cigarette smoking interferes between *S mutans* and *C.albicans* results in biofilm formation on dental restoration materials[7] . Cigarette smoke reaches not only the host cells but also the microorganisms of the oral cavity. More contact between cigarette smoke and the oral microbes can enhance development of diseases like periodontitis. Cigarette smoke may also fine-tune phenotypic and other traits of *C. albicans* which promote oral candidiasis[8]. Smoking can affect oral colonization due to *Candida* species. Both overall have a bad effect on oral health[9]. Oral *Candida* infection is usually seen in an immunocompromised host and the compromise may be either local or systemic. Local compromising factors like diminished salivation, poor oral hygiene, wearing dentures, and other systemic factors like Diabetes mellitus, nutritional deficiencies, HIV infection and others also promote oral infections like oral Candidiasis[10].

## Conclusion

Exposure to cigarette smoke enhances fungal growth and biofilm formation. More studies are needed in this aspect.

## References

1. Ye P, Chen W, Huang F, Liu Q, Zhu YN, Wang X, et al. Smoking increases oral mucosa susceptibility to Candida albicans infection via the Nrf2 pathway: In vitro and animal studies,Journal of Cellular and Molecular MedicineVolume 25, Issue 16 p. 7948-7960
2. Pourbaix A, Rapnouil BL, Guéry R, Lanternier F, Lortholary O, Cohen JF. Smoking as a Risk Factor of Invasive Fungal Disease: Systematic Review and Meta-Analysis, Clinical Infectious Diseases 2020;71(4):1106–1119.
3. Akpan A, Morgan R. Oral candidiasis. Postgrad Med J 2002;78(922):455–9.
4. Singh A, Verma R, Murari A, Agrawal A. Oral candidiasis: An overview. J Oral Maxillofac Pathol. 2014;18(Suppl 1):S81 –S5
5. Navabi N, Ayatollahi-Mousavi SA, Anvari N. A Comparison of the Prevalence Rate of Oral Candida Colonization between Opium Users and Cigarette Smokers in Kerman, Iran. Addict Health. 2021 Apr;13(2):106-113. doi: 10.22122/ahj.v13i2.301.
6. Coronado-Castellote L, Jimenez-Soriano Y. Clinical and microbiological diagnosis of oral candidiasis. J Clin Exp Dent 2013;5(5):e279–e86.
7. Ye P, Wang X, Ge S, Chen W, Wang W, Han X. Long-term cigarette smoking suppresses NLRP3 inflammasome activation in oral mucosal epithelium and attenuates host defense against Candida albicans in a rat model. Biomed Pharmacother. 2019;113:108597.

8. Semlali A, Killer K, Alanazi H, Chmielewski W, Rouabhia M. Cigarette smoke condensate increases C. albicans adhesion, growth, biofilm formation, and EAP1, HWP1 and SAP2 gene expression. BMC Microbiol. 2014 ;12;14:61. doi: 10.1186/1471-2180-14-61.

9. Muzurović S, Hukić M, Babajić E, Smajić R. The relationship between cigarette smoking and oral colonization with *Candida* species in healthy adult subjects. Med. Glas 2013; 10(2):397-399.

10. Krishnan PA. Fungal infections of the oral mucosa,Indian Journal of Dent. Res 2012;. 23(5):650-59.

**Citation:** Tiwari SS, Raj A, Bhattacharyya S, Ganguli A. Study of Comparison of Oral Fungal Flora of Smokers vs Non-Smokers in a Metropolitan City. *SVOA Microbiology 2023,* 4:3, 91-97.

# Study of Comparison of Oral Microbial Flora of Smokers vs Non-Smokers in a Metropolitan City

**Article** *in* Research in Medical & Engineering Sciences · October 2023

DOI: 10.31031/RMES.2023.10.000743



**4 authors**, including:

Shyam Sundar Tiwari

**2** PUBLICATIONS **0** CITATIONS

SEE PROFILE

Atul Raj

All India Institute of Hygiene and Public Health

**44** PUBLICATIONS **49** CITATIONS

SEE PROFILE

Sayan Bhattacharyya

All India Institute of Hygiene and Public Health

**152** PUBLICATIONS **206** CITATIONS

SEE PROFILE

Crimson Publishers
Wings to the Research

Research Article

# Study of Comparison of Oral Microbial Flora of Smokers vs Non-Smokers in a Metropolitan City

**Shyam Sundar Tiwari[1], Atul Raj[2]*, Sayan Bhattacharyya[2]* and Abhirup Ganguli[3]**

[1]M.Sc. Biotechnology student, Swami Vivekanand Institute of Modern Science, Sonarpur, India

[2]Department of Microbiology, All India Institute of Hygiene and Public Health, India

[3]Department of Microbiology, Swami Vivekananda Institute of Modern Science, Sonarpur, India

**ISSN: 2576-8816**

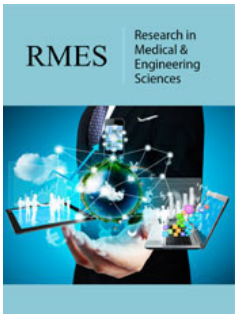


***Corresponding author:** Atul Raj and Sayan Bhattacharyya, Department of Microbiology, All India Institute of Hygiene and Public Health, Kolkata, India

**Submission:** September 19, 2023

**Published:** October 20, 2023

Volume 10 - Issue 4

**How to cite this article:** Shyam Sundar Tiwari, Atul Raj*, Sayan Bhattacharyya* and Abhirup Ganguli. Development of High-Content Adult Sensory Neuron Gene Silencing Screening Assay to Study Mechanisms of Neurite Growth. Res Med Eng Sci. 10(4). RMES.000743. 2023. DOI: 10.31031/RMES.2023.10.000743



## Abstract

There are more than 700 different bacteria found in oral cavity. Epidemiological studies show significantly higher risk for periodontal disease in smokers compared to non-smokers. The increased risk is proportional to the duration and rate of smoking. This is an important area of public health research. In our study we found that MRSA was significantly more in oral cavity of smokers when compared to non-smokers.

**Keywords:** Oral Microbiome; Pathogenic microorganisms; Smokers; Nonsmokers

**Abbreviations:** MRSA: Methicillin Resistant *Staphylococcus aureus*

## Introduction

### Oral microbiome

The inside of our mouth is the perfect place for bacteria to thrive: it's dark, it's warm, it's wet and the foods and drinks we consume provide nutrients for them to eat. But when the harmful bacteria build up around our teeth and gums, we are at risk of developing periodontal (or gum) disease, experts say, which is an infection and inflammation in the gums and bone that surround your teeth. Such conditions in your mouth may influence the rest of your body. A growing yet limited body of research, for instance, has found that periodontal disease is associated with a range of health conditions including diabetes, heart disease, respiratory infections and dementia. There are more than 700 bacteria found in the oral cavity ,2nd highest after gut.

The community of microbial residents in our body is called the microbiome. The term "microbiome" is coined by Nobel Prize laureate Joshua Lederberg, to describe the ecological community of symbiotic, commensal and pathogenic microorganisms. These microorganisms literally share our body space. Oral microbiome was first identified by the Dutchman Antony van Leeuwenhoek who first identified oral microbiome using a microscope constructed by him. He was called the father of microbiology and a pioneer who discovered both protists and bacteria. In 1674, he observed his own dental plaque and reported "little living animalcules prettily moving." Collective genome of microorganisms that reside in the oral cavity is called oral microbiome. In periodontal disease, tooth loss, and possibly gastrointestinal cancers oral bacteria playing a critical role and several physiological functions. The bacterial community structure of the oral microbiome is formed principally by Firmicutes, Bacteroidetes, Proteobacteria, Actinobacteria, Spirochaetes, and Fusobacteria, with only 4% of species belonging to other phyla. The number of microbes present in our bodies is almost the same or even more [1].

## Oral microbiome and disease

The oral microbiome is known to participate in metabolic functions that include the deglycosylation of complex carbohydrates by *Streptococcus oralis* (Byers et al., 1999) and sulfate reduction by Desulfobacter and Desulfovibrio (van der Hoeven et al., 1995). Proteolytic activities of periodontal bacteria also are important for amino acid absorption. Proteolysis is mostly produced by Porphyromonas, Prevotella, and Fusobacterium species (Jie Bao et al., 2008), and an aminopeptidase effect has been observed from *Fusobacterium nucleatum* (Rogers et al., 1998) [2].

The oral microbiota contains one of the highest diversities of bacteria in the human body. Many of these bacteria are believed to contribute to the development of cancer. *Fusobacterium nucleatum* (*F. nucleatum*) is one such bacteria and is considered an oncobacterium. *F. nucleatum* is a Gram-negative anaerobic bacterium that is found primarily in the oral mucosa under normal conditions. However, *F. nucleatum* has been implicated in several disease states including colorectal cancer. *F. nucleatum* is more abundantly found in diseased lesions. Multiple studies have shown that F. nucleatum is found to be present in potentially high numbers in cancerous tissues [3].

The stability of the oral microbiome may be important for resistance against colonization by pathogens (Vollaard and Clasener, 1994) and is mainly produced by the presence of commensal streptococci, which produce a high amount of bacteriocins and inhibit the growth of Gram negatives. *Streptococcus salivarius* has been identified as a member of the normal oral microbiome that may maintain the bacterial community structure and has been suggested as a possible probiotic.

Smoking has been recognized as a major risk factor for periodontal disease, affecting the prevalence, severity, progression and treatment response of the disease, second only to the dental plaque. Epidemiological studies have presented a significantly higher risk for periodontal disease in smokers compared to non-smokers and the increased risk is proportional to the duration and rate of smoking. Cigarette smoking is a public health problem. It decreases the commensal population of normal flora in the oral cavity leading to an increase of pathogenic microbes [4].

Active smokers and those exposed to second hand smoke are at increased risk of bacterial infection. Tobacco smoke exposure increases susceptibility to respiratory tract infections, including tuberculosis, pneumonia and Legionnaires disease; bacterial vaginosis and sexually transmitted diseases, such as chlamydia and gonorrhoea; Helicobacter pylori infection; periodontitis; meningitis; otitis media; and post-surgical and nosocomial infections. Tobacco smoke compromises the anti-bacterial function of leukocytes, including neutrophils, monocytes, T cells and B cells, providing a mechanistic explanation for increased infection risk. Further epidemiological, clinical and mechanistic research into this important area is warranted [5].

## Gingivitis

It is not uncommon to have some form of periodontal disease. In its early stages, called gingivitis, the gums may become swollen, red or tender and may bleed easily. If left untreated, gingivitis may escalate to periodontitis, a more serious form of the disease where gums can recede, bone can be lost, and teeth may become loose or even fall out. With periodontitis, bacteria and their toxic byproducts can move from the surface of the gums and teeth and into the bloodstream, where they can spread to different organs, said Ananda P. Dasanayake, a professor of epidemiology at the New York University College of Dentistry, US. This can happen during a dental cleaning or flossing, or if you have a cut or wound inside your mouth, he said.

If you have inflammation in the mouth that is untreated, some of the proteins responsible for that inflammation can spread throughout the body and potentially damage other organs.

## Diabetes

Of all the associations between oral health and disease, the one with the most evidence is between periodontal disease and diabetes. And the two conditions seem to have a two-way relationship. periodontal disease seems to in-crease the risk for diabetes, and vice versa. Researchers have yet to understand exactly how this might work, but in one review published in 2017, researchers wrote that the systemic inflammation caused by periodontal disease could worsen the body's ability to signal for and respond to insulin, leading to diabetes.

In another study, published in April 2023, scientists found that diabetics who were treated for periodontal disease saw their overall healthcare costs decrease by 12 to 14 per cent. "You treat periodontal disease, you improve the diabetes," Dasanayake said.

## Pneumonia

If large amounts of bacteria from the mouth are inhaled and settle in the lungs, that can result in bacterial aspirations pneumonia. This phenomenon has been observed mainly in patient who are hospitalized or older adults in nursing homes and is a concern for those who can't floss or brush their teeth on their own.

## Cardiovascular diseases

In a report published in 2020, an international team of experts concluded that there is a significant link between periodontitis and increased chances of heart attack stroke, plaque buildup in the arteries and other cardiovascular conditions. A 2012 statement from the American heart association noted that inflammation in the gums has been associated with higher levels of inflammatory proteins in blood that have been linked with poor heart disease [6].

## Pregnancy complications

A number of studies and reviews have found association between severe periodontal disease and preterm, low birth weight babies. Though more research is needed to confirm this link.

In 2019 reviews, researchers found that treating periodontal disease during pregnancy improve birth weight and reduced the risk of preterm birth and the death of foetus or the newborn. And in 2009 study researchers found that oral bacteria could travel to the placenta-potentially playing a role in chorloamnionitis a serious infection of the placenta and amniotic fluid that can lead to

an early delivery or even cause life threatening complications if left untreated [7].

### Cystic fibrosis

Cystic fibrosis is a life-shortening autosomal recessive disease affecting the pulmonary, gastrointestinal and genitourinary systems. Lung colonization with a succession of pathogens, such as *Staphylococcus aureus* and *H. influenzae* is likely to occur in affected individuals. Ultimately, persistent colonization by the opportunistic pathogen *Pseudomonas aeruginosa* contributes to significant morbidity and mortality in cystic fibrosis [5-8]. Epidemiological studies have shown that second hand smoke exposure is associated with poor prognosis in cystic fibrosis patients [9] and that a dose-dependent relationship exists between number of cigarettes smoked and severity of disease amongst young patients [7,8,10]. In keeping with these data, mice infected with *P. aeruginosa* and exposed to tobacco smoke exhibit delayed clearance of infection and increased morbidity compared to control mice which were infected but not exposed to smoke [8,9].

### Bacterial meningitis

Carriage of *H. influenzae*, pneumococcus, and meningococcus has been shown to be more common in both active and second-hand smokers than in nonsmokers (34-38). Indeed, the relationship may be dose-dependent, and, in a study of military recruits, smoke exposure gave an attributable risk for meningococcal carriage of 33% (38). In addition to increased carriage, meningitis cases have a two-to fourfold higher risk of exposure to cigarette smoke than controls [10-12]. Furthermore, second-hand smoke exposure predisposes to nasopharyngeal colonization with specific *Staphylococcus aureus* variants that may have altered capacity to compete with pneumococci subtypes. Passive exposure to tobacco smoke has also been associated with *Haemophilus influenzae* and pneumococcus meningitis in Australian children [13-15].

## Aim of study was

The aim of this study was to find out the difference in oral microbial flora between smokers and Non-Smokers.

## Objectives of study were

A. Identification of Microbes.

B. Comparison of microbial flora from the sample of Smokers and Nonsmokers.

Sample collected from volunteer Before taking swab, written, informed and voluntarily consent was taken from the participants in English, Bengali and Hindi.

## Materials and Methods

### Time of study

The study was carried out from February 2023 to May 2023.

### Place of study

Department of Microbiology, BN campus, All India Institute of Hygiene and Public Health, Kolkata.

### Type of study

**Laboratory based observational study:** 2.4 Fifty-four (54) subjects, representing both genders, ranging in age from 18 to 60. Fifty-four (54) samples were tested. This sample size had been calculated by method of convenience. In case of smokers the swabs were taken from those, who smokes from minimum 5 years. There were 27 swabs taken from smokers and 27 swabs from non-smokers. Two swabs were taken from each volunteer, one for culture and another for Gram stain and Albert's stain. Gram stain for seeing gram positive and gram-negative bacteria while Albert stain for seeing bacteria containing Metachromatic Granules (MCG) [16,17].

### Methodology proper

These volunteers are from

A. Bidhannagar

B. Urban health unit, All India Institute of Hygiene and Public health, Chetla

C. Central Avenue

D. Sonarpur

E. Howrah

Samples from the following nine sites were analysed for each subject: dorsum of the tongue, lateral sides of the tongue, buccal fold, hard palate, soft palate, labial gingiva and tonsils of soft tissue surfaces, and supragingival and subgingival plaques from tooth surfaces. samples were be collected by swab from the adjacent area and was brought to the laboratory. Then samples were transported to laboratory in ice-pack or within 4 hours of collection. Then the samples were processed for bacteria and Yeast. Samples were inoculated on the following media:

A. Mac Conkey agar with neutral red as pH indicator (Peptone, Neutral red, agar agar, Lactose, Sodium taurocholate, deionized water) for distinguish bacteria based on their lactose-fermenting properties into LF (Lactose-fermenting) and NLF (Non-Lactose-fermenting) colonies.

B. Sabouraud's dextrose agar plate (pH 5.6-6) (glucose -2gm, Peptone 2 grams, Agar agar 2 grams, deionized water 100ml) for fungi.

C. Robertson's cooked meat medium (RCM) for culturing anaerobes, made as per manufacturer's instruction.

D. Blood agar plate for differentiate bacteria based on their hemolytic properties.

E. Muller Hilton Agar for Antibiotic Susceptibility Test.

F. Nutrient Agar with 6.5% NaCl and Tellurite Agar for inoculation of *Enterococcus* spp.

G. Egg Yolk Agar for inoculation of *Bacillus* spp.

Gram's stain, Albert's stain was done from samples directly to detect Gram positive or gram-negative bacteria, bacteria with

metachromatic granules respectively. Sample inoculation and identification of Microorganisms.

The pure bacterial cultures were obtained by inoculating the sample on Blood agar media plates, MacConkey agar media plate, SDA tube and RCM broth. For this purpose, samples were streaked on different media and agar plates with the help of sterilized inoculating loops. The inoculated nutrient agar plates were then incubated for 18-24 h at 37 °C. After incubation the isolated bacterial colonies were picked from growth plates and quadrant streaking were done aseptically to new plates in order to obtain pure strains of bacterial culture. Four quadrants streaking were done by rotating the plates at 90° anticlockwise at four different areas of plate. This was done by dragging the culture across the agar with the help of sterilized inoculating loop from previously streaked area to new one. The plates were then incubated at 37 °C for 24h. After incubation isolated colonies were picked and cultured again to purify the samples [12,13].

Blood agar plate was used to grow fastidious microorganisms and to After culture, the plates were placed in incubator at 37 °C for a period of 18-24 hours for the development of colonies of bacteria, and after 24 hours the plate was taken out from incubator and different bacterial colonies were identified. Gram stain performed and after that the subculture of bacterial colony took place from the mixture. Biochemical tests like Indole, urease, motility, Citrate utilization, acid and H2S on TSI agar were also done from colonies of Gram-negative bacteria, and from Gram positive colonies, standard biochemicals like Catalase (with 3% $H_2O_2$), coagulase and oxidase were done [18,19].

## Result

In the end of study, we were able to access the presence of pathogenic and normal bacteria in oral microbiome. Which are important of public health point.

### How many samples tested

In this study we collected total 54 samples out of which 14 were taken from females and 40 from males. Out of 14 females 7 were smokers and 7 were non-smokers. Out of 40 males 20 were smokers and 20 were non-smokers. Out of 27 smokers 7 were occasional smokers while 20 were regular/chain smokers. Out of all the smokers, only one smokes bidi while others were cigarette-smokers. Out of all the smokers, 4 individuals were also consuming oral tobacco. The most common bacterial species we isolated overall, was *Enterococcus* spp. (44 isolates out of 54, 81.25%). Out of these 44 isolates, 34 were *Enterococcus faecalis* (77.27%) and 10 were *Enterococcus* non-*faecalis* (22.73%). *Streptococcus pneumoniae* was also isolated; 2 from smokers and one from non-smokers. In smokers most common pathogen found was MRSA (Methicillin Resistant *Staphylococcus aureus*) (50%) followed by *Klebsiella aerogenes* (20%) *Streptococcus pneumoniae* (15%) *Pseudomonas aeruginosa* (15%) and oral *Streptococcus* (10%) (Figures 1-3).

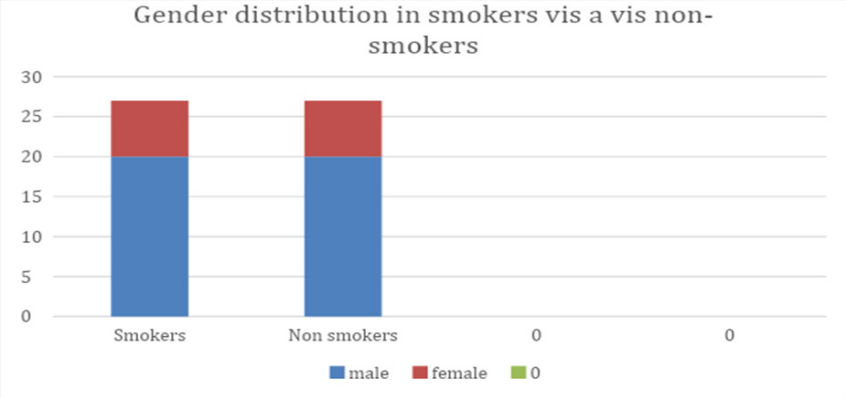


**Figure 1:** Gender distribution of Smokers vs nonsmokers.

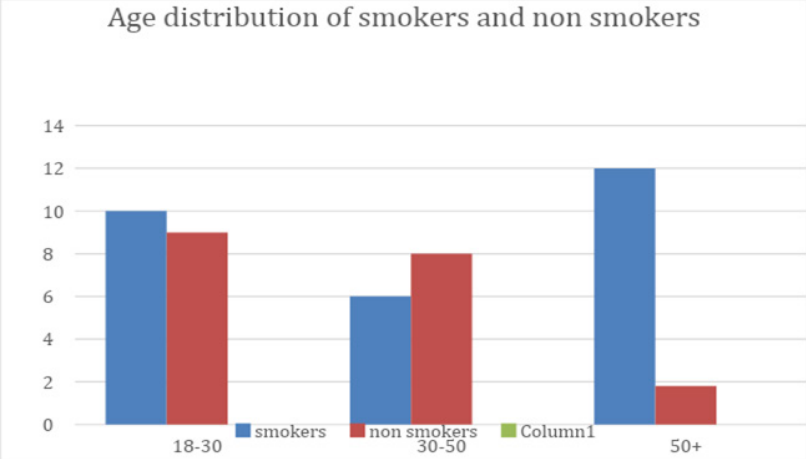


**Figure 2:** Age distribution of Smokers vs nonsmokers.

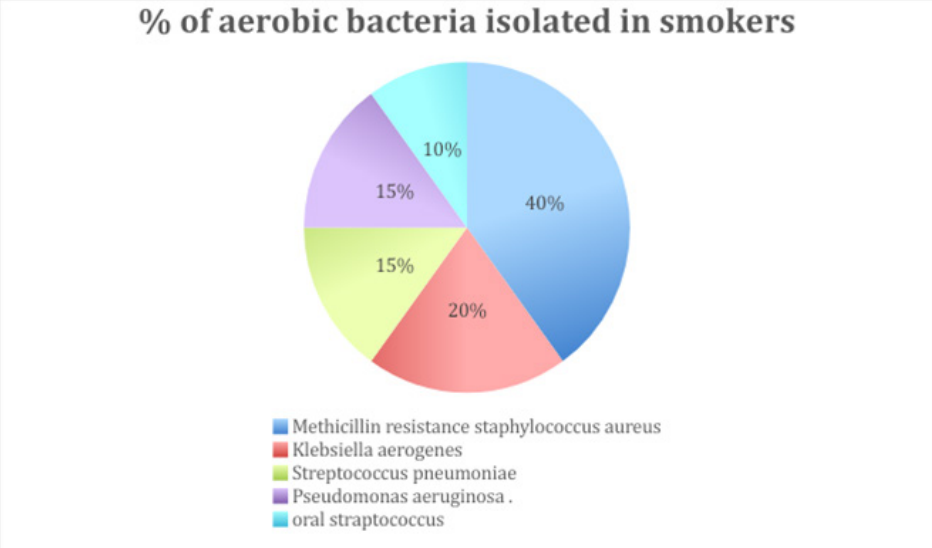


**Figure 3:** percentage of aerobic bacteria isolated from smokers.

While in non-smokers the microbial flora isolated were more vivid as compared to smokers, *Enterococcus faecalis* and *Enterococcus* non- *faecalis* are most common as but no yeasts were found, the most common bacteria found in non-smokers were *Bacillus* non-cereus (40%) followed by coagulase negative *Staphylococcus* spp. (*Staphylococcus saprophyticus*) (5%). Apart from that the other common bacteria found were *Enterobacter cloacae (5%), Aeromonas schubertii* (10%), *Escherichia coli* (20%), *Micrococcus* (10%) and *Klebsiella pneumoniae* (10%). *Prevotella, Veillonella* and *Streptococcus spp.* were the predominant genera in the saliva of both groups. Although the overall composition and diversity of the microbiota were similar, *Prevotella* was significantly more abundant in salivary samples of current smokers compared to non-smokers (Figure 4).

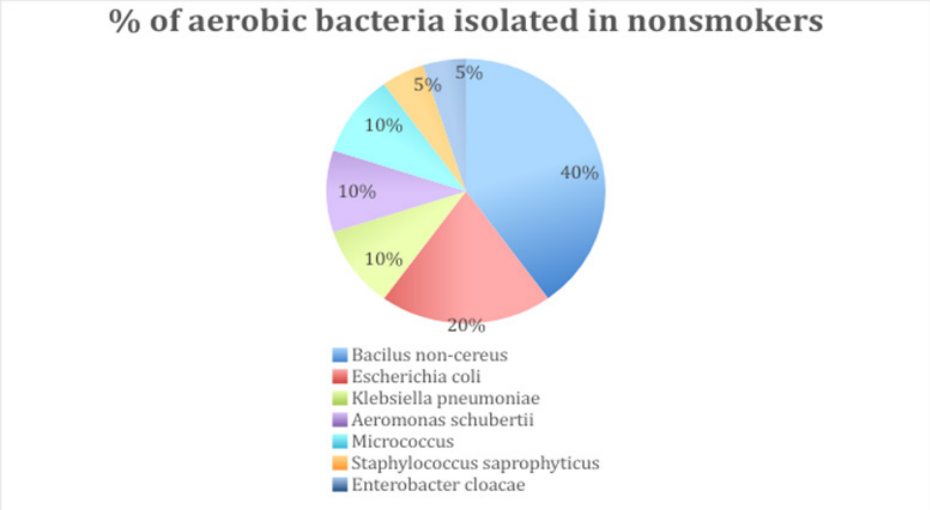


**Figure 4:** percentage of aerobic bacteria isolated from Non-smokers.

### Statistical calculation

MRSA was found more in smokers (14 out of 27) than Nonsmokers (0 out of 27). By taking 95% confidence interval and degree of freedom 1, with the help of chi-square test, this difference was found to be highly significant (p value <0.0001).

## Discussion

Oral microbes are mostly Commensal, but they can also cause oral and periodontal disorders. They can vary according to the oral hygiene, and the smoking pattern of the host. At the end of the study, we were able to assess the burden of normal as well as pathogenic Microorganisms in smokers' vis a vis nonsmoker. This type of study has not been done previously from this part of our country. Hence these findings were important from the public health viewpoint. The purpose of this study is to define the predominant Microbial flora of the healthy oral cavity by identifying and comparing the cultivable and the not-yet-cultivated bacterial species on different soft tissues and supra- and subgingival plaques. Our study was also helpful for finding the details about oral microbes. The microbiome of each organ is distinct and substantial variability occurs even within the oral cavity, partly due to spatial variations in the availability of

Oxygen. The oral rinse samples used in this study are likely to over-represent microbes present in the surface of the oral cavity as well as saliva, and less likely to include microbes from dental plaques or gingival crevicular fluid, which may explain the dominance of Firmicutes, as noted in buccal mucosa. Salivary microbiome has been reported to have higher richness and diversity compared with gingival plaque microbiome, and to be less susceptible to changes in periodontal conditions [17].

## Conclusion

In conclusion, there is a distinctive bacterial flora in the healthy oral cavity which is different from that of smokers' oral cavity. For example, many species specifically associated with periodontal disease, such as *Porphyromonas gingivalis*, *Tannerella forsythia*, and *Treponema* spp. were not detected in any samples tested. In addition, the bacterial flora commonly thought to be involved in dental caries and deep denticavities, represented by *Streptococcus mutans*, *Lactobacillus* spp., *Bifidobacterium* spp., and *Atopobium* spp., were not detected in supra- and subgingival plaques from clinically healthy teeth. More such studies are needed to delineate the exact difference of microbial flora between smokers and non-smokers.

## Source of Funding

None.

## Conflict of Interest

There are no Conflicts of Interest.

## References

1. Ogba OM, Ewa JJ, Olorode OA, Mbah M (2017) Effect of tobacco smoking on oral microbial flora and the relationship with oral health in Calabar, Nigeria. Int J Bio Lab Sci 6: 1-5.
2. Yamashita Y, Takeshita T (2017) The oral microbiome and human health. J Oral Sci 59(2): 201-206.
3. Sedghi L, DiMassa V, Harrington A, Lynch SV, Kapila YL (2021) The oral microbiome: Role of key organisms and complex networks in oral health and disease. Periodontol 2000 87(1): 107-131.
4. Costalonga M, Herzberg MC (2014) The oral microbiome and the immunobiology of periodontal disease and caries. Immunol Lett 162(2 Pt A): 22-38.
5. Solbiati J, Frias Lopez J (2018) Metatranscriptome of the Oral Microbiome in Health and Disease. J Dent Res 97(5): 492-500.
6. Yu G, Phillips S, Gail MH, Goedert JJ, Humphrys MS, et al. (2017) The effect of cigarette smoking on the oral and nasal microbiota. Microbiome 5(1): 3.
7. Mason MR, Preshaw PM, Nagaraja HN, Dabdoub SM, Rahman A, et al. (2015) The subgingival microbiome of clinically healthy current and never smokers. ISME J 9(1): 268-272.
8. Cole JR, Chai B, Farris RJ, Wang Q, Kulam SA, et al. (2005) The Ribosomal Database Project (RDP-II): Sequences and tools for high-throughput rRNA analysis. Nucleic Acids Res 33(Database issue): D294-D296.
9. Camelo Castillo AJ, Mira A, Pico A, Nibali L, Henderson B, et al. (2015) Subgingival microbiota in health compared to periodontitis and the influence of smoking. Front Microbiol 6: 119.
10. Moalic E, Gestalin A, Quinio D, Gest PE, Zerilli A, et al. (2001) The extent of oral fungal flora in 353 students and possible relationships with dental caries. Caries Res 35(2): 149-155.
11. Fujimori I, Goto R, Kikushima K, Ogino J, Hisamatsu K, et al. (1995) Isolation of alpha-streptococci with inhibitory activity against pathogens, in the oral cavity and the effect of tobacco and gargling on oral flora. Kansenshogaku Zasshi 69(2): 133-138.
12. Van Schooten FJ, Besaratinia A, De Flora S, D Agostini F, Izzotti A, et al. (2002) Effects of oral administration of N-acetyl-L-cysteine: a multi-biomarker study in smokers. Cancer Epidemiol Biomarkers Prev 2002 11(2): 167-175.
13. Wirth R, Maróti G, Mihók R, Simon Fiala D, Antal M, et al. (2020) A case study of salivary microbiome in smokers and non-smokers in Hungary: analysis by shotgun metagenome sequencing. J Oral Microbiol 12(1): 1773067.
14. Shankargouda P, Rao Roopa S, Sanketh DS, Amrutha N (2013) Microbial flora in oral disease. J Contemp Dent Pract 14(6): 1202-1208.
15. Shankargouda P, Rao Roopa S, Sanketh DS, Amrutha N (2013) Oral microbial flora in health. World Journal of Dentistry 4(4): 262-266.
16. Peter R, Emilia S, Uittamo J, Malcolm R, Riina R (2009) Novel method for sampling the microbiota from the oral mucosa. Clin Oral Investig 13(2):243-246.
17. Chowdhry R, Singh N, Sahu DK, Tripathi RK, Mishra A, et al. (2018) 16S rRNA long-read sequencing of the granulation tissue from nonsmokers and smokers-severe chronic periodontitis patients. Biomed Res Int 2018: 4832912.
18. Cintron F (1992) Initial processing, inoculation, and incubation of aerobic bacteriology specimens. In: Isenberg HD (Ed.), Clinical Microbiology Procedures Handbook, American Society for Microbiology, Washington DC, USA, 1: 1.4.1-.4.1.9.
19. https://www.medcalc.org/calc/comparison_of_proportions.php